ISSN 0859 144X

THE ASEAN JOURNAL OF RADIOLOGY

January - April 1995
Volume I Number I

Published by The Radiological Society and
the College of Radiologists of Thailand,
Bangkok, Thailand.

Supported through an educational grant from Bracco International

THE ASEAN JOURNAL OF RADIOLOGY

January - April 1995

Volume I Number I

Published by The Radiological Society and
the College of Radiologists of Thailand,
Bangkok, Thailand.

Supported through an educational grant from Bracco International

1. The AAR Journal of Radiology publishes the papers on Radiological Sciences, such as research work, review articles, case reports, innovations in Medical Sciences related to all branches of Radiology, and letters to the editor. The aforementioned materials can be written in English only.

2. The authors have to submit 2 copies of the manuscript and a diskette: **to Prof. Dr. Kawee Tungsubutra,** 318 Kaweevej Hospital, Tarksin Road, Dhonburi, Bangkok 10600, Thailand.
or to the Associate Editors at the Radiological Society of Malaysia, Indonesia, Phillippine, Singapore and Brunei. The names and addresses of the Associate Editors in each country were published in the front page of this Journal.

3. The original copy to be submitted must be typed in a double space on one side of the page of 8″ × 11″ paper.

4. The format of the article must include:

a. Title page and address of the author (s)

b. Abstract

c. Introduction (Background)

d. Material and Method

e. Results and discussion (Tables and Illustrations)

f. Acknowledgement (it any)

g. References (Follow the Vancouver style developed by ICMJE)

5. We will provide 25 copies of reprints for the author (s) who submit (s) and article for publication in the AAR Journal.

6. The illustrations and tables must be clearly prepared with legends in English as they are the art works to be reproduced.

7. The authors are responsible for the contents of the article as to its facts and findings.

8. Ethics.

Paper reporting studies which might be interpreated as human experimentation (e.g. controlled trials) should conform to the standards of the Declaration of Helsinki (see British Medical Journal 1964:2:177) and should indicate that approval that such studies may proceed has been granted by the local or hospital Ethics Committee.

When reporting experiments on animals indicate whether the institution's or the National Research Council's guide for, or any national law on, the care and use of laboratory animals was followed.

Messages from Prof. Dr. Kawee Tungsubutra

Editor-in-Chief, The Asean Journal of Radiology

It was my believe that the only difference between a professional society and a social society is that; a professional society must have a regular journal which the members can read to follow up the progresses in their specialties of their professions and can send their article to be published in this journal as well.

This ASEAN Journal of Radiology which you are holding in your hands has been successful with the co-operation of our professional friends who are the radiologists from all the member countries and with the kind considerations of the Bracco International Co., especially Dr. Paul Synaeve who has given a strong support and encouragement since I have sold this idea to him 4 years ago at the AAR congress in Bali, Indonesia. In this first issue, we are publishing in a haste to be able to distribute this first volumes at the AAR congress in Manila, Phillippines as requested by our Phillippines co-editor. This is the reason why in this first volume all the articles are the works from Thailand. I hope that the next volume we will have the international articles from the AAR member countries as well as from others in the world.

I hope our journal can be published 3 volumes in a year as the first start and gradually increase to 4,6 and 12 per annum i.e. monthly journal as the B.J.R. or the yellow journal, gray journal, etc.

Kawee Tungsubutra

Prof. Dr. Kawee Tungsubutra

4 January 1995

The Asean Journal of Radiology

Volume 1 Number 1 January 1995

CONTENTS

Volume 1 Number 1 January 1995

CONTENTS

The lesions in the brains detected by CT scan in the Thai patients Investigated due to seizure.

P. Pekanan[1], P.Sirivongspairat[1], S.Nirapathapongporn[1], S.Balachandra[1], C.Chatchavala[1], K.Osathavanichvongs[2] and R.Vejrak[1]

Retrospective study of the CT scan of the brains of the 931 outpatients who had seizure problems. Fifty five percents showed positive findings. The most common findings of all ages were cysticercosis and the second most common findings were infarction. The third most common lesions were the single mass lesion. Cysticercosis was the most common lesion of the age group 11-40 yrs old, infarct was the most common finding in the age group 41-93 yrs old and brain atrophy was the most common lesion in the age group 0-10 yrs old. The age of the patients ranged from 2 days to 93 yrs old and 75% were 11-60 yrs old. There was a tendency to detect the lesions more in the older ages.

Key words: Seizure, CT scan of the brains

A Seizure is a sudden change in body functioning due to abnormal, excessive electrical discharges of neurons in the brain (1). Epilepsy is a symptom complex in which there is a tendency to have repeated seizures. It follows that not everyone who has seizures has epilepsy, but everyone who has epilepsy has seizures. Neither seizures nor epilepsy is a final diagnosis but a symptom complex requiring a search for underlying etiologic factors. Consideration of seizures should arise whenever a patient presents with loss of consciousness or any sudden brief change in functioning with or without loss of consciousness. Paroxysmal changes in consciousness, sensation, emotion, or through all processes may be manifestations of a seizure disorder. A diagnosis of a seizure disorder is especially likely if such changes are repetitive, sterotyped, and preceded by a premonition or warning (aura) or followed by (postictal) confusion, exhaustion, or headache. The physician's initial task when a patient presents with what might be a seizure is to determine whether the episode was indeed a seizure, or some other episodic, periodic, or recurrent paroxysmal event that is nonepileptic, such as syncope, migraine, pseudoseizure, transient ischemic attack or narcolepsy. When the diagnosis of a seizure is made, the patient should be evaluated for common toxic-metabolic or structural abnormalities. These commonly include hypoglycemia, infection, alcohol or drug withdrawal, stroke or tumor.

The purpose of the study was to determine the detected structural abnormalities in the brain by CT scan as the causes of seizures in Thai population.

Materials and methods

Retrospective study of the CT scan of the patients who presented with seizure was performed during the year 1983 and 1991. The CT scan of the brain included plain and intravenous contrast studies. There were 931 patients consisting of 552 male and 279 female patients. The age ranged from 2 days to 93 yrs old. Seizure was the major indication that made the physicians request for the CT scan of the brains in this study. The positive results of the detected lesions were grouped according to the patient's age, as shown in the Table 1-9 and the incidence of each lesion was summarized in Table 10. The patients were sent from many hospitals in Bangkok and outside Bangkok to the diagnostic CT center where the data were

[1]Department of Radiology, Ramathibodi Hospital, Rama 6 street, Bangkok 10400, Thailand

[2]Medical software development project, Mahidol University, Pin-Klao-Nakornchaisri Street, Bangkok, Thailand

analyzed. The detailed clinical data and the final pathological results would not be obtained. The reported lesions were purely imaging diagnosis by the qualified radiologists.

Results

From 931 patients, there were 512 positive results which was equal to 55%. The majority of the patients were between 11-60 yrs old, comprising 76%. The rate of the positive detection of the lesions increased with the patient's age. The cystic lesion, ring or nodular enhanced lesions associated with surrounding brain edema of cysticercosis as shown in Fig. 1, was the most common findings in the age group of 11-40 yrs old. Infarct was the most common finding in the age group of 41-93 yrs old. Brain atrophy was the most common finding in the age group of 0-10 yrs old. For overall lesions, infarct was the most common lesion, comprising of 27%, cystic lesions and active cysticercotic lesions were the second most common lesions, representing 17% each. If the live and dead forms of the cysticercosis were combined, then the cysticercotic lesions were the most common lesions detected by CT scans. These lesions were diagnosed cysticercosis, based on the previous experiences of proved such cases by the operation and the therapeutic treatment. The ring or nodular enlarged lesions were seen as the single lesion at the cortico-medullary area, size were not more than 2 cm, most lesions were near the vertex. The calcified cysticercosis lesions were seen as small rounded dense calcified lesion, size were not more than 2 cm, occurred anywhere in the brains. The 4th most common lesion was single mass, representing 10%. Almost half of them were labelled as meningioma and almost another half were labelled as gliomatous tumors, the rest, fews were lipoma of the corpus callopsum, acoustic tumor at the CP angle, lymphoma, trigeminal neuroma. Multiple masses were believed to be metastatic lesions. Infarct lesions were usually multiple and small size.

Table 1. Positive lesions by CT scan, No. (%) of each lesion, at the age of 0-10 yrs old.

Lesions	No.	(% of total lesions)
1. Tuberous sclerosis	2	(7)
2. AVM	3	(10)
3. Low density of white matter	2	(7)
4. Subdural or epidural hematoma	3	(10)
5. Intracerebral hematoma	1	(3)
6. Single mass lesion	2	(7)
7. Cyst or ring enhanced or enhanced nodules of cysticercosis	4	(14)
8. Calcified cysticercosis	1	(3)
9. hydrocephalus	1	(3)
10. Brain atrophy	5	(17)
11. Intraventricular cyst	1	(3)
12. Dandy-Walker cyst	1	(3)
13. Abnormal meningeal enhancement	2	(7)
14. Porencephaly	1	(3)
Total	29	(100)

Table 2. Positive lesions by CT scan, No. (%) of each lesion, at the age of 11-20 yrs old.

Lesions	No.	(% of total lesions)
1. brain atrophy	2	(4)
2. Diffuse brain swelling	1	(2)
3. Thickened cortex at both insula	1	(2)
4. Hydrocephalus	1	(2)
5. AVM	1	(2)
6. Low density of the white matter	3	(5)
7. Intracerebral hematoma	1	(2)
8. Single mass	1	(2)
9. Infarct	10	(19)
10. Cyst, ring enhanced or nodular enhanced lesion with surrounding edema	16	(30)
11. Calcified cysticercosis	16	(30)
Total	53	(100)

Table 3. Positive lesions by CT scan, No. (%) of each lesion, at the age of 21-30 yrs old.

Lesions	No.	(% of total lesions)
1. Diffuse brain swelling	1	(1)
2. Brain atrophy	4	(5)
3. Hydrocephalus	4	(5)
4. AVM	8	(10)
5. Low density of the white matter	4	(5)
6. Subdural or epidural hematoma	3	(4)
7. Intracerebral hematoma	5	(7)
8. Single mass lesion	5	(7)
9. Infarct	9	(12)
10. Cyst, ring enhanced or nodular enhanced lesions with surrounding edema	16	(22)
11. Calcified cysticercosis	15	(20)
Total	74	(100)

Table 4. Positive lesions by CT scan, No. (%) of each lesion, at the age of 31-40 yrs old.

Lesions	No.	(% of total lesions)
1. Brain abscess	1	(1)
2. Brain atrophy	4	(4)
3. Thick cortex at both insular areas	1	(1)
4. AVM	2	(2)
5. Subdural or epidural hematoma	4	(4)
6. Intracerebral hematoma	9	(9)
7. Single mass lesion	15	(16)
8. Infarct	12	(13)
9. Cyst, Ring enhanced or nodular enhancement with surrounding edema	25	(27)
10. Calcified cysticercosis	20	(21)
Total	93	(100)

Table 5. Positive lesions by CT scan, No. (%) of each lesion, at the age of 41-50 yrs old.

Lesions	No.	(% of total lesions)
1. Cranial vault destruction	1	(1)
2. Subarachnoid hemorrhage	1	(1)
3. Abnormal meningeal enhancement	1	(1)
4. Diffuse brain swelling	1	(1)
5. Brain atrophy	2	(3)
6. Hydrocephalus	2	(3)
7. AVM	4	(6)
8. Low density of the white matter	1	(1)
9. Subdural or epidural hematoma	4	(6)
10. Intracerebral hematoma	4	(6)
11. Single mass lesion	10	(15)
12. Infarct	17	(26)
13. Cyst, ring enhanced or nodular enhanced lesions with surrounding edema	5	(7)
14. Calcified cysticercosis	13	(20)
Total	66	(100)

Table 6. Positive lesions by CT scan, No. (%) of each lesion, at the age of 51-60 yrs old.

Lesions	No.	(% of total lesions)
1. Subarachnoid hemorrhage	1	(1)
2. Abnormal meningeal enhancement	1	(1)
3. Intraventricular hemorrhage	1	(1)
4. Hydrocephalus	3	(3)
5. AVM	4	(4)
6. Low density of the white matter	1	(1)
7. Subdural or epidural hematoma	1	(1)
8. Multiple masses	2	(2)
9. Intracerebral hematoma	8	(9)
10. Single mass	9	(10)
11. Infarct	28	(30)
12. Cyst, ring or nodular enhanced lesions with surrounding edema	17	(18)
13. Calcified cysticercosis	16	(18)
Total	92	(100)

Table 7. Positive lesions by CT scan, No. (%) of each lesion, at the age of 61-70 yrs old.

Lesions	No.	(% of total lesions)
1. Intraventricular hematoma	1	(2)
2. Calcification of the basal ganglia and dentate nucleus	1	(2)
3. Hydrocephalus	2	(3)
4. Low density of the white matter	1	(2)
5. Subdural or epidural hematoma	2	(3)
6. Multiple masses	1	(2)
7. Intracerebral hematoma	3	(5)
8. Single mass	7	(12)
9. Infarct	31	(54)
10. Cyst, ring or nodular enhanced lesions with surrounding edema	4	(7)
11. Calcified cysticercosis	4	(7)
Total	57	(100)

Table 8. Positive lesions by CT scan, No. (%) of each lesion, at the age of 71-80 yrs old.

Lesions	No.	(% of total lesions)
1. Aneurysm	1	(3)
2. Hydrocephalus	1	(3)
3. AVM	1	(3)
4. Low density of the white matter	1	(3)
5. Subdural or epidural hematoma	1	(3)
6. Intraventricular hemorrhage	3	(8)
7. Single mass lesion	4	(11)
8. Infarct	18	(51)
9. Cyst, ring or nodular enhanced lesions without surrounding edema	1	(3)
10. Calcified cysticercosis	4	(11)
Total	35	(100)

Table 9. Positive lesions by CT scan, No. (%) of each lesion, at the age of 81-93 yrs old.

Lesions	No.	(% of total lesions)
1. Hydrocephalus	2	(12)
2. Multiple masses	1	(5)
3. Intracerebral hematoma	1	(5)
4. Infarct	12	(70)
5. Cyst or ring or nodular enhanced lesion with surrounding edema	1	(12)
Total	17	(100)

Table 10. Number of each lesion compared with the total lesions detected by CT scan, in all age groups.

Lesions	No.	(% of the total lesions)
1. Calcified cysticercosis	89	(17)
2. Cyst, ring enhanced or nodular enhanced lesions with surrounding edema	89	(17)
3. Infarct	137	(27)
4. Intracerebral hematoma	32	(6)
5. Subdural or epidural hematoma	18	(3)
6. Hydrocephalus	16	(3)
7. Multiple masses	4	(1)
8. Single mass	53	(10)
9. Aneurysm	1	(0.2)
10. AVM	23	(4)
11. Low density of white matter	13	(2)
12. Intraventricular hematoma	2	(0.4)
13. Calcification of the basal ganglia and dentate nucleus	1	(0.2)
14. Subarachnoid hemorrhage	2	(0.4)
15. Abnormal meningeal enhancement	4	(1)
16. Cranial vault destruction	1	(0.2)
17. Diffuse brain swelling	4	(1)
18. Brain atrophy	17	(3)
19. Brain abscess	1	(0.2)
20. Thick cortex at both insular areas	2	(0.4)
21. Intraventricular cyst	1	(0.2)
22. Dandy-Walker cyst	1	(0.2)
23. Porencephaly	1	(0.2)
24. Thickened cortex at both insula	2	(0.4)
Total	512	(100)

Table 11. Incidence of positive CT scan in each age group and in all ages

Age group	Total pts in gr. (% of total pts)	No. % of group of lesions No.	%	% of total positive patients
0 - 10	84 (9)	29	34	6
11 - 20	149 (16)	53	35	10
21 - 30	154 (16)	74	48	14
31 - 40	147 (15)	93	63	18
41 - 50	131 (14)	66	50	13
51 - 60	138 (15)	92	67	18
61 - 70	64 (6)	57	90	11
71 - 80	45 (5)	35	78	7
81 - 93	19 (2)	17	89	3

Total patients were 931, total positive patients were 512

Discussion

The normal CT findings in the patients with seizure was seen in 45% of 931 patients which is slightly lower than the reports of McGahan (60%) (2) and of Bogdanoff (64%) (3).

The small calcified nodules (assumed calcified cysticercosis) cysts of cysticercosis and ring or nodular enhanced lesions with surrounding edema (assumed just dead cysticercosis) were the most common lesions of overall lesions. Thailand is known as one of the endemic area of cysticercosis, so that these lesions were not mentioned in the reports of McGahan or of Bogdanoff. These lesions were also presented in the age group 0-10 yrs old, shared the first rank with the brain atrophy. The overall incidence was 34% of the total lesions.

Infarction was seen as the most common lesion for the age 61-93 yrs old and was the 2nd most common lesion for the age 11-30 yrs old and 41-60 yrs old. It was the third most common lesion for the age 31-40 yrs old. The overall incidence was 27% of the total lesions. It was seen 15% of the detected lesions reported by McGahan (2). In the McGahan's report, the infarct lesion was not seen in the patient younger than 45 yrs old. There was no infarct lesion in Bogdanoff's report (3)

The single mass lesion was the third common lesion of the overall lesions and was the second most common lesion for the age 31-40 yrs old. It was seen in 10% of all positive lesion by us, 10% by McGahan (2) and 11% by Bogdanoff (3). However, both authors included every kind of neoplasm. If we included multiple masses lesion, the incidence would be 11% of the overall lesion.

Bachman et al (4), reported CT scan in chronic seizure disorders of childhood in 98 children of age 3 months to 20 yrs old. Seventy one percents were normal scans and brain atrophy was the most common lesion seen in 46%. We found 82 positive cases in 233 patients, the negative findings was 65% and brain atrophy was the third most common lesion comprising of 8%. The most common lesion was cysticercosis, seen in 39% and infarct the second most common lesion representing 12%. There were no cysticercotic or infarct lesion by Bachman's study, except for 11% post-op changes.

There was a tendency to increase incidence of the detection of the lesion with advancing age, similar findings as that of Zimmerman (5). The detection rate was 34-48% at age 0-30 yrs old, 50-67% at age 31-60 yrs old and 78-90% at age 61-93 yrs old.

MRI of the brain might detect the temporal lobe lesions, such as focal temporal lobe atrophy, small gliomas, hamartomas, heterotopias, cavernous angiomas and arteriovenous malformation as the causes of seizure better than CT scan (6-9). However, in Thailand, where the calcified cysticercosis are quite common, CT scan is still needed in the investigation of seizure, because MRI cannot detect calcification well.

Acknowledgement : We would like to thank Urupong Medical Center to provide us the materials for this study.

References

1. Olson WH, Brumback RA, Gascon G, Iyer V. Handbook of Symptom-Oriented Neurology. 2nd Ed. Baltimore: Mosby, 1994.
2. McGahan JP, Dubling AB, Hill RP. The evaluation of seizure disorders by computerized tomography. J Neurosurg 50: 328-332, 1979.
3. Bogdanoff BM, Stafford CR, Green L, Gonzalez CF. Computerized transaxial tomography in the evaluation of patients with focal epilepsy Neurology 25: 1013-1017, 1975.
4. Bachman DS, Hodges FJ, Freeman JM. Computerized axial tomography in chronic seizure disorders of childhood. Pediatrics 58: 828-832, 1976.
5. Zimmerman RA, Gonzalex C, Bilaniuk LT et al. Computed tomography in focal epilepsy, Computed Tomogr 1: 83-91, 1977.
6. de Leon MJ, Golomb J, George AE et al: The radiologic prediction of Alzheimer disease: the atrophic hippocampal formation. AJNR 14: 897-906, 1993.
7. Cendes F, Leproux F, Melanson D et al: MRI of amygdala and hippocampus in temporal lobe epilepsy. J Comp Asst Tomogr 16: 206-210, 1993.
8. Jackson GD, Barkovic SF, Duncan JS, Connelly A: Optimizing the diagnosis of hippocampal sclerosis using MR imaging. AJNR 14: 753-762, 1993.
9. Holtas S: Neuroradiological approach to the epileptic patient, Riv Di Neuroradiol (suppl) 2: 27-32, 1993.

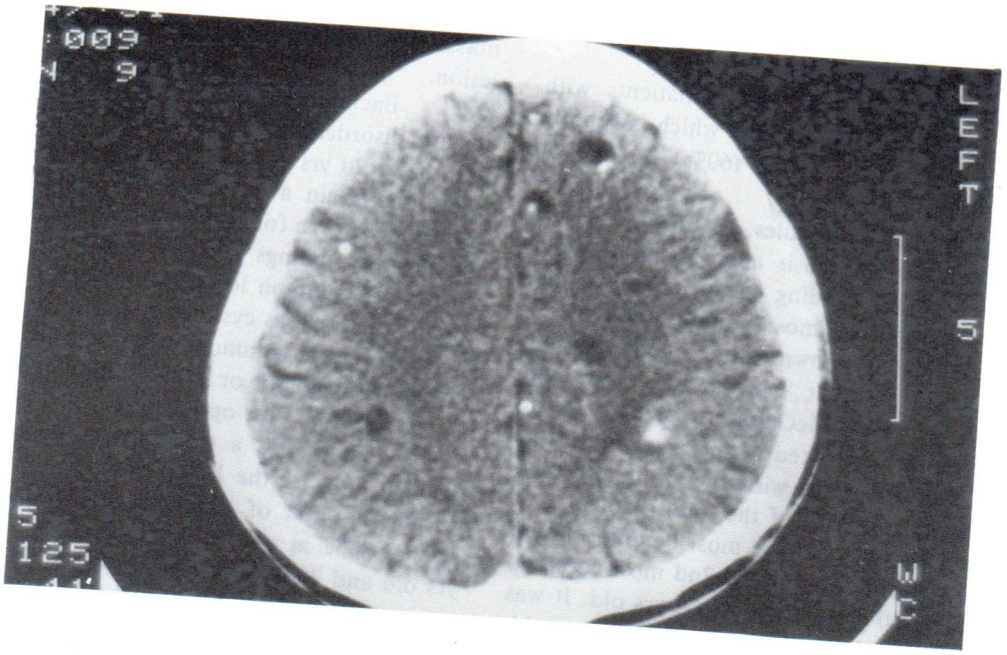

Fig. 1a Cysticercosis. Non i.v. enhanced CT scan of the brain, supraventricular level showed small calcified nodules, small cystic lesions with and without calcified scolex at both frontoparietal lobes.

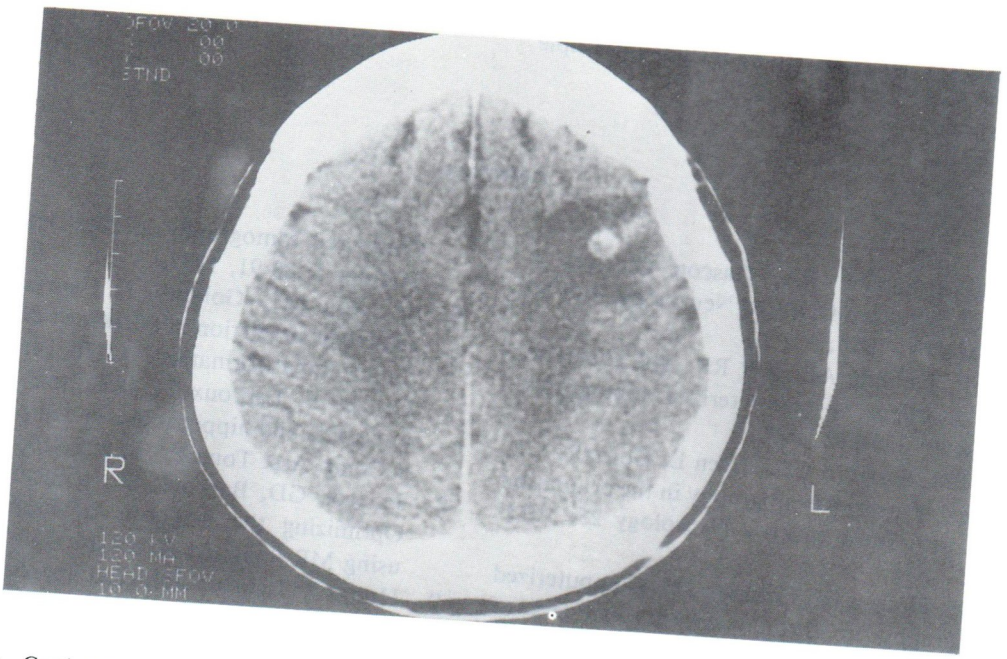

Fig. 1b Cysticercosis. I.V. enhanced axial CT scan of the brain, supraventricular level showed small ring enhanced lesion with surrounding white matter edema at corticomedullary area at high Lt. frontoparietal lobe. Just-dead cysticercotic lesion.

The ability of the routine head computed tomography in the detection of the non-giant intracranial aneurysms-A reappraisal

S. Hirunpat[1], P. Pekanan[1], W. Thanomkiat[1], N. Ruxayos[1]

Abstract.

Retrospective review of the routine CT scan of the brain of the patients who were operated for ruptured and unruptured aneurysms. Angiography was performed in every case which was studied. There were 28 ruptured aneurysms and two unruptured aneurysms. The rate of the detection of the ruptured aneurysms by CT scan depended on the size of the aneurysm, the time interval from the onset of the subarachnoid hemorrhage to the time of performing CT scan and the site of the aneurysm. The detection rate was high when the size of the aneurysms were larger than 6 mm, when CT scans was performed after 4 days of onset of subrachnoid hemorrhage and when the aneurysms were at the basilar tip and middle cerebral artery.

key words: CT brain, non giant aneurysms

Introduction

CT has long been the important diagnostic tool in subarachnoid hemorrhage. CT scans without intravenous contrast; blood in the subarachnoid space initially is seen as increased density in the cisterns, sulci and fissures of the brain. It can detect 90% of SAHs within the first 24 hours and by the end of the first week it can still detect more than 50% (1-4). If SAH is obvious on CT more than 1 week following the initial event, rebleeding has probably occurred. Most aneurysms are in the subarachnoid space, when they bleed, they usually cause SAH. The location of blood (particularly parenchymal hemorrhage) following aneurysm rupture often provides useful information regarding aneurysm location (5). Most of the published data reported about the ability of the special CT technique such as thin slices (1.5 mm) (6) and high resolution angio-CT in the detection of the cerebral aneurysms (6-8). Our study was done to reappraise the ability of the routine CT scan in detecting non- giant aneurysms.

SAH = Subarachnoid Hemorrhage

Patients and method

Ninety-six patients were operated for intracranial aneurysms during Janaury 1990 to October 1992, in Ramathibodi Hospital. Complete data including plain and intravenous enhanced CT scan of the brain, angiographic studies and proved surgical reports, were obtained only from 30 patients with 30 aneurysms.

The CT scan were obtained from multiple diagnostic centers, all included scan areas from the foramen magnum to the vertex. The slice thickness varied from 5-10 mm at the posterior fossa and 10 mm at the supratentorial level.

The conventional angiography in all patients were performed by using a cut film biplane technique. In each study, all four major intracranial vessels, were visualized. Anteroposterior, lateral and oblique views were done with carotid injection and AP and lateral views with vertebral injection.

Correlation of the aneurysms detected by CT scan, angiographic studies and surgical findings were retrospectively analysed.

[1] Department of Radiology, Ramathibodi Hospital, Rama 6 Street, Bangkok 10400, Thailand.

Results

The patients were 18 males and 12 females. The age ranged from 29 to 76 yrs old. Subarachnoid hemorrhage was present in 28 cases and focal neurological sign without subarachnoid hemorrhage in 2 cases.

From 30 aneurysms, 20aneurysms (66.7%) were retrospectively detected by enhanced CT scan as rounded enhanced area in close proximity to the circle of Willis, with good correlation with angiographic and surgical findings. The size of the aneurysms ranged from 4 to 14 mm and all aneurysms are saccular type. The detection rate of unruptured aneurysms by CT scan was 100% (2 aneurysms)

The size of the aneurysms, the number of the aneurysms and the detection rate by CT scan was shown in Table 1.

The time interval between performing CT scan and the onset of the subarachnoid hemorrhage, number of the aneurysms and the rate of detection by CT scan was shown in Table 2.

The number of the successfully detected aneurysms by CT scan and the site of the aneurysms are shown in Table 3.

The CT detected aneurysms and angiographic demonstration of the aneuryms at internal carotid artery, anterior communicating artery, middle cerebral artery, posterior communicating artery, basilary tip were shown in figures 1-5 respectively and the looping of the anterior cerebral artery misinterpreted by CT scan as an aneurysm was illustrated in figure 6.

Overall incidence of the multiple aneurysms was 1.5% (1 out of 70 cases) by angiographic and surgical findings.

Table 1. The numbers of the detected aneurysms by CT scan, relating to the size of the aneurysms.

Aneurysm's size(mm) measured by Angio + CT	No. of aneurysms by Angio&Surg.	No. detected by CT	
		No.	%
4	3	1	33
5	6	2	33
6	3	2	66
7*	6	6	100
8	3	2	66
9	—	—	—
10	6	4	66
11	1	1	1100
12	—	—	—
13	—	—	—
14	2	2	100

* There was only one aneurysm that was measured 3 mm by angiographic study and 7 mm by CT study, due to spasm of the aneurysm in the presence of subarachnoid hemorrhage; so that the figure 7 mm was used.

Aneurysm's size 4-5 mm, CT detection rate would be 3 in 9 = 33%

6-14 mm, CT detection rate would be 17 in 21 = 85%

Table 2. Number of the detected aneurysms by CT scan relating to the time interval between the CT scan performed and the episode of the subarachnoid hemorrhage

Time interval from SAH episode and CT scan performed (days)	No. of aneurysms by Angio and Surg.	No. detected by CT	
		No.	%
0	3	2	67
1	11	5	46
2	2	1	50
3	2	1	50
4	2	2	100
5	3	2	67
6-9	—	—	—
10	3	3	100
11	—	—	—
12	1	1	100
13	—	—	—
14	1	1	100

Note; time interval day 0-3, CT detection rate would be 9/18 = 50%
4-14, " 9/10 = 90%

Table 3. The number of detected aneurysms by CT scan according to the location of the aneurysms

Location of the aneurysms	No. of aneurysm by Angio & Surg.	Detection by CT scan	
		No.	%
Anterior communicatiing a.	14	9	64
Posterior communicating a.	5	2	40
Internal carotid a.	3	2	66
Middle cerebral a.	6	5	83
Basilary tip	2	2	100

Discussion

The overall detection-rate of the non-giant aneurysms by routine CT scan in our series was 66.7% which was not as low as that mentioned by Ghoshhajra et al (2). The detection rate rised to 81% if the size of the aneurysms were between 6-14 mm, which were the size of the major aneurysms that ruptured (10). The accuracy of high resolution axial CT in the diagnosis of cerebral aneurysms 3 mm and larger has been reported at about 97% (6).

CT could detect 18 aneurysms in 28 cases of subarachnoid hemorrhage in our series (64%). The CT detection rate for the interval of 0-3 days from the SAH episode to the performed CT, would be 50% (9 in 18 aneurysms) and the rate of detection would rise up to 90% after the 4th day (9 in 10 aneurysm), due to the decreased blood attenuation in the subarachnoid space and render the aneurysms to be more obvious. The detection of the aneurysms in the absence of subarachnoid hemorrhage was very successful in our 2 cases. (detection rate = 100%) Delayed CT scanning after the episode of subarachnoid hemorrhage would be another way to detect the ruptured aneurysms.

The highest detection rate of the aneurysms by CT scans was obtained when the aneurysms were at basilary tip and middle cerebral a. which represented 100% and 83% respectively. The detection rate of the aneurysms of other arteries of the circle of Willis detected by CT scan was approximately equal. Ghoshhajra et al (2) reported highter detection rate at anterior and middle cerebral arteries (76%). Because of the close relationship between the aneurysms at the supraclinoid internal carotid artery (ICA), ICA bifurcation and posterior communicating artery, precisely locating the origin of the aneurysm from the ICA complex was impossible by CT alone. Confirmation by angiography or surgical findings was necessary. The aneurysms at the junction of the anterior cerebral artery and the anterior communicating artery were the most frequent ones found to be ruptured, similar to other reports (11).

Looping vessels and non-identical cuts of the plain and post intravenous enhanced studies might give the false positive findings by CT scan.

In conclusion; routine CT scan of the brain could detect 64% of the ruptured aneurysm and 100% of the unruptured aneurysm. The detection rate was high after 4 days from the onset of the subarachnoid hemorrhage due to decreased blood density in the subarachnoid space. The aneurysms at the basilar tip were the easiest ones to be detected, followed by those at the middle cerebral artery. The detection rate would be up to 81% if the size of the ruptured aneurysms were 6 mm or larger.

References

1. Inoui Y, Saiwai S, Miyamato T, et al: Post contrast computed tomography in subarachnoid hemorrhage from rupture aneurysms. J Comput Assist Tomogr 1981; 5: 341-344
2. Ghoshhajra K, Scotti L, Marasco J, et al: CT detection ofintracranial aneurysm in subarachnoid hemorrhage, AJR 1979; 132: 613-616
3. Liliequist B, Lindquist M, Valdimarsson E: Computed tomography and subarachnoid hemorrhage. Neuroradiology 1977; 14: 21-26
4. Lim ST, Sage DJ: Detection of subarachnoid blood clot and other thin flat structures by computed tomography. Radiology 1977; 123: 79-84
5. Silver AJ, Pederson ME, Ganti SR, et al : CT of subarachnoid hemorrhage due to ruptured aneurysm. AJNR 1981; 2: 549-552
6. Schmid U, Steiger HJ, Huber P: Accuracy of high resolution computed Tomography in direct diagnois of cerebral aneurysms. Neuroradiology 1987; 29: 152-159
7. Asari S, Sato T, Sakurai M, et al: Delineation of unruptured cerebral aneurysms by computerized angiotomography. J Neurosurg 1982; 57: 527-534
8. Newell DW, Leroux PD, Dacey RG, et al: CT infusion for the detection of cerebral aneurysms. J Neurosurg 1989; 71: 175-179
9. Nehls DG, Flom RA, Carter LP, Spetzler RF. Multiple intracranial aneurysms: determining the site of rupture. J Neurosurg 1985; 63: 342-348
10. McCormick WF, A Costa-GJ: The size of intracranial saccular aneurysm: An autopsy study. J Neurosurg 1970; 33: 422-427

January - April 1995 Volume 1 Number 1

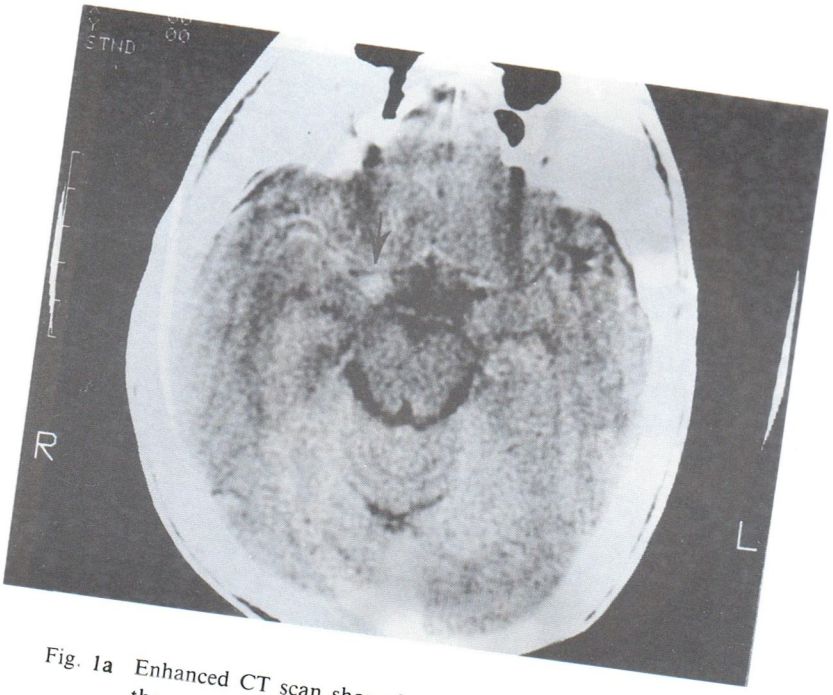

Fig. 1a Enhanced CT scan showed enhanced small nodule at the rt margin of the suprasellar cistern-aneurysm of distal rt internal carotid artery.

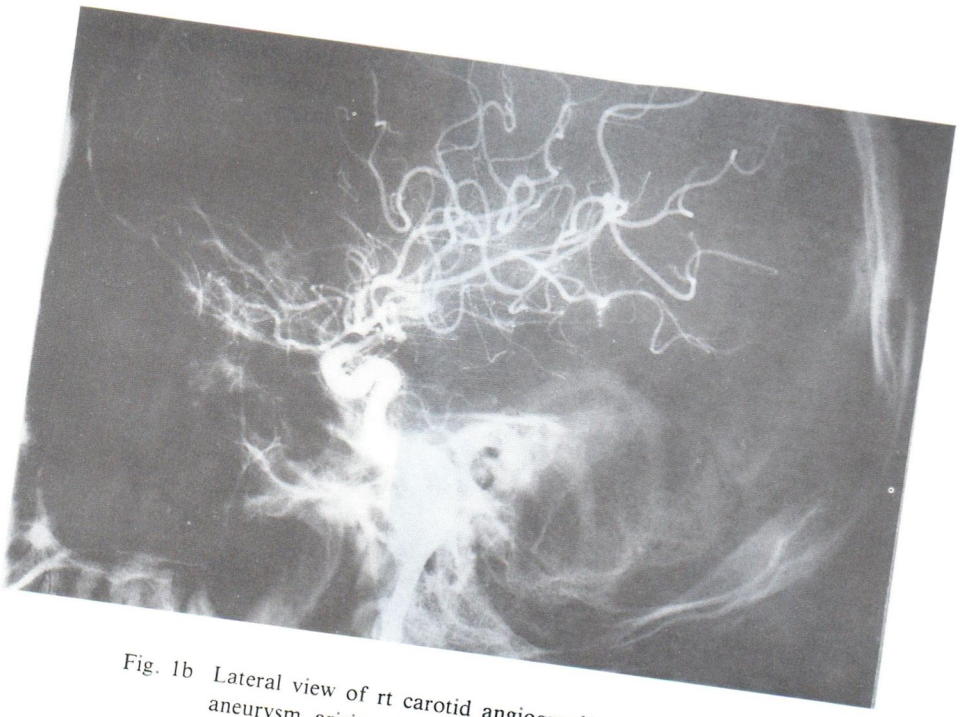

Fig. 1b Lateral view of rt carotid angiography showed small aneurysm arising from posterior part of rt internal carotid a., difficult to differentiate from posterior communicating a. aneurysm.

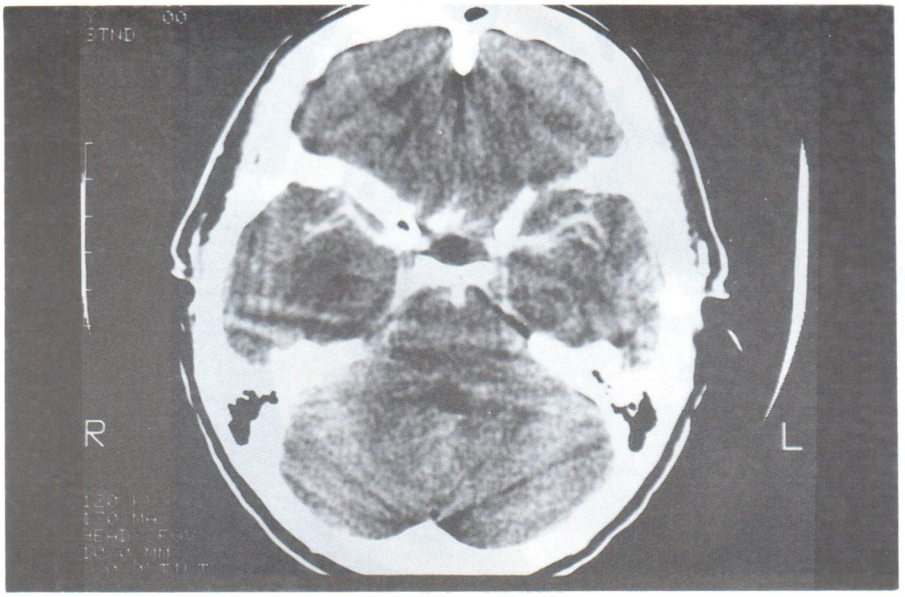

Fig. 2a Enhanced CT scan of the brain at suprasellar area showed enhanced nodule at anterior rt paramedian area of immediate suprasellar region-aneurysm of anterior communicating artery

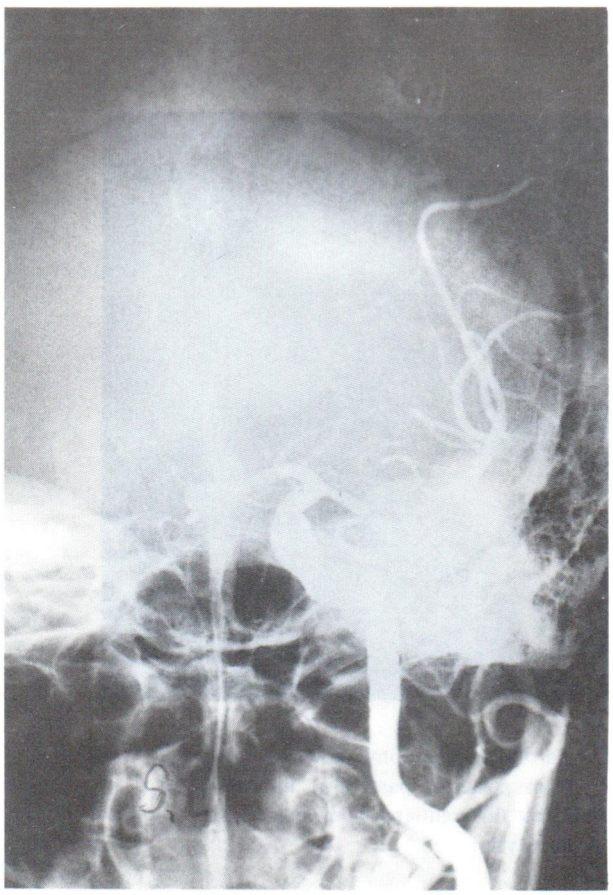

Fig. 2b Left carotid injection showed lobulated aneurysm at anterior communicating artery.

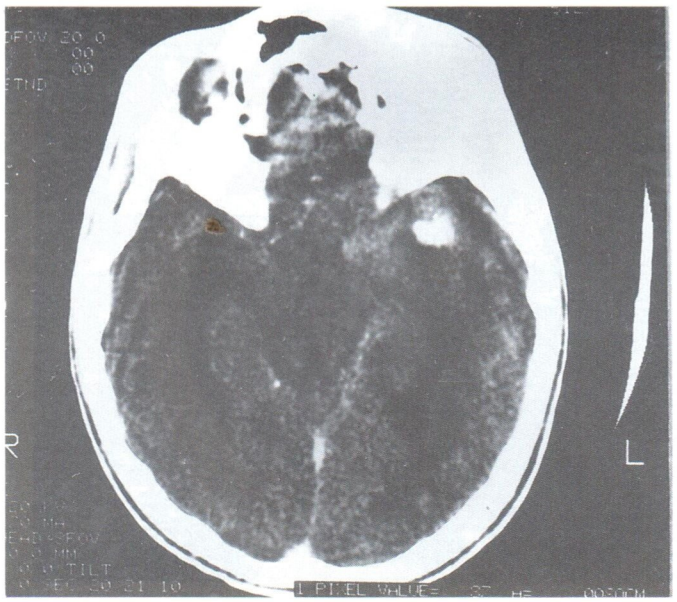

Fig. 3a Enhanced CT scan of the brain showed enhanced nodule at anterior-inferior portion of left temporal fossa-aneurysm of left middle cerebral a.

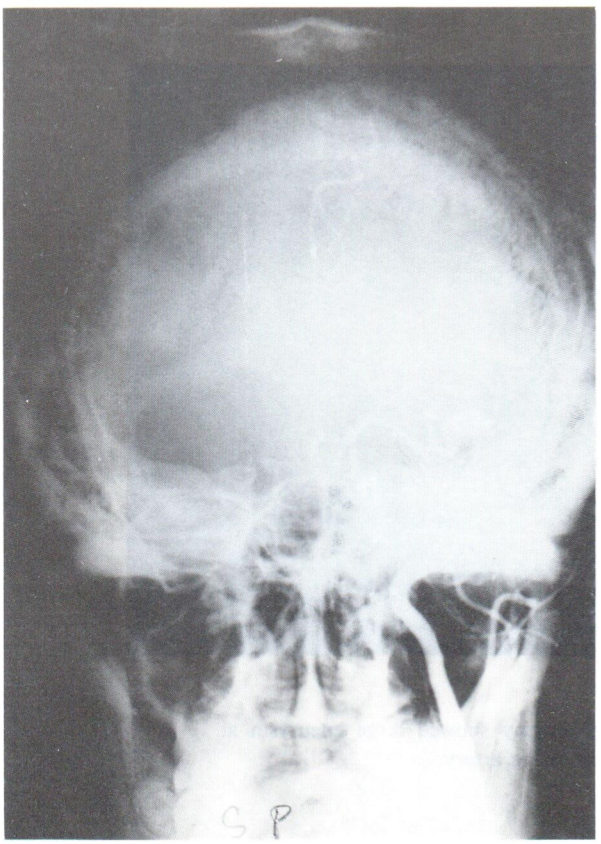

Fig. 3b Left carotid injection showed aneurysm arising from genu of left middle cerebral artery.

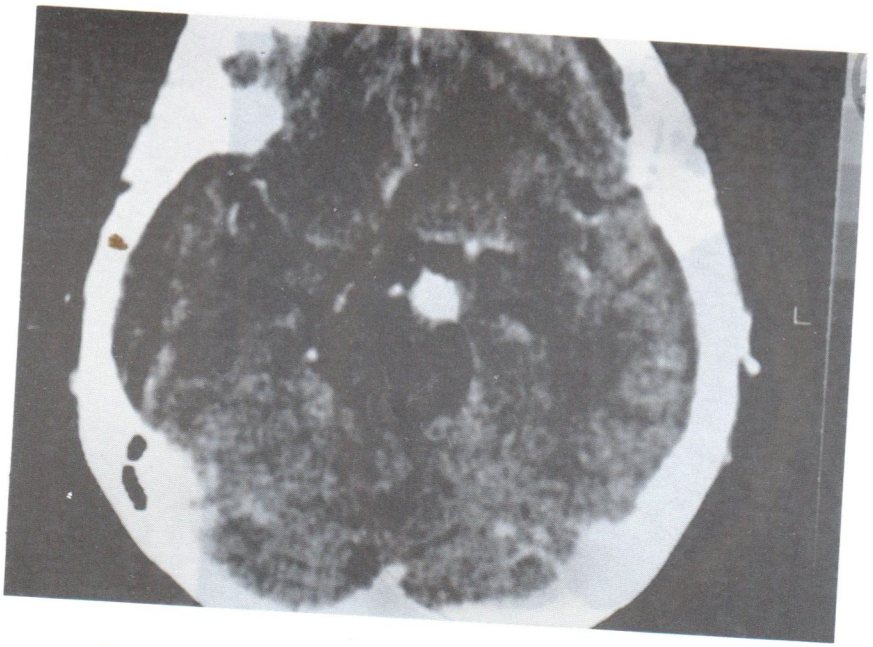

Fig. 4a Enhanced CT scan of the brain showed enhanced nodule at left posterior corner of the suprasellar cistern-aneurysm of posterior communicating artery.

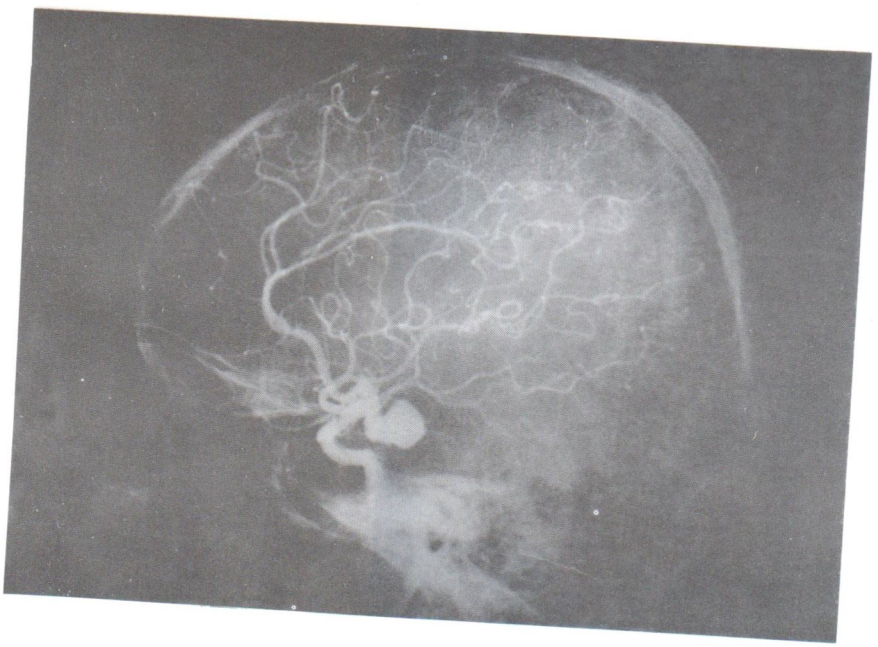

Fig. 4b Left carotid angiography showed large aneurysm at posterior communicating artery.

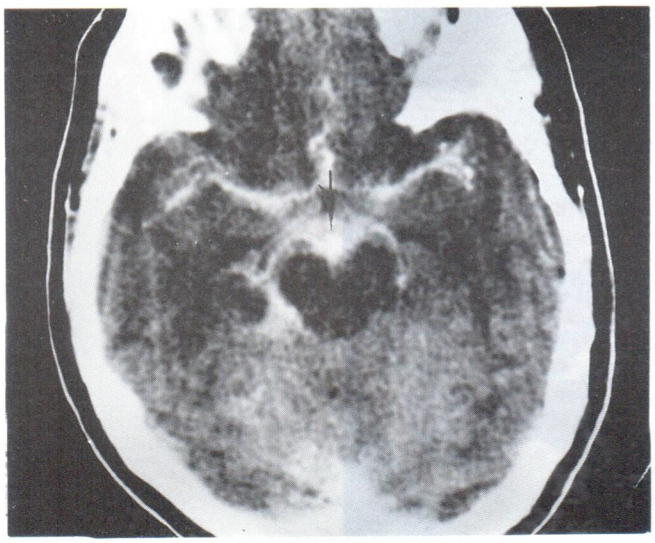

Fig. 5a Plain CT scan of the brain showed subarachnoid blood at suprasellar cistern and rt perimesencephalic cistern-aneurysm of basilar tip.

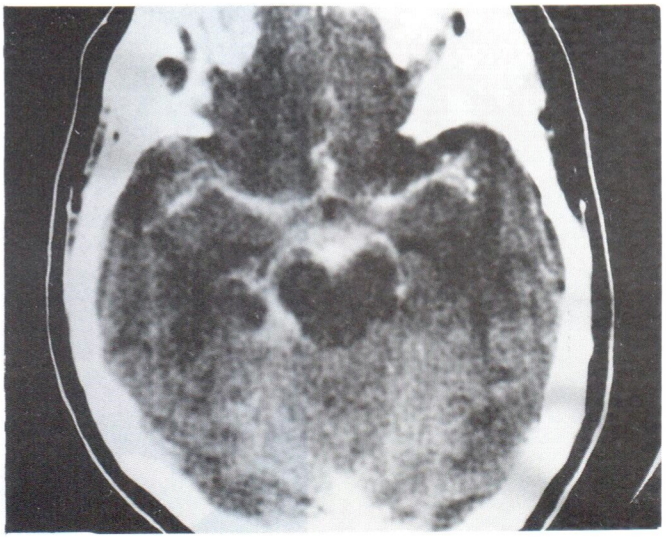

Fig. 5b Enhanced CT scan of the brain showed enhanced nodule at midline of posterior aspect of suprasellar cistern-aneurysm of basilar tip.

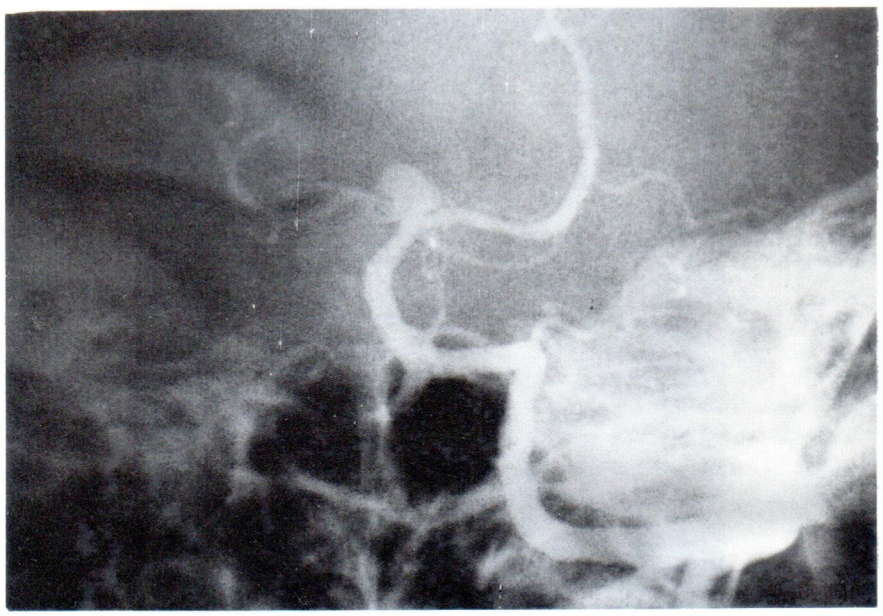

Fig. 5c Left vertebral injection showed lobulated aneurysm at basilar tip.

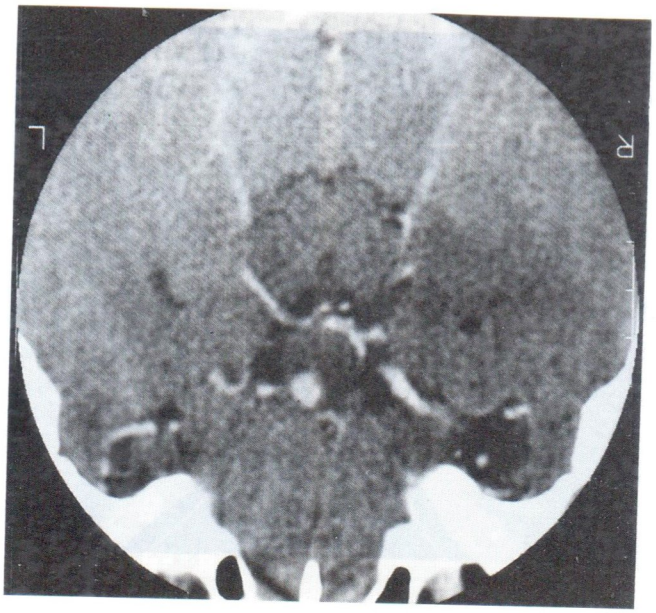

Fig. 6a Enhanced CT scan of the brain showed enhanced small nodule at left paramedian area of the suprasellar cistern-looping of anterior cerebral a.

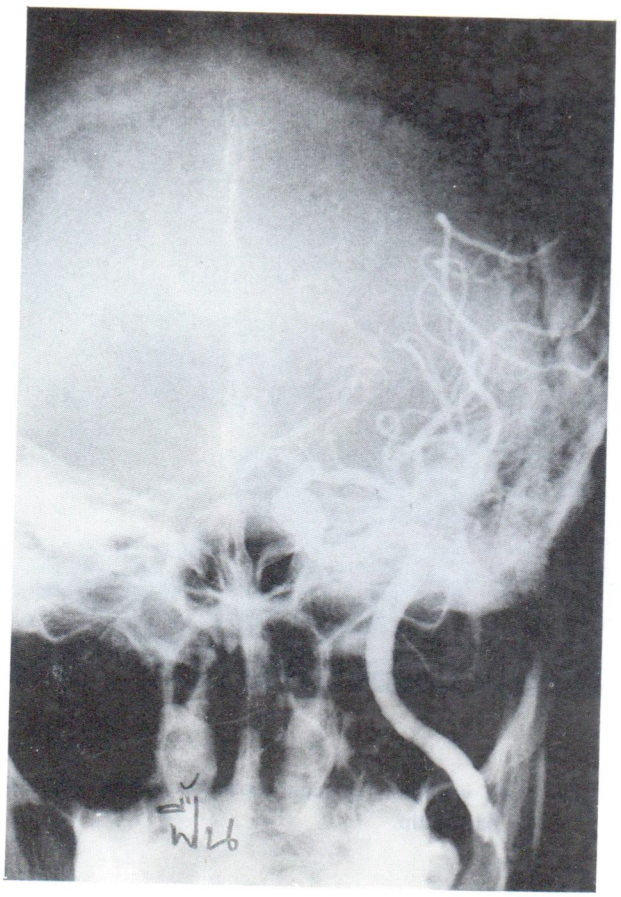

Fig. 6b Left carotid injection showed looping vessel of lt ACA, simulating aneurysm in CT scan.

CT FINDINGS OF BRAIN-INFECTIONS IN THE HIV-POSITIVE PATIENTS WITH THE CORRELATED PATHOGENS

C. Chaisirirat[1], P.Pekanan[1]

Summary. Sixty HIV-positive patients admitted because of brain infection. Cryptococcosis, toxoplasmosis and tuberculosis were the main infectious processes. Twenty-eight cases had CT brain images. Causing organism of the neurological problems were verified by CSF-culture, CSF-PCR and serum titer. Every case showed a good response to the treatment. Fifteen patients had cryptococcosis; 60% showed normal pattern, 20% showed mild atrophy, 6.7% showed mild hydrocephalus, abnormal enhancement and enhanced nodule without surrounding edema. Eight cases were toxoplasmosis and all cases presented with multiple ring enhanced lesions with surrounding edema. Three cases had mixed infections of cryptococcosis and tuberculosis and showed normal pattern. One case of tuberculosis showed low density of white matter without nidus and another case showed infarction of the basal ganglia.

Key words: AIDS-Brain computed tomography-Brain infections

The central nervous system is commonly affected in the HIV-positive patients. Approximately forty percents of them have neurological symptoms as the initial presentation (1).

This study described the CT images of the infected brains in the HIV-positive patients. Correlation of the image-patterns with the organisms involved were made.

Materials and methods

From September 1992 to August 1994, 238 AIDS patients were admitted due to various problems. Sixty patients had meningitis and/or infectious processes in the brain parenchyma and/or ventricular systems. Computed tomography of the brains were performed with standard technique, including plain and i.v. contrast enhanced studies, in 28 cases.

The diagnosis of HIV infection was made by both gelatin agglutination test and ELISA test. The diagnosis of the brain infection was made by positive CSF-culture, CSF-PCR, India ink preparation, CSF-gram stain, CSF-AFB-stain, CSF-crypto-antigen, and serum toxo-titer. Every diagnosed case showed a good response to the specific treatment for that pathogen.

*Deparment of Radiology, Ramathibodi Hospital, Bangkok, Thailand

Results

Various infectious processes involving brains of 60 AIDS-patients was shown in Table I. The age of the patients who had CT scans performed varied from 21 to 56 yrs. old. There are 13 cases (46%) ages between 21-30 yrs, 11 cases (39%) ages between 31-40 yrs. 4 cases (14%), ages between 41-50, and 1 cases (41%) ages between 51-56 yrs.

The causative pathogens, CT patterns and numbers of the patients were shown in Table 2. Examples of the lesions of toxoplasmosis were shown in Fig 1. Abnormal enhancement and small enhanced nodule of cryptococcosis were seen in Fig. 2, Fig. 3 and Fig. 4. Low density white matter lesion and ganglionic infarction in tuberculous cases were shown in Fig. 5 and Fig. 6 respectively.

Neurological manifestations included headache, fever, seizure, hemiparesis, and stiff neck. Most of the cases presented with neurological problems as the first episode and the HIV-infected condition was made known at the time of the admission. Duration of the illnesses from the onset to the admission time was 3 days to 2 months, mostly 2-3 weeks.

Discussion

Infectious processes involving brains were seen in 25% of all admitted AIDS-patients (60 in 238 patients). Cryptococcosis appeared in 62% of our cased with brain infection (60 cases) but occurred in only 6% of 35 infectious cases, reported by Levy et al in 1986 (2). Toxoplasmosis appeared more (77%) in his report comparing with 17% in our series. Tuberculosis were seen in 10% of our cases but none in Levy's cases. This probably reflected the changing of the prevalence of the causative organisms in the 1990 or reflected different behavior of the infectious processes in the different parts of the world.

Normal CT pattern was the most common finding in cryptococcosis, in our series (64%) and in Papovich's cases (43%) (3). Brain atrophy occurred less in our series (14%), compared with that in Tien's series (45%) (4), in Mathews cases (44%) (5) and in Papovich's cases (34%). The difference was probably due to short duration of the illnesses from the onset of symptoms to the admission day and/or due to the first attack of brain infections in most of our patients. In addition, most of the patients were young, i.e. 85% were less than 40 yrs. old. Focal lesioin in the form of enhanced small nodule withiout surrounding edema was shown only 7% in our cases, 17% in Tien's series and 11% in Paovich's series. It appeared in more percentage in Mathews' cases (44%); however his involving cases with CT study were not many. The lack of surrounding edema was in corresponding with those found in other series.

Abnormal enhanced pattern in cryptococcosis was seen as illdefined border areas of atchy enhancement, shown at both putamen, and vermis, were probably more than 3 mm cryptococcomas, described in Mathews' article (5). These lesions diasppeared after treatment in our series.

Abnormal meningeal enhancement was seen in only one case in our series at supracerebellar cistern, and was also less seen in the reports of Mathew (5), Tien (4) and Chag (6). This enhancement occurred together with abnormal enhanced parenchyma and increased enhancement of the choroid plexus, probably reflected more extensive infection in this patient.

Enlarged and intense enhancement of the choroid plexus was shown at both sides of posterior horns of lateral ventricle in one case. Similar findings at choroid plexus of the temporal horns of this infectious process of cryptococcosis, was described in two cases studied by MRI enhanced study, reported by Nicholas (7). However, there was no CSF entrapment as in his cases.

MRI studies was not performed in our institution in these AIDS-brain infectious cases. They did CT studies just to detect focal lesions, so that we did not have such MRI cases. MR was more effective than CT in detecting dilated perivascular spaces and cryptococcomas (5).

All cases of toxoplasmosis in our cases, presented with ring enhanced lesions with surrounding edema which were similar to the reports of LEVY (2), Dina (8). Cases of ring-enhanced lesion with surrounding edema which did not respond to toxolasmosis treatment, could represent other processes, like lymphoma (9) (10) (11) and tuberculosis as was shown in this series though ring lesions are not clearly visualized.

Two cases of tuberculosis were seen as areas of infarction at both basal ganglia and as white matter edema or cerebritis or early abscess formation. Infarction is probably secondary vasculitis.

Interestingly, mixed infections of tuberculosis and cryptococcosis appeared as normal CT findings. This should be explained by mild degree of meningitic forms.

Table 1: Sixty HIV-positive patients, who had brain infections, admitted between September 1992 to August 1994.

INFECTIOUS PROCESSES	No. of PATIENTS Cases % of total HIV.
1. Cryptococcosis	37 (62)
2. Toxoplasmosis	10 (17)
3. Tuberculosis	6 (10)
4. Tuberculosis + Cryptococcosis	2 (3)
5. Tuberculosis + Toxoplasmosis	2 (3)
6. Toxoplasmosis + Cryptococcosis	1 (1.5)
7. Bacterial meningitis	1 (1.5)
8. Meningitis, unknown cause	1 (1.5)

Table 2: Disease processes, CT patterns in 28 cases and numbers of patients in each process

Disease processes	**CT patterns**	**No. of patients (%)**
Cryptococcosis	Normal	9/15 (60)
	Mild atrophy	3/15 (20)
	Mild hydrocephalus	1/15 (6.7)
	Abnormal enhanced area at vermis, basal ganglia, meningeal enhancement at sup. cerebellar cistern and enlarged enhanced choroid plexus of lat. ventricles	1/15 (6.7)
	Small enhanced nodule without surrounding edema	1/15 (6.7)
Toxoplasmosis	Ring enhanced lesions with surrounding edema	8/8 (100)
Cryptococcosis + tuberculosis	Normal	3/3 (100)
Tuberculosis	Low density of white matter without enhanced nidus	1/2 (50)
	Ganglionic infarct	1/2 (50)

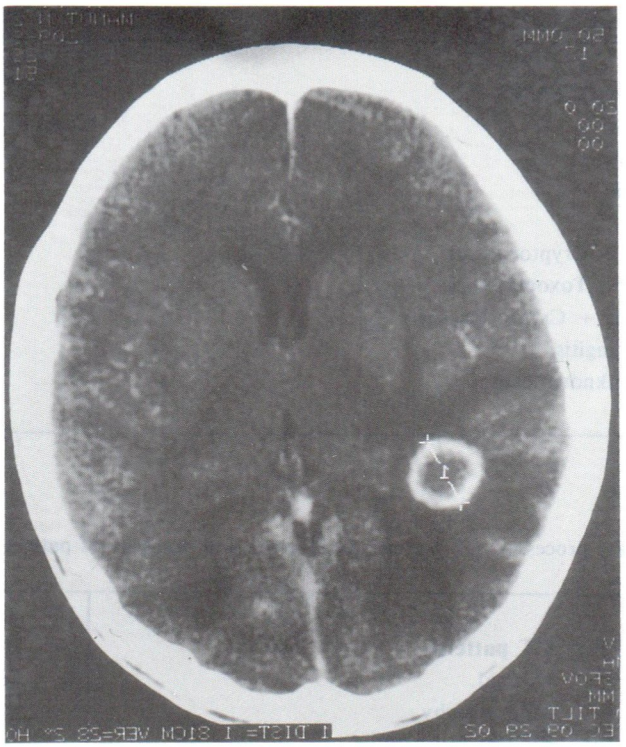

Fig. 1. Enhanced CT scan showed a ring enhanced lesion with surrounding edema in toxoplasmosis

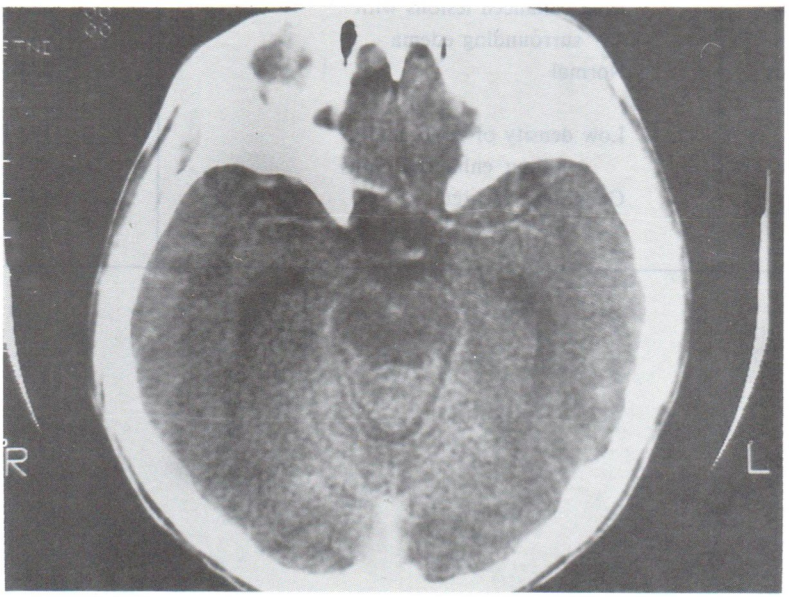

Fig. 2. Enhanced CT scan showed enhanced tentorial and supra-cerebellar cistern meninges, in cryptococcosis

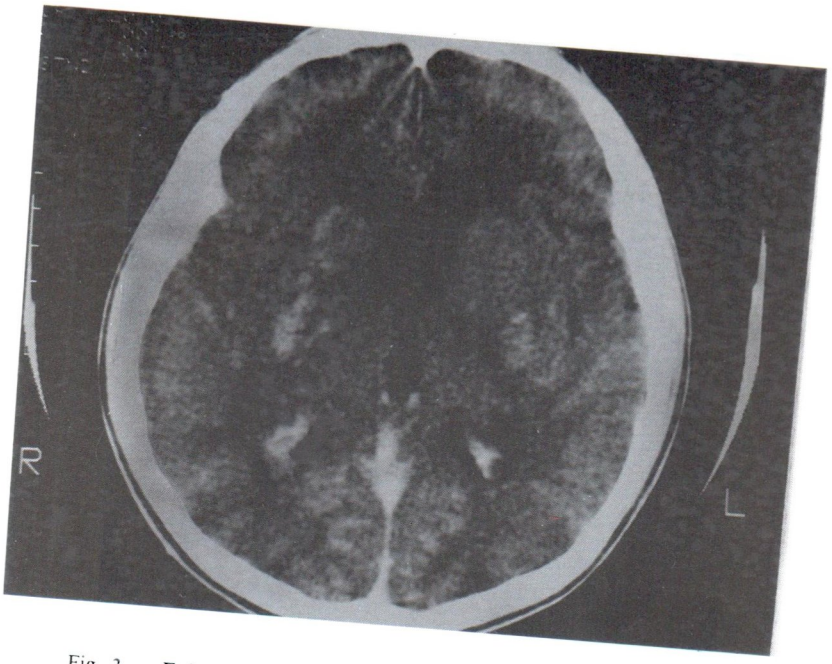

Fig. 3. Enhanced CT scan showed patchy enhancement of both sides of basal ganglia and enlarged enhanced choroid plexus of both posterior horns, in cryptococcosis

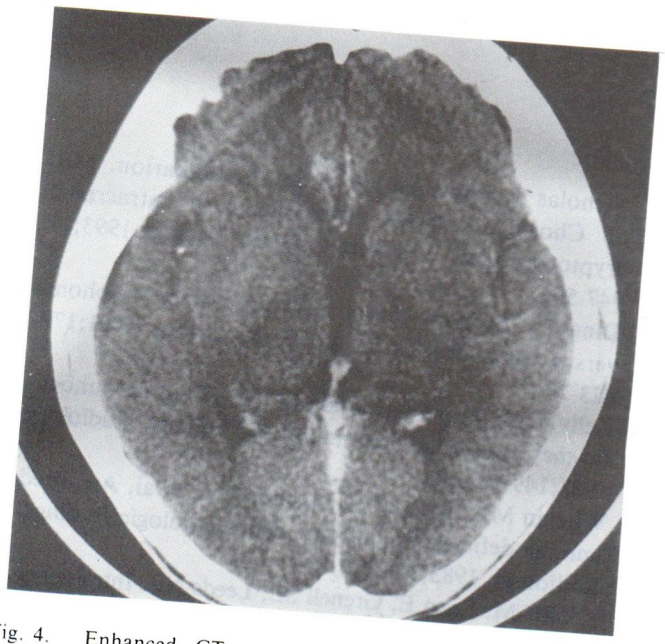

Fig. 4. Enhanced CT scan showed enhanced small nodule without surrounding edema at right genu of Corpus Callosum, in cryptococcosis

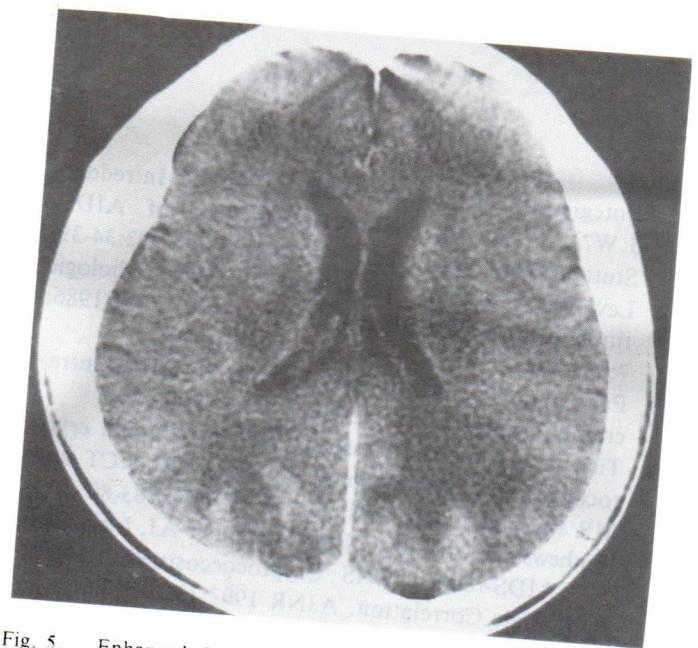

Fig. 5. Enhanced CT scan showed low density of white matter of both parieto-occipital lobes without enhanced nidus lesion, in tuberculosis.

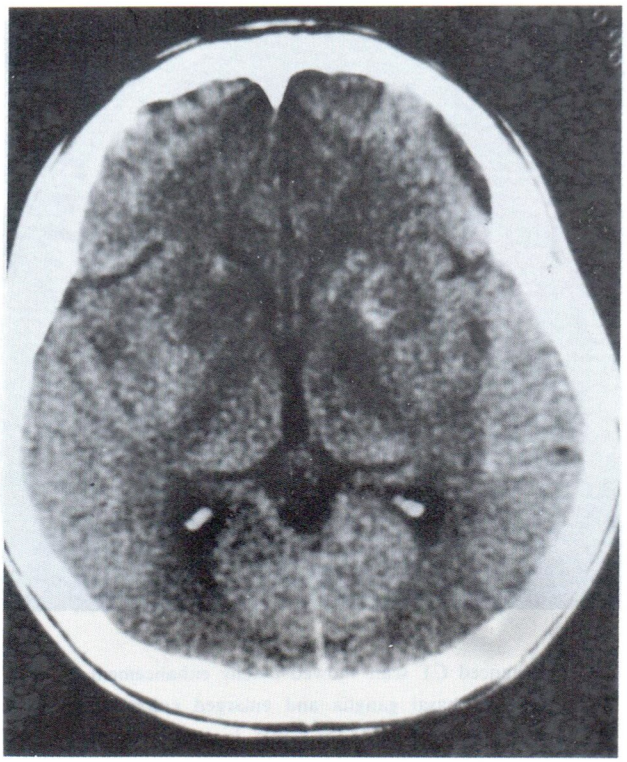

Fig. 6. Enhanced CT scan shows enhanced infarction at both basal ganglia, in tuberculosis.

References

1. Potegies P. Clinical neurology of AIDS. In:redders J.W.A.J., et al Diagnostic imaging of AIDS. Stuttgart New York:Georg Thieme Verlag,1992:34-39.
2. Levy RM, Rosenbloom S, Perrett CV. Neuroradiologic findings in AIDS:A review of 200 cases. AJNR 1986; 7:833-39.
3. Papovich MJ, Arthur RH, Helmer E. CT of intracranial cryptococcosis.AJNR 1990;11;139-42.
4. Tien RD, Chu PK, Hesseling JR. Intracranial cryptococcosis in immunocompromised patients:CT and MR findings in 29 cases. AJNR 1991;12:283-89.
5. Mathews VP, Alo PL, Glass JD, Kumar AJ, McArthur JC. AIDS-related CNS Cryptococcosis:Radiologic-Pathologic Correlation. AJNR 1992;13:1477-86.
6. Chang KH, Han MH, Roh JK, KIm IO, Hans MC, Kim C-W. Gd-DTPA enhanced MR imaging of the brain in patients with meningitis. Comparison with CT. AJNR 1990;11:69-76.
7. Nicholas J, Patronas and Erini V, Makariou. MRI of Choroidal Plexus involvement in intracranial cryptococcossis. J Comput Assist Tomogr.1993;17: 547-50.
8. Dina TS. Primary central nervous system lymphoma versus toxoplasmois in AIDS. Radiology 1991;179: 823-28.
9. Kelly WM, Brant-Zawadzki M. Acquired immunodeficiency syndrome: neuroradiologic findings. Radiology 1983;149:485-91.
10. Whelan MA, Kricheff II, Handler M, et al. Acquired immunodeficiency syndrome:neuroradiologic findings. Radiology 1983;149:477-84
11. Elkin CM, Leon E, Grenell SL, Leeds NE. Intracranial lesions in the acquired immunodeficiency syndrome: radiological (computed tomographic) features. JAMA 1985;253:393-96.

Mammographic Features of Fat Necrosis

Malai Muttarak, M.D.*, Nimit Martin, M.D.**,
Benjaporn Chiwun, M.D.***

ABSTRACT

Fat necrosis of the breast is a benign, nonsuppurative inflammatory process with variable presentation. Occasionally it mimic malignant lesions both clinically and mammographically. Four cases of fat necrosis are presented which illustrate the spectrum of mammographic features of this condition. The appearances vary from one indistinguishable from carcinoma to single or multiple lucent lesions with ring-like calcification. Biopsy is performed when clinical signs, mammographic findings or clinical history suggest malignancy.

INTRODUCTION

Fat necrosis of the breast is common benign condition that has an extremely variable presentation. It occasionally mimic malignant lesion clinically and mammographically.[1-2] We report 4 cases of different mammographic presentation of fat necrosis. An appreciation of some of these appearances may prevent unnecessary biopsy.

CASE REPORTS

Case 1.

An obese 51-year-old woman had right breast mass with pain for a week. She had no history of breast trauma. Physical examination showed a firm mass in the upper, inner quadrant of the right breast and the overlying skin was dimple. Mammograms revealed a fatty breast and a focal irregular increased density without calcification in the upper, inner quadrant of the right breast (Fig 1). The clinical and mammographic diagnosis of suspicious carcinoma called for excisional biopsy. The pathologic diagnosis was fat necrosis (Fig 2).

Case 2.

An obese 41-year-old woman had mammograms performed for a lump in the left breast for 2 years. First mammograms showed a fatty breast with a 8 mm. circumscribed mass with irregular border in the left breast. Two years later a repeat mammograms showed enlargement of the left breast mass (Fig 3). Excisional biopsy was performed to exclude malignancy and revealed fat necrosis (Fig 4).

Case 3.

A 57-year-old woman had bilateral mammograms for screening. Mammograms showed moderate dense breasts. There were 2 mm. radiolucent cyst with calcified wall, 10 mm. radiolucent cyst with thick calcified wall in the right breast and a 3 mm. radiolucent cyst with calcified wall in the left breast (Fig 5). Follow up mammograms 2 years later showed no significant change of these lesions.

* Department of Radiology, ** Department of Surgery, *** Department of Pathology, Faculty of Medicine, Chiang Mai University, Chiang Mai 50200 THAILAND.

Case 4.

A 73-year-old woman had mammograms performed for screening. There were multiple small radiolucent cysts with calcified wall in both breasts (Fig 6). A repeat examination was done 20 months later showed stability of these lesions.

DISCUSSION

Fat necrosis of the breast is a nonsuppurative inflammatory process that varies in appearance depending on the stage of the lesion.[2] It occurs most often in the fatty, pendulous breasts of middle-aged women. Trauma has been thought to be the primary cause of fat necrosis, although a history of trauma is elicited in only about 40% of cases.[2] A biopsy or other surgical procedure can also lead to fat necrosis.[2-5] Fat necrosis may result from mammary duct ectasia with stagnation of the secretory contents, subsequent effusion of irritative material into the stroma. There is a death of tissue, saponification of fat occurs, leading to the formation of vacuoles. Macrophages are then found surrounding the vacuoles engulfing debris. The necrotic focus may cavitate and the wall of the cavity may calcify. Healing by fibrosis begins at the periphery and eventually may replace the entire area or leave a persistent cystic cavity. Calcification may occur in the necrotic area.[2]

Clinically, the patient may be asymptomatic or present with a mass that may or may not be painful. Associated localized thickening and retraction of skin over the lesion may be present and indistiguishable from carcinoma. Mammographic feature in fat necrosis is variable. They include; (1) a spiculated density often indistinguishable from carcinoma, (2) a circumscribed mass, (3) a poorly defined mass or asymmetric density, (4) localized skin thickening and/or retraction, (5) round, branching, rodlike or angular microcalcification, often resembling those seen in carcinoma, (6) single or multiple cysts, which are often lipid-filled, and may or may not have calcified walls, and (7) any combination of these findings.[1-8]

All our cases had no history of trauma or previous breast surgery. Two cases presented with a lump and mammograms disclosed a mass. Fat necrosis characteristically is situated near the skin or areolar region. In case 1, lesion is closed to skin but lesion in case 2 is deep in the breast. Both cases (1 and 2) are obese and pendulous breasts. Mammographic appearance in case 1 and 2 is indistinguishable from carcinoma, leading us to perform biopsy. Pathologically was not proved in cases 3 and 4 because it represents one of the characteristic mammographic appearances of fat necrosis. Although microcalcification resembling carcinoma is frequent, none could be demonstrated in our patients.

With increasing use of mammography, we can anticipate increasing numbers of fat necrosis. Biopsy of these lesions need not be performed unless other signs, mammographically or clinically, suggest malignancy. Familiarity with the variable appearance of fat necrosis will help to prevent inaccurate interpretations and unnecessary biopsies.

Acknowledgement

We are greatful to professor Dr. Sanan Simarak for reviewing the manuscript.

REFERENCES:

1. Minagi H, Youker JE. Roentgen appearance of fat necrosis in the breast 1968; 62-5.

2. Bassett LW, Gold RH, Cove HC. Mammographic spectrum of traumatic fat necrosis: The fallability of "pathognomonic" signs of carcinoma. AJR 1978; 130: 119-22.

3. Andersson I, Fex G, Pattersson H. Oil cyst of the breast following fat necrosis. Br J Radiol 1977; 50: 143-6.

4. Baber CE, Libshitz HI. Bilateral necrosis of the breast following reduction mammoplasties. AJR 1977; 128: 508-9.

5. Bassett LW, Gold RH, Mirra JM. Nonneoplastic breast calcifications in lipid cysts: Development after excision and primary irradiation. AJR 1982; 138: 335-8.

6. Orson LW, Cigtay OS. Fat necrosis of the breast: Characteristic xeromammographic appearance. Radiology 1983; 146: 35-8.

7. Evers K, Troupin RH. Lipid cyst: Classic and atypical appearances. AJR 1991; 157: 271-3.

8. Leborgne R. Esteatonecrosis quistica calcificada de la mama. Torax 1967; 16: 172-5.

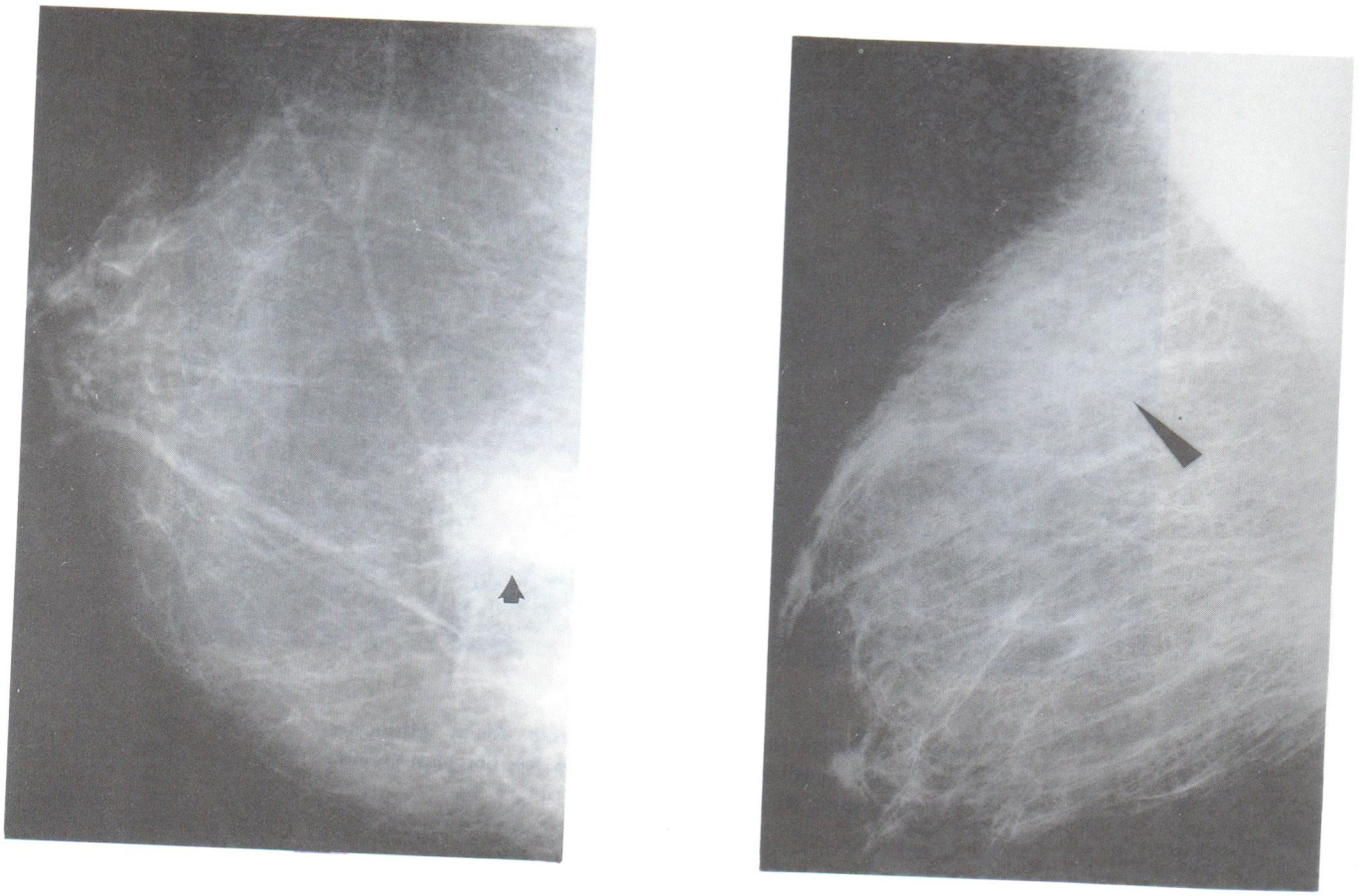

Fig 1 A. craniocaudal, B. mediolateral oblique and C. focal compression mammograms of the right breast show an area of focal irregular increase density (arrow).

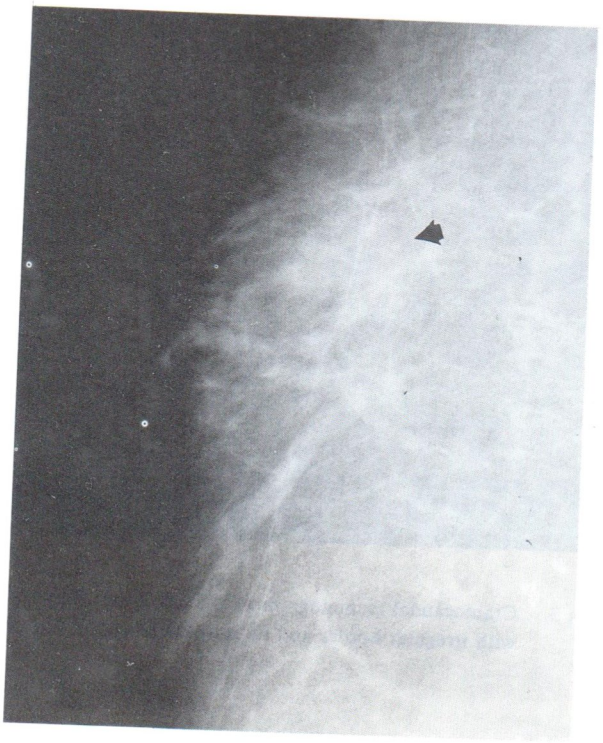

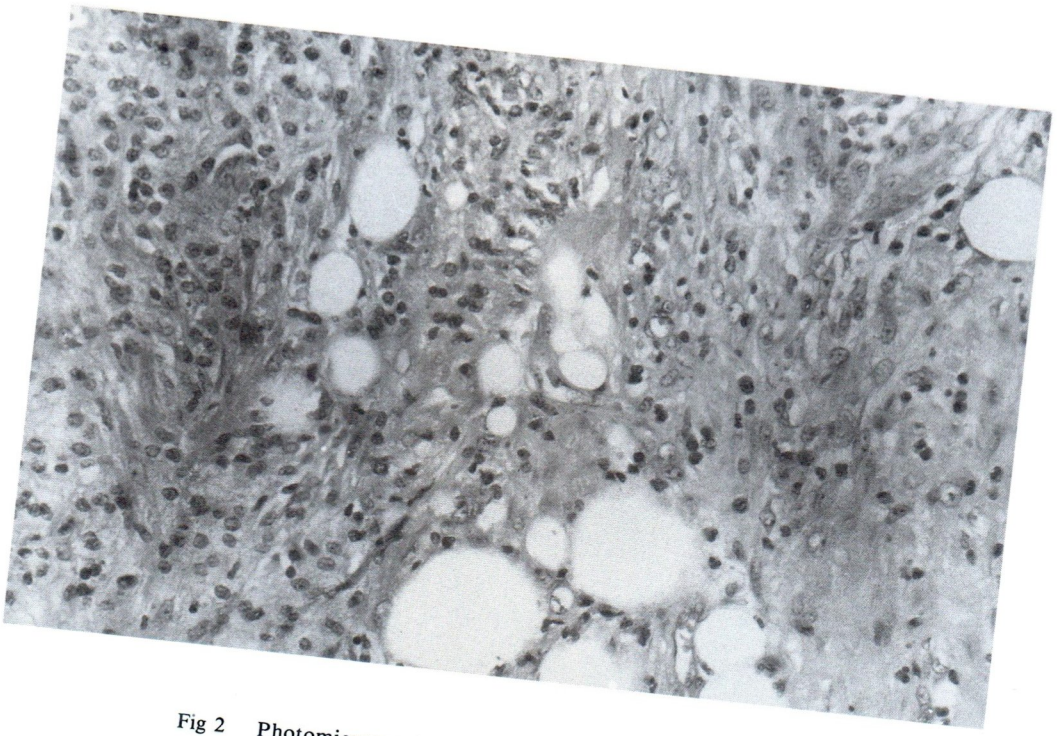

Fig 2 Photomicrograph shows numerous foamy histiocytes intermingling with lymphocytes. A few fibroblast are also evident. (H & E × 200)

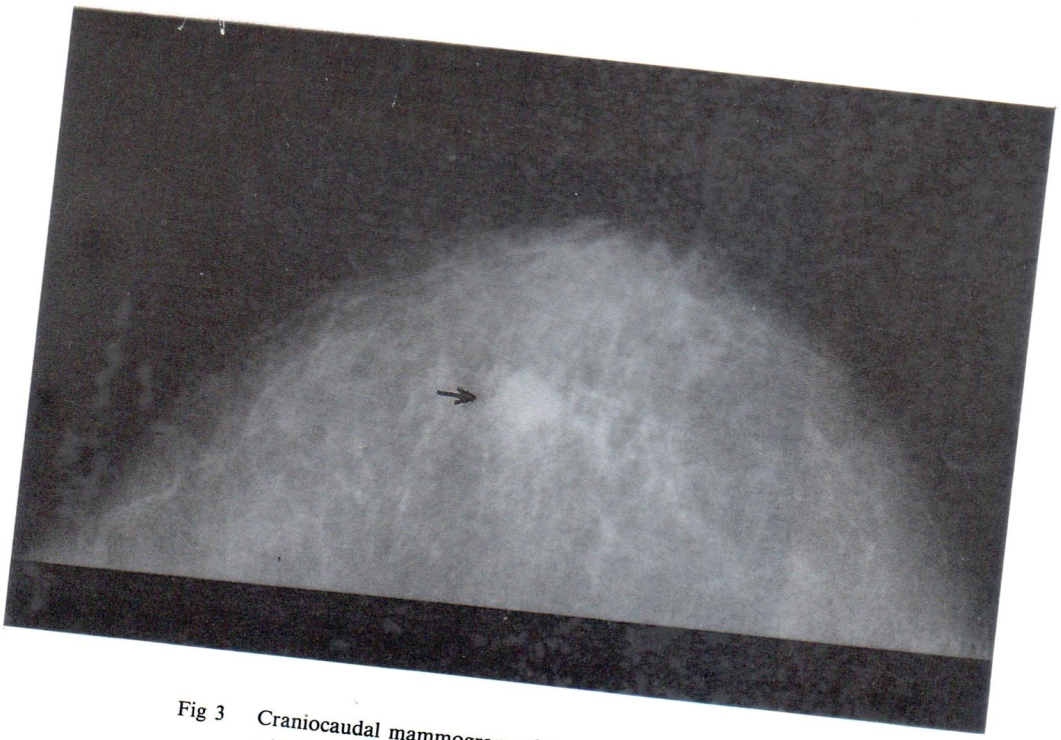

Fig 3 Craniocaudal mammogram of the left breast shows a mass with irregular border and no microcalcification (arrow).

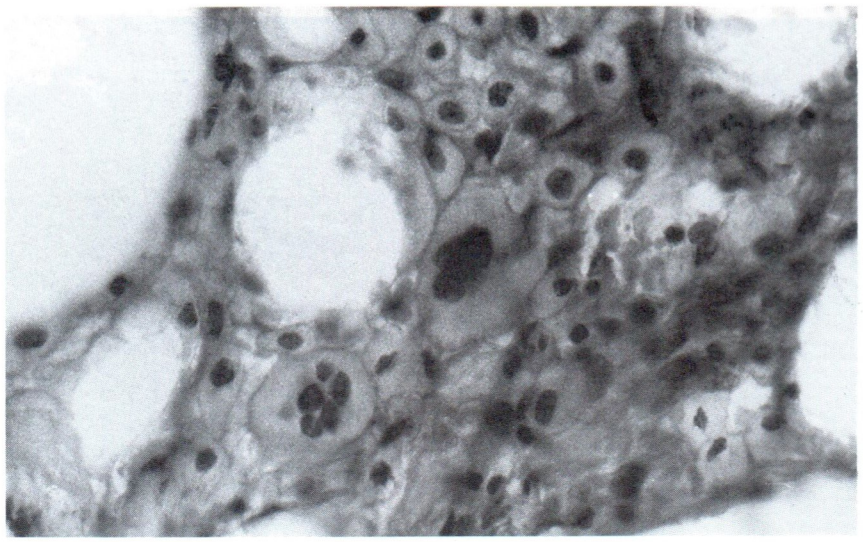

Fig 4 Photomicrograph shows numerous foamy histiocytes surrounding small cystic spaces. A few multinucleated giant cells are also seen. (H & E × 400)

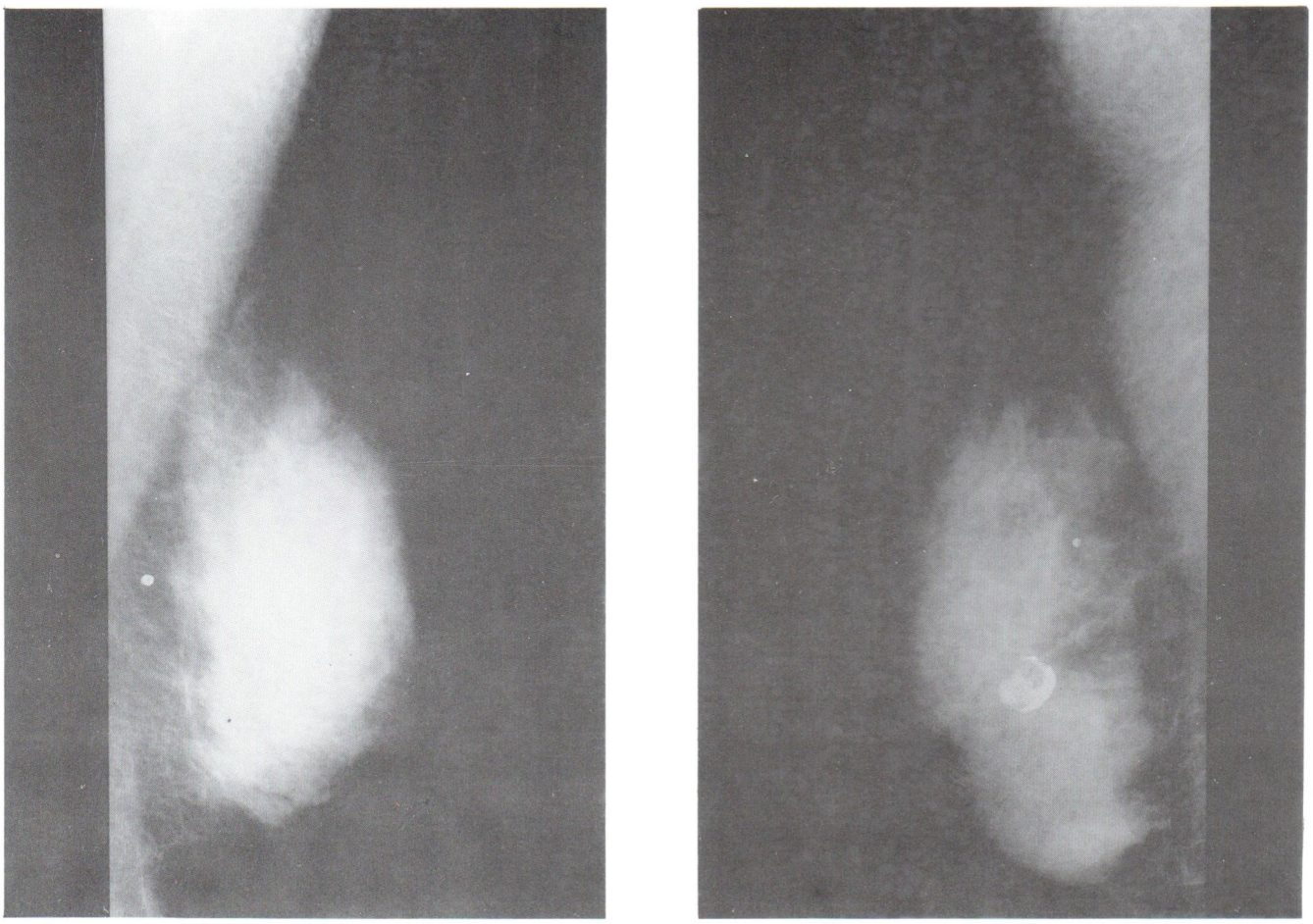

Fig 5 Bilateral mediolateral oblique mammograms A. right and B. left show moderate dense breast for a 57-year-old woman and bilateral calcified radiolucent masses.

Fig 6 Craniocaudal view of the left breast shows multiple small radiolucent cysts with calcified wall.

THE ROENTGENOGRAPHIC FINDINGS OF ORTHOPEDIC MELIOIDOSIS

J. Jatchavala, P. Siriwongpirat, P. Pekanan, B. Sathaphatayavongs

Abstract

The purpose of our study was to describe roentgenographic appearance of Melioidosis in musculoskeletal system, discuss its differential diagnosis and its associated diseases.

We review the conventional radiographs of the 8 proven cases of Melioidosis involving bones and joints on the basis of the type of bony destruction, location and periosteal reaction.

The result of serological analysis, history of associated diseases were discussed.

5 patients with osteomyelitis involved large tubular bones. The types of bony destruction were geographic, permeative, punched-out and mixed permeative and punched-out osteolytic destruction. Most common location was metaphyses.

There are two cases of periosteal reaction, codman and solid buttress.

Of the 2 patients with septic arthritis, larged joints were involved. Roentgenographic findings were joint effusion and bony erosion.

There were variable radiographic features of Melioidosis. Osteolytic destruction with or without periosteal reaction was shown. Lack of reactive sclerosis may not be differentiated from primary or secondary bone tumor and osteomyelitis from other organisms. The roentgen findings of arthritis could not be differentiated from Tbc.

DM was the most common associated disease. Indirect hemagglutinin titer over 1:160 was helpful in the diagnosis.

Key words: The Roentgenographic findings of Orthopedic Melioidosis, geographic, permeative, punched-out and mixed bone destruction. Metaphyses. Periosteal reaction. Effusion. Erosion.

Introduction

Melioidosis, an infectious disease caused by the gram negative bacillus, Pseudomonas Pseudomallei, was first reported in 1912 by Whitmor. (1) It is commonly found in soil and rice paddies of the Southeast Asia and other tropical areas. (1,2) In Thailand, the first case was reported by Chitti Chitivej in 1955. The highest incidence was in the Northeastern part.

There is wide spectrum of the clinical presentation of Melioidosis, range from subclinical to acute fulminating septicemia. (4,5) Multiple organs involvement (6,7) is frequency encountered. The lungs are the site most commonly affected. Musculoskeletal system involvement is rare and usually found in association with infection in other organs. Several reports of the orthopedics Melioidosis has been presented (8,9) but no roentgenographic findings had been illustrated.

The purpose of this study is to describe the roentgenographic appearance of melioidosis in bones and joints and to emphasize the features which may help to differentiate it from other mimicking diseases.

Department of Radiology, Ramathibodi Hospital, Rama VI Road, Bangkok 10400, Thailand.

Patients and Methods

Retrospective analysis of the proven cases of Melioidosis infection of bones and joints were performed during 1985-1989. The diagnosis was made by means of positive culture from pus, bone biopsy, joint effusion or positive serological test (titer ober 1:160).

The conventional radiographs of the involved bones or joints were reviewed, on the basis of the types of bony destruction, location, and periosteal reaction.

RESULT

The result (as in table 1) revealed 5 male and 3 female patients, the age-range was 28-75 years (mean 54.5 years). The majority of the patients lived in the Northeastern part of Thailand. Duration of symptoms ranged from 2 months to 8 months.

Osteomyelitis was diagnosed in 5 cases, involving 2 humerus, 1 femur, 1 tibia and 1 radius. Septic arthritis was diagnosed in 2 cases, involving 2 knees and 2 ankles. Osteomyelitis with septic arthritis in 1 case involved right distal tibia and right femur.

An isolated musculoskeletal system involvement was found in 3 cases (case No.1,2,7) and those associated with systemic infection were seen in 5 cases. (case No. 4,5,6,8)

Diabetes millitus is the most common associated disease. (6 in 8 cases)

Positive Indirect Haemagglutinin (IHA) titer, more than 1:160 was seen in 6 cases (100%)

TABLE 1

No.	Sex/age	Occupation	Clinical presentation	Duration	Associated disease	Positive culture	IHA titer
1	M/43	Northeast	Fever,swelling	8 M	DM		1:160
2	M/28	North	Pain at Rt. hip weight loss	6 M	Asthma	Bone biopsy & culture	
3	M/75	Northeast	Fever, anemia and swelling & pain at Rt. knee & Rt. ankle	2 M		pus from urine & blood	
4	M/55	Northeast	Fever,swelling of Rt. and Lt. ankles, liver abscess, pneumonia,skin pustules	2 M	DM past history of pulm. Tbc.	joint eff. from Lt. ankle & blood	1:320
5	F/57	Northeast	Fever, Lt. ankle pain sepsis and pneumonia	2 M	DM		1:1280
6	M/66	Northeast	Pain chronic ulcer at Rt. forearm swelling Lt. ankle	3 M	pus from osteomyilitis at Rt. forearm		1:320
7	F/62	Northeast	Fever,pain & swelling at Rt. arm	3 M	DM	bone biopsy & C/S	
8	F/50	Northeast	Fever,pain at Rt. knee	3 M	DM	joint effusion & blood	1:640

TABLE 2

Case No.	Bone or joint involved	Roentgen findings
1.	Rt.	Permeative and punched out bony destruction at superior medial aspect of humerus including its neck with Codman periosteal reaction. Normal glenoid cavity
2.	Rt. femur	Well-defined geographic bony destruction of the intertrochanteric region with sharp border.
3.	Rt. knee	Bony erosion of lateral femoral condyle and lateral tibial condyle.
	Rt. ankle	Degenerative change with effusion and small osteolytic lesion at distal fibula.
4.	Lt. ankle	Joint effusion, no bony destruction
5.	Lt. tibia	Permeative bony destruction of distal tibia. Normal joint space.
6.	Rt. distal radius	Punched out osteolytic lesion at radial side, no periosteal reaction. Periarticular osteoporosis.
7.	Rt. humerus	Muliple, punched-out osteolytic expansile destruction involved metaphyses and diaphyses. Solid, buttress periosteal reaction.

Roentgen findings

Osteomyelitis

Patterns of bony destruction

Geographic destruction (case 2 fig 1)

Punch-out osteolytic destruction (case 6 fig 2, case 7 fig 3)

Permeative destruction (case 5 fig 4, case 8 fig 5)

Mixed permeative and punch-out osteolytic destruction (case 1 fig 6)

Periosteal reaction

Codman (case 1 fig 6)

Solid-buttress (case 7 fig 3)

Septic arthritis

Bony erosion (case 3 fig 7)

Joint effusion (case 4 fig 8)

DISCUSSION

The clinical presentation, bacteriological, radiological and pathological findings of melioidosis may imitate many diseases. In respiratory system (10), radiographic findings of acute septicemic form may not be able to diferentiated from staphylococcal infection and in chronic form may resemble chronic pulmonary tuberculosis (7)

Musculoskeletal system symptoms may also accompany either the primary infection or disseminated disease. Bone and joint involvement in melioidosis is rare. In this sudy, osseous lesions were single and involved long tubular bone, particularly metaphyseal location. Radiologically, the lesions consisted of geographic, permeative, punched-out osteolytic destruction with or without periosteal reaction. Lack of reactive bone sclerosis is possibly the characteristic of the disease.

The geographic osteolytic destruction has well defined border without sclerotic margin. This pattern of bony destruction may be diffiult to differentiate from metastases (11), or primary bone tumor such as giant cell tumor, or Brown tumor. Clinical and chemical analysis were required. The epiphyseal or diaphyseal involvement may be helpful in the differential diagnosis.

The permeative destructive pattern may resemble osteomyelitis from other causes (12)

The punched-out osteolytic and mixed punched-out and permeative osteolytic destruction may resemble bony destruction from fungal infection, such as coccidiomycosis (12,13)

Septic arthritis in melioidosis is possibly less frequent than osteomyelitis, ankle and knee may be the most common site. Radiographs of the involved articulation

revealed effusion and marginal erosion. These findings could not be differentiated from arthritis caused by other pathogens such as tuberculosis. (12,13)

Our study confirmed previous reports that DM was the most common underlying disease. However there is no remarkable influence on the severity of the isolated articular melioidosis. (8)

The history of living in endemic area should arouse the suspicious of the disease.

Indirect hemagglutinin titer over 1:160 is helpful in the diagnosis.

REFFERENCE

1. Minick G, Zimmerman HM, Maner Go, Humphy AA. Melioidosis on Guam. JAMA 1947;130:1063-1067.
2. Rubin HL, Alexander AD, Yager RH. Melioidosis. A military medicine problem Milit Med 1963;128: 538-542.
3. Chittivej C, Buspavanij S, Chaovanasai A. Melioidosis with case report in a Thai. (English abstract) Roy Thai Army Med J 1955;8:11-8.
4. Reeder MM, Palmer PES. Melioidosis In: Reeder MM, Palmer PES, eds. The radiology of tropical diseases. 1st ed Baltimore: Williams & Wilkings 1981;595-622.
5. Cooper EB. Melioidosis. JAMA 1967;200:452-453.
6. Dhiensiri T, Puapairoj S, Susaenrat W. Pulmonary Melioidosis: Clinical-Radiologic Correlation in 183 cases in Northeastern Thailand. Radiology 1988; 166:711-715.
7. Cowsuwan W, Mahakkanukrauh C, Tassanavipas A, et al, Melioidosis in orthopedics J Bone Joint Surg (Am) 1993;108-112.
8. Saengnipathkul S. Laupattarakaserm W, Kowsuwon W, Mahaisavariya B. Isolated Articular Melioidosis Clin Ortho Rel Res. 1991;267:182-185.
9. Boonma P, Puapairoj A, Nanagura R, et al. The pelvic bone infection of meloioidosis: a report on tour cases. Intern Med 1988;4:112-115.
10. Punyagupta S. Melioidosis: The great imitator. Ramathibodi Med J 1983;6:147-153.
11. Resnick D, Niwayana G: Skeletal metastasis. In diagnosis of bone and joint disorders 2nd Edition p 9946-4010 WB Sauders company Philadelphia 1988.
12. Resnick D, Niwayama G: Osteomyelitis, septic arthritis and soft tissue infection: The organisms. In diagnosis of bone and joint disorders 2 nd edieion p WB sanders company Philadelphia 1988.
13. Theros G, Elias, Siogel A Barry: Bone disease (Fourth series) Test and syllabus p 554-555 Reston Virginia 1989.

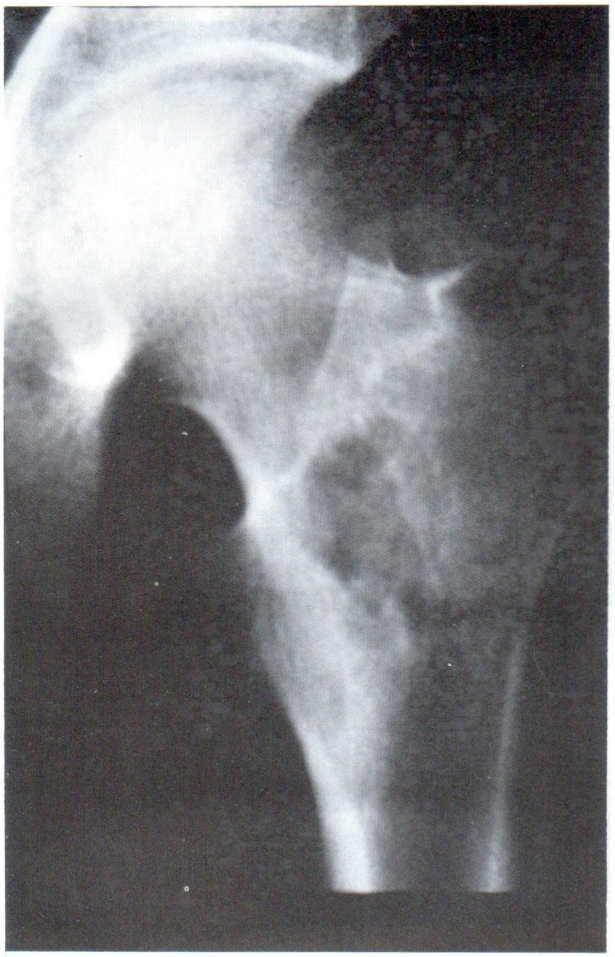

Fig.1 Case 2. 28 yr-old male with rt. hip pain and weight loss. Conventional radiograph of the pelvis shows well defined geographic osteolytic destruction of the intertrochanteric region of rt femur with sharp border

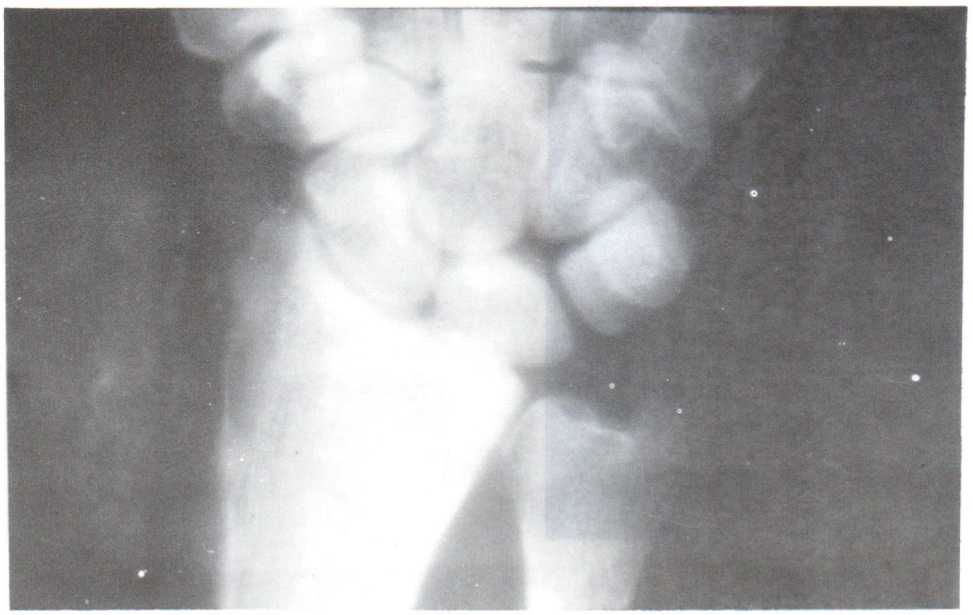

Fig.2 Case 6. 66 yrs-old male with chronic ulcer at rt. forearm. Conventional radiograph of Rt. forearm shows punched-out osteolytic destruction at radial side of Rt. distal radius without periosteal reaction. Periarticular osteoporosis is also noted.

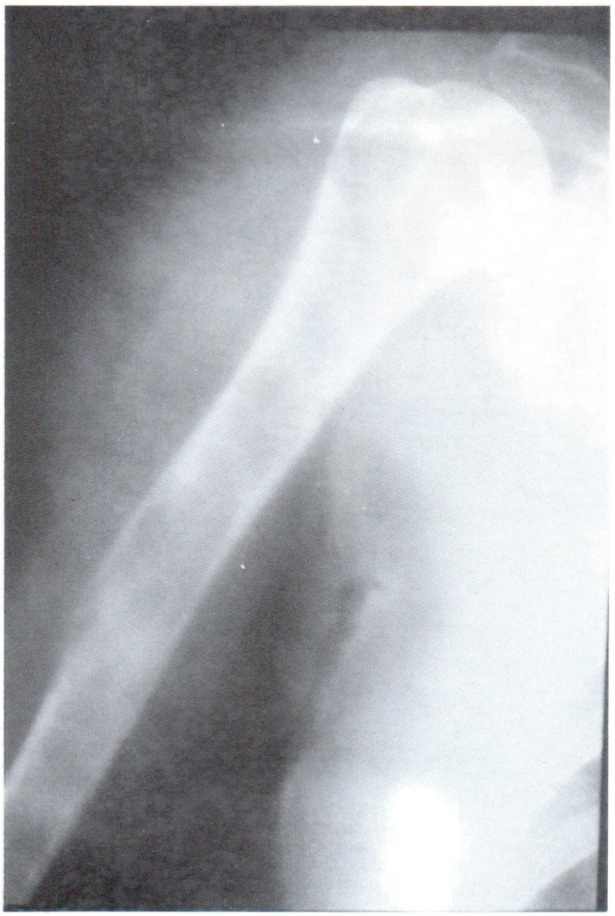

Fig.3 Case 7. 62-yr-old female with pain and swelling of Rt.arm. Conventional radiograph of Rt. humerus shows multiple punched-out osteolytic expansile lesions involving metaphysis and diaphyses. Solid buttress periosteal reaction is seen.

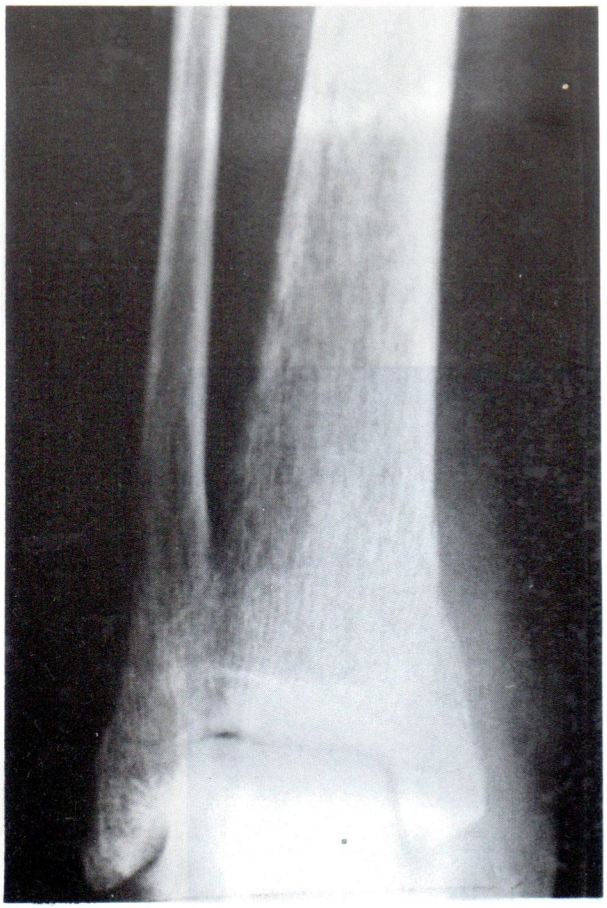

Fig.4 Case 5. 57 yr-old female with fever, Lt ankle pain, sepsis and pneumonia.
Conventional radiograph of Lt. ankle shows permeative osteolytic destruction of distal tibia. The joint space is normal.

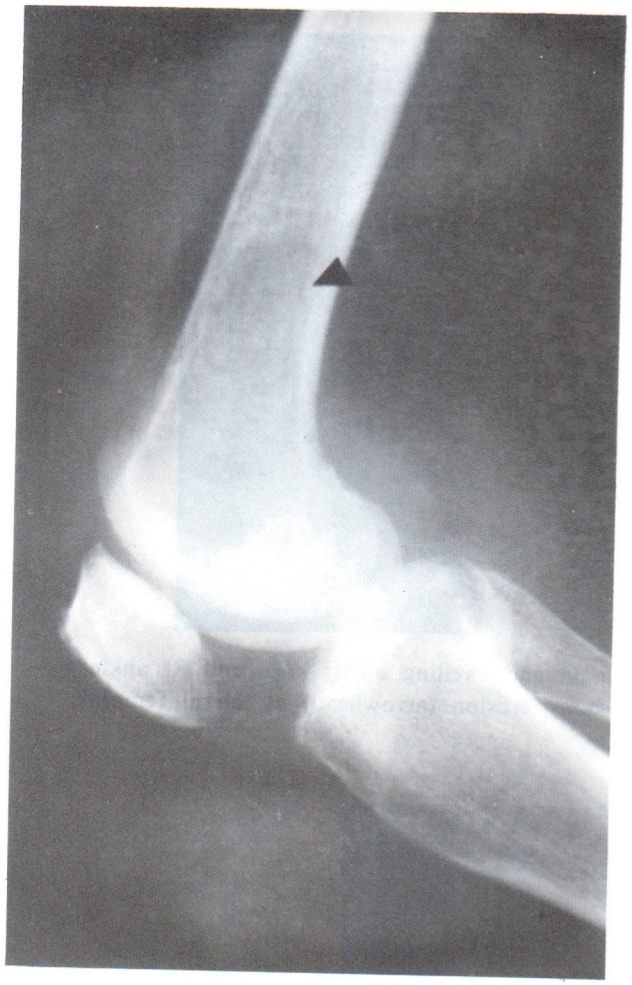

Fig.5 Case 8. 50-yr-old female with fever and pain at Rt. knee.
Conventional rediography of Rt knee shows permeative osteolytic destruction of distal femur with joint effusion

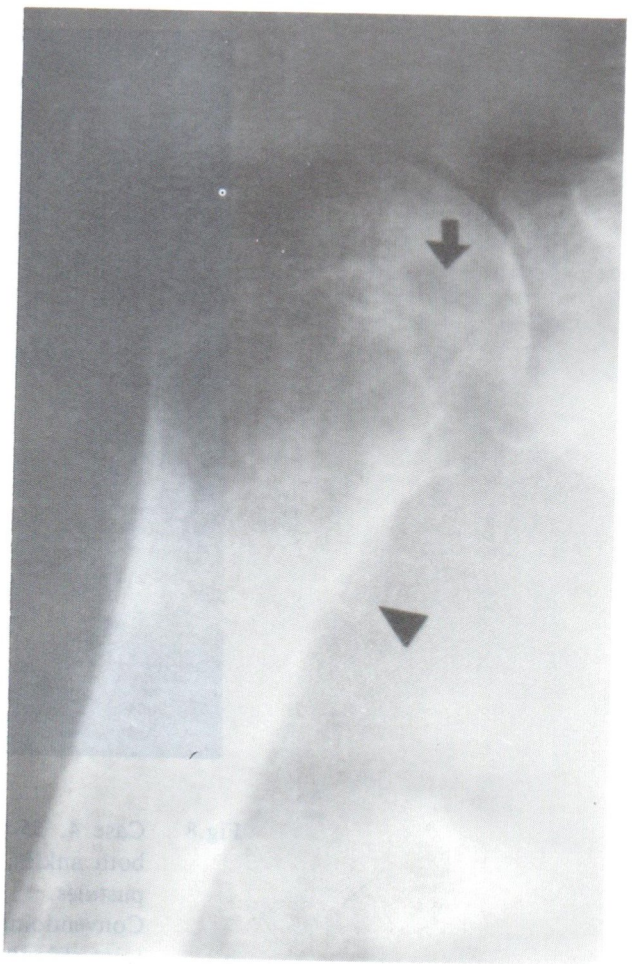

Fig.6 Case 1. 43-yr-old male with fever, pain and swelling of Rt. arm.
Conventional radiograph of Rt humerus shows permeative and punched-out osteolytic destruction at superomedial aspect with Codman periosteal reaction (arrowhead). The glenoid cavity is normal. The bony destruction involved metaphyses and epiphyses (arrow)

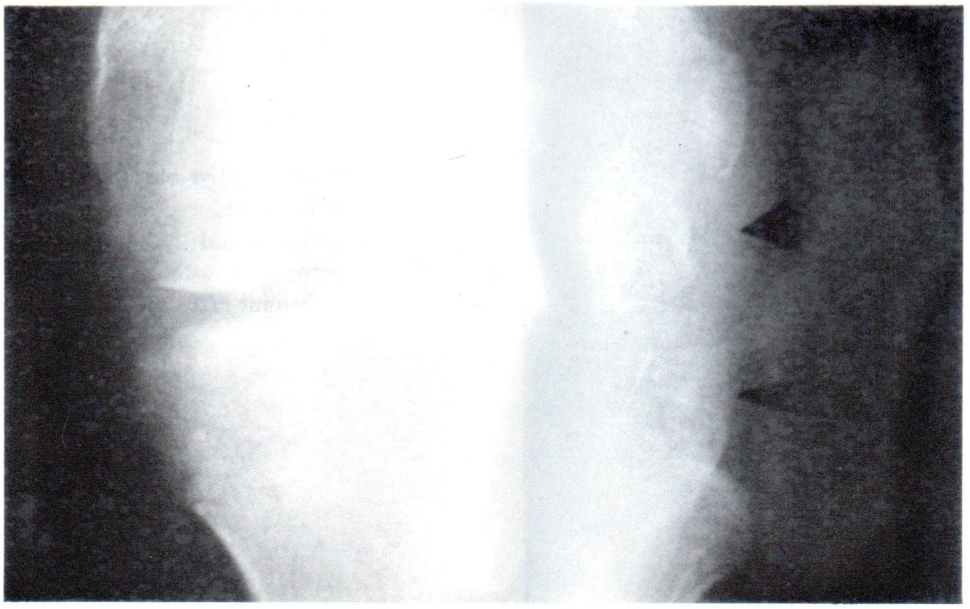

Fig.7 Case 3. 75-yr-old male with fever, anemia, pain and swelling of Rt knee and Rt ankle. Conventional radiograph of Rt knee shows bony erosion (arrowhead) at lateral femoral condyle and lateral tibial condyle

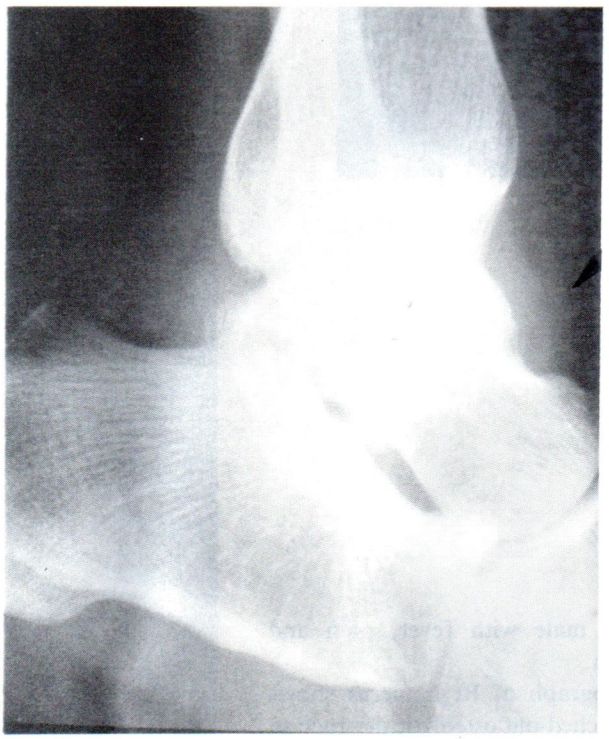

Fig.8 Case 4. 55-yr-old male with fever, swelling of both ankles, liver abscess, pneumonia and skin pustules.
Conventioinal radiograph of Lt. ankle shows joint effusion (arrowhead). No bony destruction is evident

BASAL CELL NEVUS SYNDROME A CASE REPORT

Suphaneewan Jaovisidha M.D. *
Instructor
Pimjai Siriwongpairat M.D.*
Assistant Professor
Jaovisidha S., Siriwongpairat P. *

ABSTRACT

The basal cell nevus syndrome is a multisystem disorder inherited in an autosomal dominant manner with marked penetrance and variable expression. Originally defined as the triad of nevoid basal cell carcinomas, jaw cysts, and skeletal anomalies. The syndrome complex has since been greatly expanded to include a variety of other organ system abnormalities. We recently had the opportunity to discover a family with this syndrome while evaluating a patient with atopic eczema, and describing hypopneumatization of mastoid antrum, as an associated finding in this syndrome which has not been documented before.

INTRODUCTION

Basal cell nevus sysdrome (nevoid basal cell carcinoma syndrome, Gorlin-Goltz syndrome, hereditary cutaneomandibular polyoncosis) had been recognized during the hundred years since the first cases were described by Jarisch and White. It is a rare and complex disease with multiple manifestations. The patients show characteristic facies, which together with enlarged calvaria may lead the clinician to search for the basal cell nevus syndrome very early in life, even in the absence of an indicative family history.

Although the syndrome has been well defined for over 25 years, many clinicians are familiar only with its major manifestations, such as multiple basal cell carcinomata, jaw cysts, and skeletal abnormalities. This report, we present a patient coming with atopic eczema, after closed evaluation and further investigations disclosed multisystem abnormalities of the basal cell nevus syndrome.

CASE REPORT ;

PATIENT ; A 33-year-old Thai female

PRESENT ILLNESS ; The patient came to the dermatologic clinic for evaluation of mild atopic eczema. She had a past history of undergoing excision of epidermoi inclusion cyst in March 1994.

PHYSICAL EXAMINATION ; The physical examination showed mild atopic eczema at dorsum of left hand. In addition, there were erythematous lichenified papules and plaques on lateral side of neck, flexural surface of elbows and knees. She was noted to have frontal bossing with prominent supraorbital ridge. (Fig. 1). Head circumference measured 60 cm. & mild ocular hypertelorism is observed. Also seen were multiple discrete 1-2 mm. pits on non-inflammatory base distributed on the palms (Fig 2) with similar lesions on the soles.

* Division of Diagnostic Radiology, Department of Radiology, Faculty of Medicine, Ramathibodi Hospital, Mahidol University

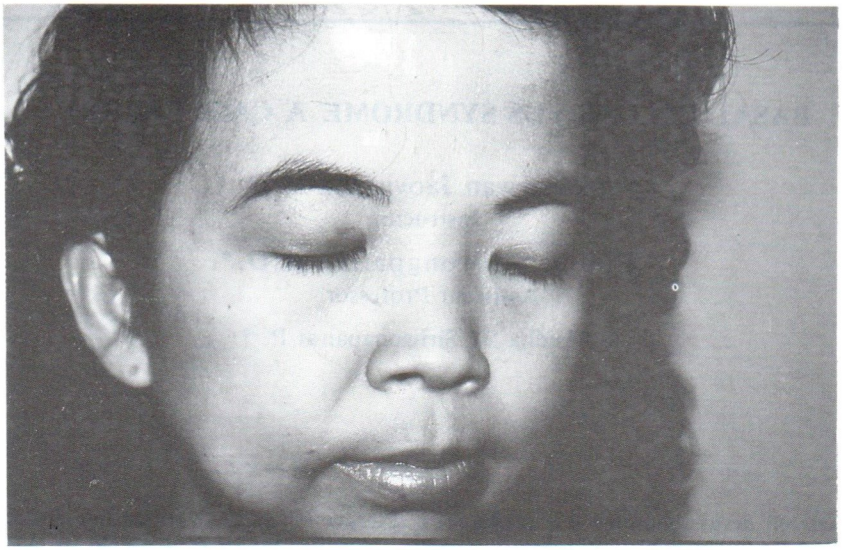

Fig.1 Photograph of the patient revealed frontal bossing with prominent supraorbital ridge

Fig.2 Photograph of the patient's palm showed numerous palmar pits

Careful evaluation of skin revealed no evidence of basal cell carcinoma, skin tags, or trichoepitheliomas. No reticulate pigmentation or nail abnormality is observed. Two pigmented nevi each were found on right arm and abdomen.

Physical chest examination reveals normal heart & lungs. Abdominal examination showed no abnormality. No palpable mass is noted. The patient showed no kyphosis or scoliosis while in standing position.

FAMILY HISTORY ; The patient's father had a history of malignancy (questionable carcinoma of nasal cavity or nasopharynx or paranasal sinus), and died at the age of 48.

No palmar pits in siblings but the patient's second sister had congenital heart disease.

The patient and siblings all have carius teeth with early tooth loss.

Her first child aborted and her second son was born with complete cleft lip, cleft palate, and strabismus (exotropia). Her son also has macrocephaly and attended the Pediatrics neurologic clinic but has normal develpment.

HISTOPATHOLOGY ; The histopathology revealed sharp demarcated area of relatively thin cornified granular and spinous layer of the epidermis from volar skin. The rete ridges are thin and increase in epidermal melamin.

Another slide showed cords, nests, and strands of uniform nevus cells (melanocytes) in the upper dermis.

RADIOGRAPHIC FINDINGS ; (Fig. 3 - Fig. 14)

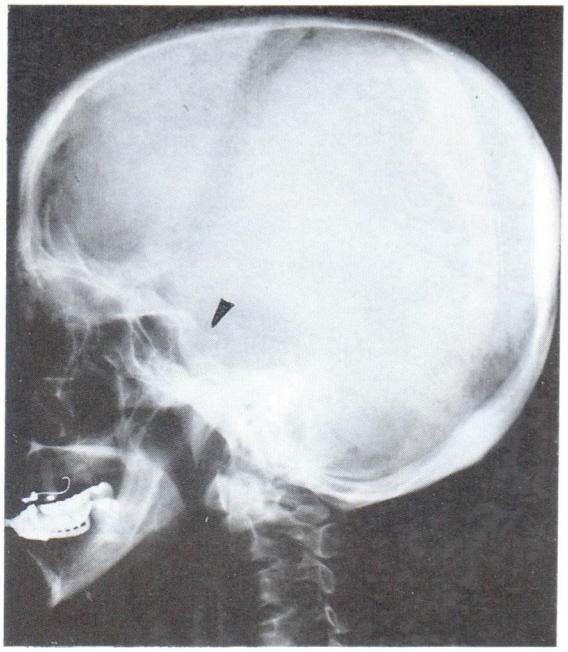

Fig.3 Film lateral skull revealed macrocephaly (increased craniofacial ratio), & bridging sella turcica

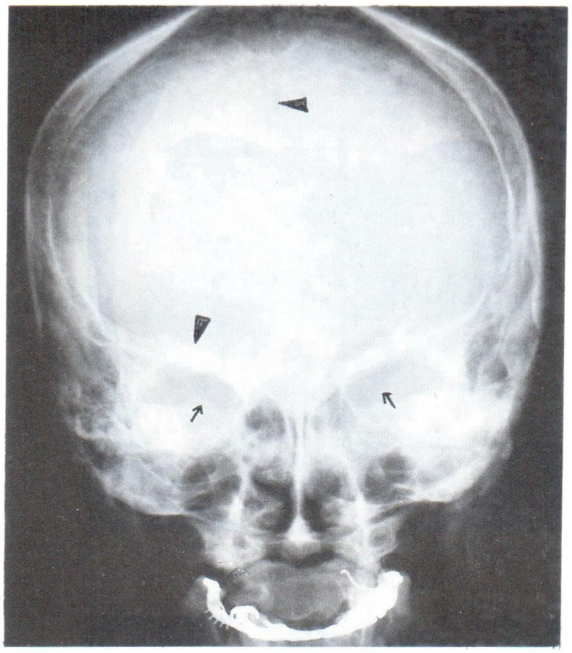

Fig.4 Film AP skull disclosed calcified falx cerebri (upper arrow), hyperostosis of Rt supraorbital ridge (mid level arrow), and symmetrical, abnormal widening of superior orbital fissures (lower small arrows)

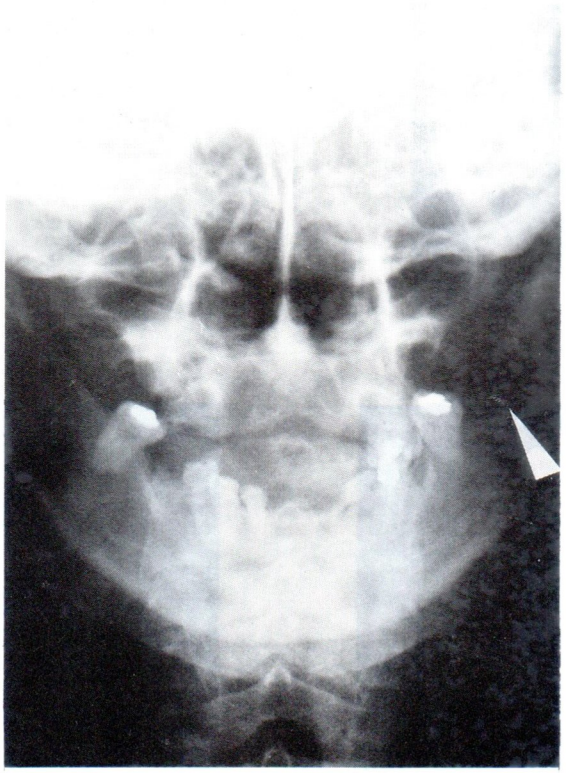

Fig.5 Film mandible revealed jaw cyst at Lt mandibular ramus

January - April 1995 Volume I Number I

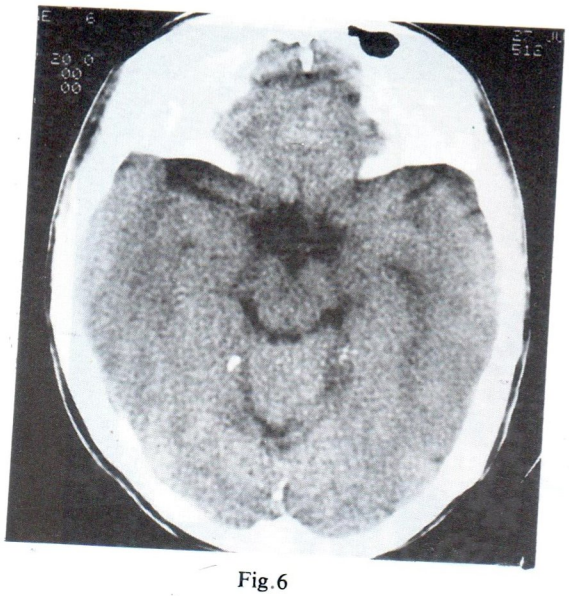

Fig.6

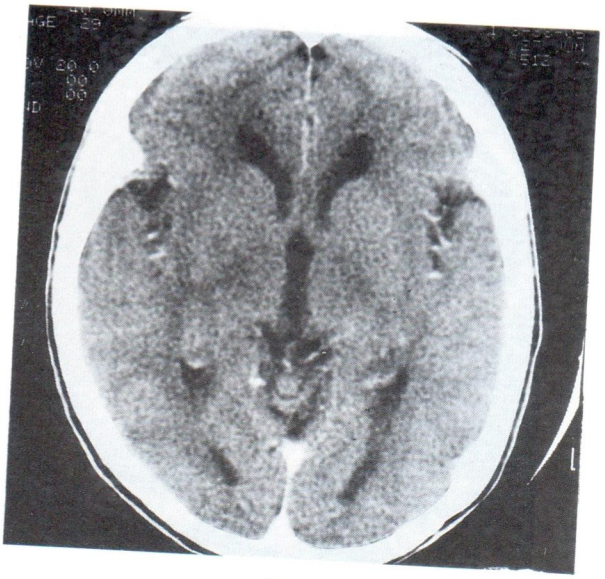

Fig.7

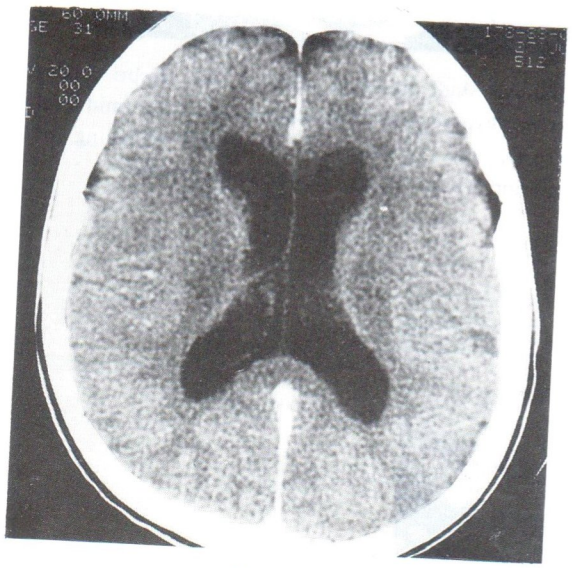

Fig. 8

Fig.6-10 CT scan of the brain
Fig.6 : calcified tentorium cerebelli
Fig.7-8 : symmetrical hydrocephalus
Fig.9 : calcified falx cerebri (lamellated calcification)
Fig.10 : hypopneumatized Lt mastoid antrum

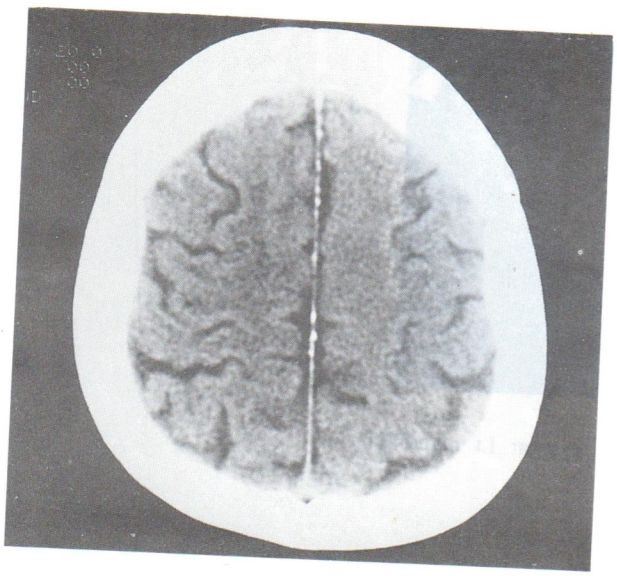

Fig.9

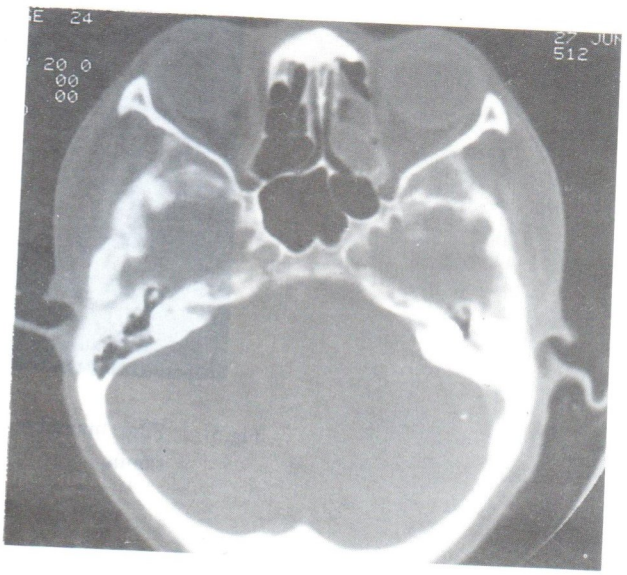

Fig.10

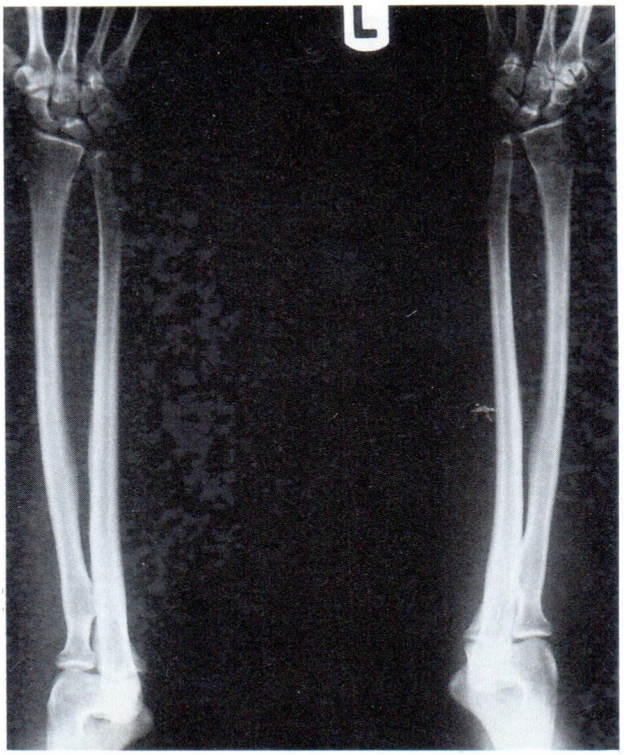

Fig.11 Film forearms showed midly deformed ulna bilaterally

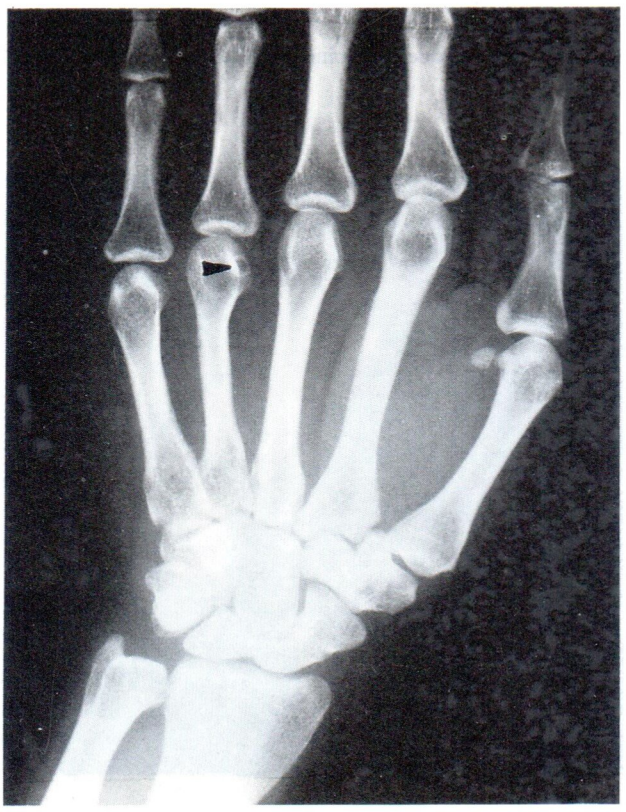

Fig.12 Film Rt. hand showed small bone cyst at 4th metacarpal head

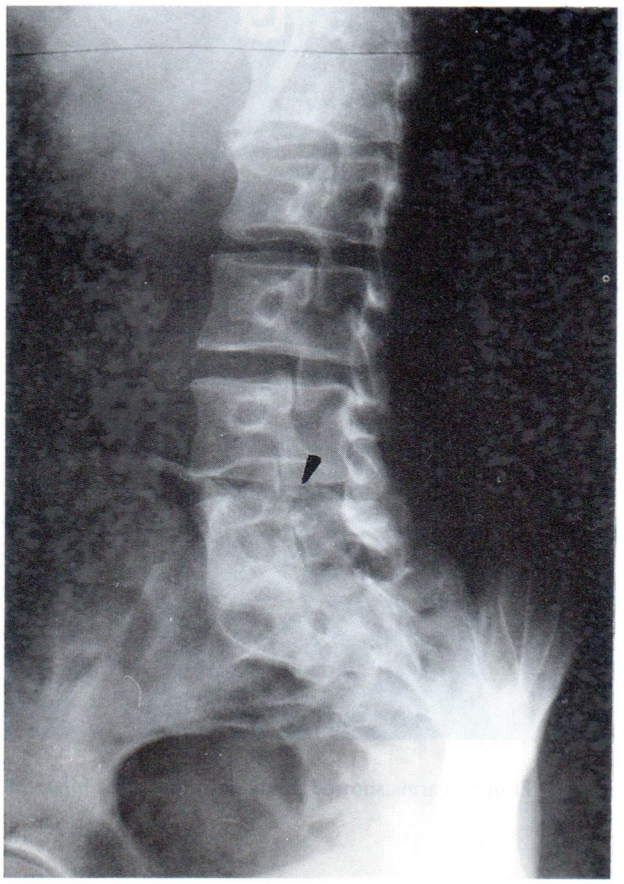

Fig.13 Film oblique L-S spine disclosed spondylolysis of L-5

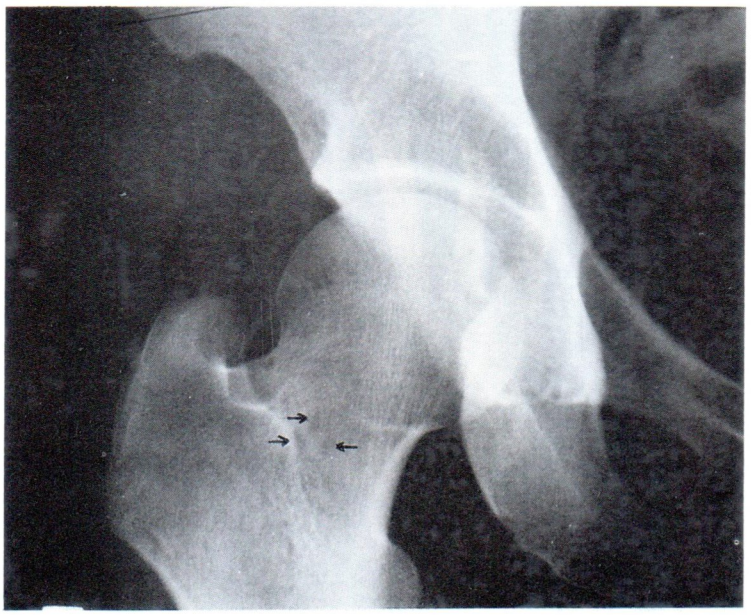

Fig.14 Film AP Rt. hip revealed multiple small bone cysts at Rt. femoral neck

DISCUSSION

The basal cell nevus syndrome had variable expression and involving multiple organ systems.

TABLE 1. Diagnostic findings in adults with nevoid basal cell carcinoma syndrome (14)

50 % or greater frequency	14 % or less
Enlarged haed circumference	Medulloblastoma (true frequency not known)
Mild ocular hypertelorism	Inguinal hernia
Multiple basal cell carcinoma	Meningioma
Odontogenic keratocysts of jaws	Lymphomesenteric cysts
Epidermal cysts of skin	Cardiac fibroma
Palmar and/or plantar pits	Fetal rhabdomyoma
Calcified ovarian cysts	Ovarian fibrosarcoma
(probable overestimated frequency)	Marfanoid build
Calcified falx cerebri	Agenesis of corpus callosum
Rib anomalies	Cyst of septum pellucidum
(splayed, fused, partially missing, bifid, etc.)	Cleft lip and/or cleft palate
Spina bifida occulta of cervical or thoracic vertebrae	Polydactyly, postaxial-hands or feet
Calcified diaphragma sella	Sprengel deformity of scapula
(bridged sella, fused clinoids)	Congenital cataract, glaucoma, coloboma of iris, retina, optic nerve, medullated retinal nerve fiberrs
Hyperpneumatization of paranasal sinuses	Subcutaneous calcification of skin
49 to 15 %frequency	(possibly underestimated frequency)
Calcification of tentorium cerebelli and petroclinoid ligament	Minor kidney malformations
Short fourth metacarpals	Hypogonadism in males
Kyphoscoliosis or other vertebral anomalies	Mental retardation
Lumbarization of sacrum	
Pectus excavatum of carinatum	
Pseudocystic lytic lesion of bones (hamartomas)	
Strabismus (exotropia)	

SKIN

The syndrome is characterized by nevoid basal cell carcinomas, which appear largely between puberty and 35 years of age, although they have been reported to occur as early as 2 years of age. It has been estimated that about 2% of the patient younger than 45 years of age with basal cell carcinoma have the syndrome, in contrast to 22% of those younger than 19 years of age. Only about 15% of patients manifest the skin lesions before puberty, and about 10% of patients over the age of 30 years have no skin lesion, as we have seen in our patient who showed no basal cell carcinoma in the 33 years of her age. The lesions are pink or pale brown papules, may resemble moles, skin tags, nevi, or hemangioma and they may range in size from 1 to 10 mm in diameter. Epidermoid cysts (1 to 2 cm) occur on the limbs and trunk in over 50% of the cases. Before puberty the lesions are harmless, even huge numbers are present. Only a few become aggressive, and they are only after adolescence, when they may be locally invasive, behaving like ordinary isolated basal cell carcinoma. Death has resulted in a few instance from invasion of the brain, lung, or peritoneum. Only in the rare case has metastasis been documented.

About 65 % present small (1 to 2 mm) asymmetric palmar and/or plantar pits. There are several cases in which basal cell carcinomas have been arisen in the base of these pits.

FACE

A characteristic facies is present in about 70 % of patients. This is due in part to increased size of the calvaria (occipitofrontal circumference, 60 cm or more in adult) due to frontal and biparietal bulging, well-developed supraorbital ridges, broadened nasal roots, low position of occiput, mild hypertelorism, exotropia, and exaggerated length of mandible associated with pouting of the lip.

Cleft lip and/or palate occur in about 5 % Congenital blindness due to corneal opacity, congenital or precoccious cataract or glaucoma and/or coloboma of iris, choroid, and optic nerve, with convertent or divergent strabismus and nystagmus, has been reported in 10-15 % of the patients.

ODONTOGENIC KERATOCYSTS

Cysts of the jaws, developed during the first decade of life (usually after the seventh year) to peak during the second or third decades. 15 % of patients do not have radiographically demonstrable cysts by the age of 40. In spite of widespread extension throughout the jaws, almost never do they cause symptoms unless secondarily infected following surgery. Most often they are detected on routine dental check ups. Adjacent teeth may be occasionally loosened. Although rare, both ameloblastoma & squamous cell carcinoma have arisen in these jaw cysts.

Odontogenic keratocysts are found in over 80%, about 3 times as often in the mandible as in the maxilla. They may be small, single, or multiple, but more often are large, bilateral, unilocular or multilocular, and asymmetric, involving both jaws. They can displace the developing permanent teeth. Recurrent rate of the cysts. between 30% to 60% after treatment.

CENTRAL NERVOUS SYSTEM

Medulloblastoma developing within the first 2 years of life has been described in several patients, in their sibs & offsprings. Accurate assessment is problematic since several patients have had their sibs or other relatives die during infancy from "brain tumour, but the estimated rate is about 20%. Meningioma & craniopharyngioma have also been described.

Mental retardation, has been reported in about 3% of cases. Calcified falx cerebri which appear early in life, is seen in about 85% (normal 5%). Calcification of the tentorium cerebelli (40%), petroclinoid ligaments (20%), dura, pia & choroid plexus is common. The sinuses are hyperpneumatized in 60% due to absence of intrasinusal septa. In our patient, she has hypopneumatization of left mastoid antrum which has not been described before, and is likely due to bony dysplasia for she had no history of otitis media. Bridging sella (calcification of the diaphragma sellae) is seen in at least 60-80% (normal 4%). The sella is amall and ofter asymmetric due to hyper-pneumatization of sphenoid bone. Platybasia, agenesis of corpus callosum, cysts of septum pellucidum, & congenital hydrocephalus have also been reported.

MUSCULOSKELETAL SYSTEM

Patients may be very tall, some exhibiting marfanoid build. Skeletal anomalies are common. About 60% have anteriorly splayed, fused, partially missing, hypoplastic, or bifid ribs. Cervical ribs are frequent. Kyphoscoliosis with or without associated pectus excavatum or carinatum is present to some degree in about 30-40%, and spina bifida occulta of the cervical and thoracic vertebrae is found in 60%. Malformation at the occipito-vertebral junction are common. These included short atlas or foramen arcuale, less often agenesis of the odontoid process, the presence of a third occipital condyle, or basilar agenesis. Cervical or upper thoracic vertebral fusion or lack of segmentation has been documented in about 40%, as well as 40% incidence of lumbarization of sacrum.

There are various other bony anomalies : polydactyly of hands and feet, hallux valgus, syndactyly of second & thrid fingers. Sprengel deformity is found in 5-10%. Medial hooking or dysplasia of the lower scapula borders has been noted. Pes planus & defective medial portion of clavicle have also been described.

Small pseudocystic lytic bone lesion are noted in 35-45%, affecting many parts of bony skeleton. Spotted sclerotic osteopoikolytic lesions have also been documented. Subcutaneous calcification of fingers & scalp has been reported.

The fourth metacarpal bone is short in 15-45% (average 20%), but this sign is not diagnostic since many studies have shown that 10% of normal population have one or both short fourth metacarpal bones.

GENITOURINARY SYSTEM

In males, there were reports of hypogonadism, anosmia, cryptorchism, female pubic escutcheon, gynecomastia and/or scanty facial or body hair. Seminoma has also been reported.

Frequently the female patients were documented to have ovarian fibromas. They may overlap near midline as a single calcified mass, simulating calcified uterine fibroid. The tumour are often not discovered unless they twisted. Ovarian fibrosarcoma has also been reported.

A variety of minor kidney malformations are noted ; horse-shoe kindney, L-shaped kidney, duplication of collecting system, renal agenesis.

MESENTERY

There has been reports of chylous or lymphatic cysts of the mesentery, which if large, can cause painless movable mass in upper abdominal quadrants. Most cases have not produced sysptom and have been diagnosed at laparotomy. They sometimes show calcification.

HEART

The isolated cardiac fibroma occur at all ages, but 85% are found in children less than 10 years old. It is solitary & can arises in many parts of the heart ; the interventricular septum, anterior wall of left ventricle, posterior wall of left ventricle, & right ventricle, in order of frequency.

The cardiac fibroma associted with the syndrome appeared no difference from the isolated tumour.

NEOPLASM OF OTHER ORGANS

This syndrome has been associated with an increased tendency of various other neoplasia ; renal fibroma, adrenal cortical adenoma, bronchogenic cysts, fetal rhabdomyoma and rhadbomyosarcoma, leiomyoma, isolated neurofibroma, melanoma.

Fibrosarcoma of jaws have been reported, but probably secondary to radiation therapy.

In conclusion, we have presented a rare case of basal cell nevus syndrome, with multiorgan abormalities. The finding of hypopneumatization of mastoid antrum has not been described before. We planned to have periodic follow up & examination for this patient.

REFERENCES ;

1. Taybi H. Radiology of Syndromes. Chicago : Year Book Medical publishers Inc., 1975 : 26-27
2. Taybi H, Ralph SL. Radiology of Syndromes, Metabolic Disorders, and Skeletal Dysplasia. 3rd Ed. Chicago : Year Book Medical Publishers Inc., 1990 : 335-7
3. Bare JW, Lebo RV, Epstein EH Jr. Loss of heterozygosity at chromosome 1q22 in basal cell carcinoma and exclusion of the basal cell nevus syndrome gene from this site. Cancer-Res. 1992 Mar 15; 52(6): 1494-8
4. Battisti C, Palmeri S, Federico A. Oculo-dento-digital syndrome (Gorlin's sysdrome) : clinical & genetical report of a new family. Acta Neurol Napoli 1992 Apr; 14(2): 103-10
5. Chenevix-Trench-G, Wicking C, Berkman J, et al. Further localization of the gene for basal cell carcinoma syndrome (NBCCS) in 15 Australasian families : linkage and loss of heterozygosity. Am J Hum Genet 1993 Sep; 53(3): 760-7
6. Chenevix-Trench-G. Basal cell naevus sysdrome. Med J Just 1992 May 4 ; 156(9): 671-2
7. Coffin CM.Congenital cardiac fibroma associated with Gorlin syndrome. Pediatr Pathol 1992 Mar-Apr; 12(2): 255-62
8. DiSanto S, Abt AB, Boal, et al. Fetal rhabdomyoma and nevoid basal cell carcinoma syndrome. Pediatr Pathol 1992 May-Jun; 12(3): 441-7
9. Evans DG, Ladusans EJ, Rimmer S, et al. Complication of the naevoid basal cell carcinoma syndrome : result of a population based study. J Med Genet 1993 Jun; 30 (6): 460-4
10. Farndon PA, Del-Mastro-RG, Evans DG, et al. Location of gene for Gorlin sysdrome. Lancet 1992 Mar 7; 339 (8793) : 581-2
11. Fryer A. Odontogenic keratocysts do not occur in Noonan syndrome. Clin Dysmorphol Apr ; 2 (2): 185-6
12. Gailani MR, Bale SJ, Leffell DJ, et al. Developmental defects in Gorlin syndrome related to a putative tumour suppressor gene on chromosome 9. Cell 1992 Apr 3; 69 (1) : 111-7
13. Goldstein AM, Bale SJ, peck GL, et al. Sun exposure and basal cell carcinoma syndrome. J Am Acad Dermatol 1993 Jul; 29(1) : 34-41
14. Gorlin RJ. Nevoid Basal-Cell Carcinoma Syndrome. Medicine 1987 ; 66 (2): 98-113
15. Horner K, Rushton V. Adontogenic keratocyst in an infant. Br Dent J 1992 Jul 25; 173 (2): 52
16. Khalique N, Rippin JW. Odontogenic keratocyst in an infant. Br Dent J 1992 Apr 11; 172 (7) 282-3
17. Kuster W, Happle R. Neurocutaneoius disorders in children. Curr Opin Pediatr 1993 Aug; 5 (4) 436-40
18. Mathur MN, Thompson JF, O'Brien CJ, et al. Naevoid basal cell carcinoma (Gorlin's) syndrome. Aust N Z J Surg 1993 May; 63(5): 413-5
19. Meyvisch K, Andre J, Song M, et al. Basal cell nevus syndrome and congenital hydrocephaly. Dermatology 1993 ; 186 (4) : 311-2
20. Pilcher R. The basal cell naevus syndrome : a case in the Falkland Islands. J R Army Med Corps 1993 Feb ; 139 (1): 20-4
21. Springate JE. The nevoid basal cell carcinoma syndrome. J pediatr Surg 1986 Oct; 21 (10) : 908-10
22. Strange PR, Lang PG Jr. Long-term management of basal cell nevus syndrom with topical tretinoin and 5-fluorouracil. J Am Acad Dermatol 1992 Nov ; 27 (5 Pt 2) : 842-5
23. Theiler R, Hubscher E, Wagenhauser Fj, et al. (Diffuse idiopathic skeletal hyperostosis (DISH) and

pseudo-coxarthritis following long-term etretinate therapy). Schweiz Med Wochenschr 1993 Apr 10; 123 (14) : 649-53

24. Tokar IP, Fraser MC, Bale SJ. Genodermatoses with profound malignant potential. Semin Oncol Nurs 1992 Nov; 8 (4) : 272-80
25. Tsuji T, Otake N, Nishimura M. Cryosurgery and topical fluorouracil : a treatment method for widespread basal cell epithelioma in basal cell nevus syndrome. J Dermatol 1993 Aug; 20 (8) : 507-13
26. Ujpal M, Szabo G. (Familial occurrence of Gorlin-Goltz syndrome). Fogorv Sz. 1992 JIul ; 85 (7) : 209-12
27. Watson RA, Harper BN. Paratesticular fibrous pseudotumour in a patient with Gorlin's syndrome : nevoid basal cell carcinoma syndrome J Urol 1992 Oct ; 148 (4) : 1254-5
28. Yee KC, Tan Cy, Bhatt KB, et all. Sclerotic bone lesions in Gorlin's sysdrome. Br J Radiol 1993 Jan ; 66 (781) : 77-80
29. Zarour H, Grobb JJ, Choux R, et al. (Basal-cell and linear unilateral adnexal harmatoma (or linear uniear unilateral basal-cell nevus)). Ann Dermatol Venereol 1992 ; 119 (11) : 901-3

PRACTICAL DEEP VEIN PHLEBOGRAPHY OF LOWER LIMB

SURIN CHONMAITRI*

Abstract:

The author has described a simple technique to visualize the deep veins of the lower extremity for the diagnosis of the possibility of having deep vein thrombosis. The technique does not need a fluoroscopy or an experienced radiologist. It needs only a radiographer and may be used in the provincial or district hospital where sophisticated equipments or experienced radiologist is not available.

Key words: Simple technique for deep vein phlebography of lower limb.

There are various technics of phlebography of deep vein of lower limb, including positioning of patient either in upright or supine, and the amount of opaque media used,[1,2,3] but there is no definite guideline for timing of exposure. Spot films under fluoroscopy need radiologist to operate on and hence are not practical. We, at the Priest's Hospital, develop a simple and practical technic that requires only a well trained radiological technician.

TECHNIC

With the patient in supine position and the feet internally rotated, a no. 21 scalp vein needle is cannulated into a superficial vein on the medial aspect of the distal half of the foot, while a tourniquet is being placed above the ankle. Then 40 ml of diatrizoate meglumine 60% are injected continuously by hand.

After the first 20 ml, the second and the last 10 ml of the opaque media have been injected, the overhead 14 × 17 films are made from the foot to below-the-knee, from below- to above-the-knee and from above-the-knee to the iliac crest levels respectively (see Fig. 1-4). The successive exposure is repeated immediately at this region. Either heparin or NSS is infused right after the last ml of the opaque media has been injected, for the purpose of reducing the possibility of phlebitis.[3,5]

RESULTS

35 lower extremity venograms were performed in a total number of 35 patients over a period of 2 months.

Our patients were requested for IVP study but instead of upper limb venous injection, lower limb phlebography was performed.

The adequacy of venous opacification in the leg, the thigh and the pelvic veins were judged into 3 categores : 2^+, when the dense contrast was seen : 1^+, when the opacification was not dense enough but was adequate to exclude the disease; and O, when there was no contrast material filling the vein or the density was so poor that an adequate interpretation was not possible.

*Radiologist and the Medical Director of the Priest's Hospital, Sri Ayudhya Road, Bangkok 10400, Thailand.

DISCUSSION

As far as we know, no definite guideline has been mentioned in any literatures regarding the timing of exposure in deep vein phlebography of lower limb.

The author believes that the technic, that has been described in this literature, is the easiest and simplest one that can be performed in any hospitals in our country no matter what the radiologist or the sophisticated x-rays equipment is available or not.

The timing of exposure of various part of the leg can be done with the help of the amount of radiopaque media used, which is small and can be safely repeated. The inadequacy of the opacification of the pelvic vein can be overcome by using the technic of femoral vein compression.[6]

The procedure is quite convenient for both of the patient and the technician as it does need rotating of the table or the sport films which are not practical in the small hospitals in our country.

REFERENCES :

1. Rabinov K, Paulin S. Roentgen diagnosis of venous thrombosis in the leg. Arch Surg 1972; 104:134-144.
2. Tisnado J. Tsai F. & Beachley M. An alternate technic for lower extremity venography. Rad. 1979; 133:787-788.
3. Thomas M. Phlebography. Arch Surg 1972; 104: 145-151.
4. Coel M. Adequacy of lower limb venous opacification. AJR 1980; 134:163-165.
5. Arndt R. et al. The heparin flush : Aid in Preventing post-venography Thrombophlebitis. Rad 1979; 130: 249-250.
6. Smith T. et al. Lower extremity venography value of Femoral-Vein Compression AJR 1986; 147:1025-1026.

Table shows the number of patients with ratings of venous opacification in the leg, the thigh and the pelvic veins

35 cases of venous opacification	2^+ (dense opacification)	1^+ (adequate opacification)	0 (inadequate opacification)
in the leg vein	34	1	-
in the popliteal vein	35	-	-
in the thigh vein	31	3	1
in the pelvic vein	6	13	16

Fig.1 After the first 20 ml injection of the opaque media

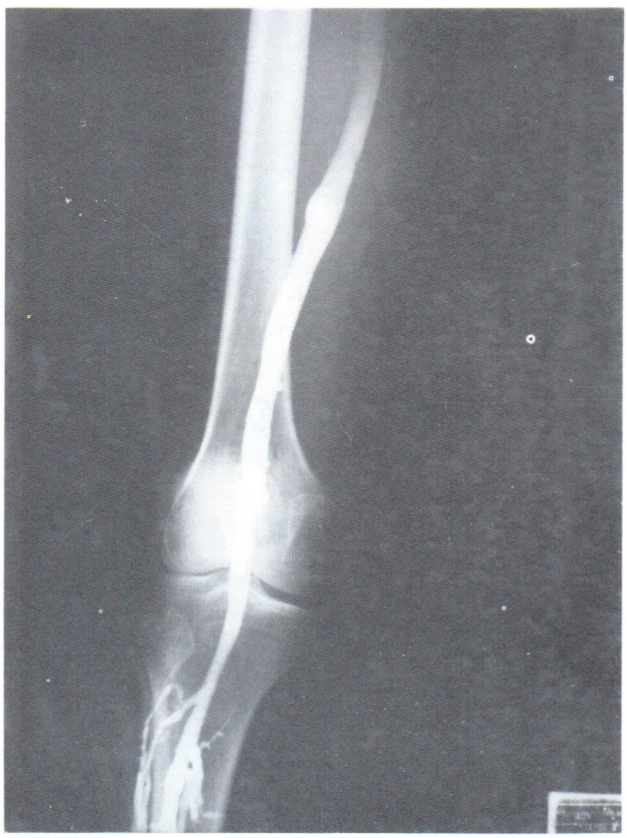

Fig.2 After the second 10 ml injection of the opaque media

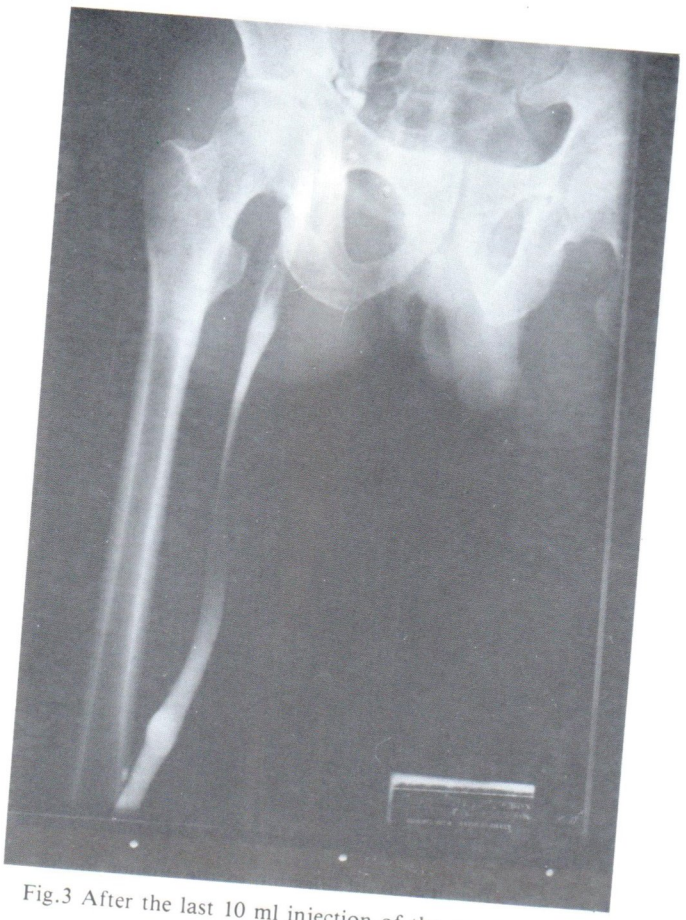

Fig.3 After the last 10 ml injection of the opaque media

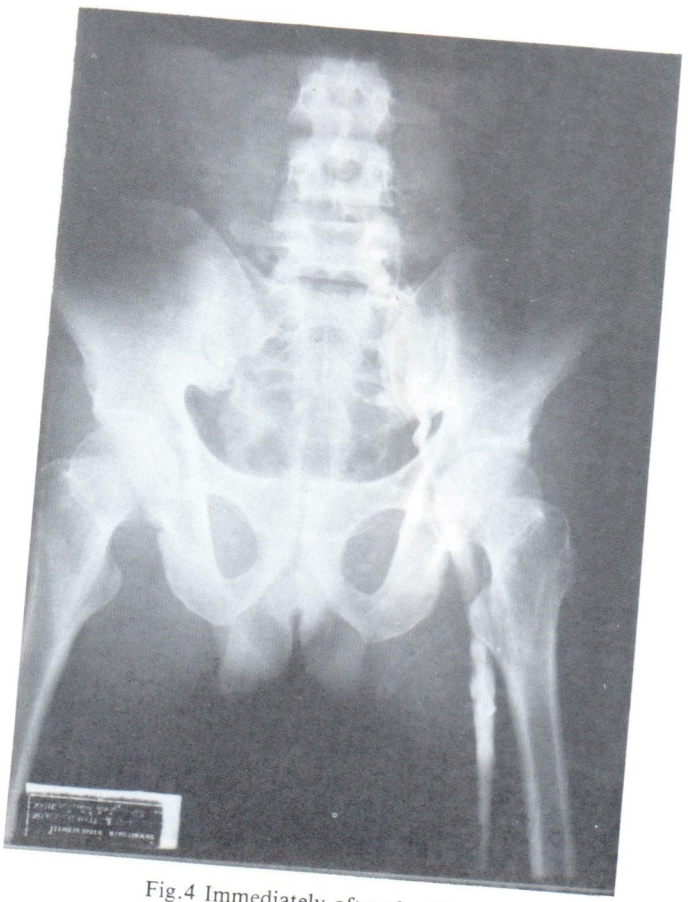

Fig.4 Immediately after the Fig.3

Loss of compressibility by ultrasonography in deep venous thrombosis of the lower extremities: a prospective evaluation.

N. Kiathirannon[1], P. Pekanan[1], C. Euavilaichit[1], N. Ruxayos[1]

Abstract:

Compressibility of the deep veins of the lower extremities by real time ultrasonography, in the cases suspected to have deep vein thrombosis was analyzed, using contrast venography as the standard in the diagnosis of the deep venous thrombosis. A prospective study was performed in 25 cases. There was no false positive cases. Thirteen contrast venography diagnosed DVT showed 11 positive ultrasonography. The sensitivity was 87% and the specificity was 100%. The false negative studies should be avoidable if more careful examination was performed. The diagnosis of DVT by determination of the loss of compressibility by ultrasonography was very simple and accurate. With careful examination, it should obviate the need to performed more traumatic contrast venography, at least in the ultrasonographic DVT positive cases.

Key words: deep vein thrombosis, Ultrasound, venous compressibility

Deep vein thrombosis (DVT) is an important disease because of its two major sequelae; chronic venous insufficiency and pulmonary embolism. Pulmonary embolism is potentially lethal and the vast majority of them originate from the pelvis and lower extremities. Clinical diagnosis of DVT is unreliable. In a group of more than 1000 patients who were suspected to have DVT clinically, only 30% was found to have DVT, according to Hirsh et al (1). Contrast venography was considered to be the diagnostic tool for determination of DVT with good demonstration of the anatomic detail. Its disadvantages include invasiveness, contrast material toxicity, local irritation and contrast induced thrombus formation (2). The non invasive imaging methods to detect DVT include technetium-99m- labeled red blood cell venography, iodine-125-labeled fibrinogen scintigraphy, impedence plethysmography (IPG) and ultrasonography.

Real-time compression ultrasonography has been shown to be effective in the assessment of the DVT (3, 4). We assessed the ability of the high resolution ultrasonography to demonstrate the presence and absence of DVT in the lower extremities on the basis of the compressibility of the vein. Simplicity of the examination was considered paramount, since the on-call examination could be performed.

[1] Department of Radiology, Ramathibodi Hospital, Rama 6 Street, Bangkok 10400, Thailand.

Materials and methods

During February 1994 to October 1994, every patient who was sent to the Department of Radiology, Ramathibodi hospital, for contrast venography of the lower extremities with the possible diagnosis of DVT, was performed with the compressive ultrasonographic study within 4 hrs after contrast venography. Both studies were performed by different radiologists and were interpreted independently.

The contrast venography was performed using the technique, modified from that described by Rabinov and Paulin (5). 100-150 ml of 40% water soluble contrast medium was injected into a dorsal pedal vein while the patient was examined on the moving tabletop fluoroscopic-radiographic unit. The examination was interpreted by the vascular radiologists. The criterias for the diagnosis of DVT by venography included a constant filling defect or thrombus in the lumen, persistent nonfilling of a venous segment despite adequate technique, or the abrupt termination of the opaque column of the contrast medium in the venous segment.

The ultrasonographic evaluation of the lower extremity was performed with 7.5 MHz linear-array transducer. The examination began with the patient in a supine position with the leg in slight external rotation. Assessment included the common femoral veins down to the level of the adductor hiatus. Effort was made to image the femoral vein within the hunter canal and at the adductor hiatus, but this was not always possible. The saphenous vein was also visualized and the point of the union was always observed. The position and the appearance of the femoral artery was also noted, as well as any mass or fluid collection in the perivascular area. The deep femoral vein and the iliac vessels were not studied. After direct visualization of the veins in both transverse and longitudinal projections, the compression was applied. The degree of compression normally required to collapse the vein is small, only to dimple the skin; this has been estimated to be equal to 10^4 dyne/cm^2. The compression was routinely applied while the transducer was transversely oriented, so that the transducer did not roll off the vein. The vein was compressed and released at approximately 1 cm intervals.

After evaluation of the common femoral, superficial femoral and saphenous veins, the patient was placed in a prone position. The knee was bent about 30 degree and the distal part of the leg was supported with the towels for the optimal visualization of the venous lumen. The popliteal vein, both above and below the knee was studied to the region of its trifurcation. Routine imaging and compression of the proximal 1-2 cm of the posterior tibial vein was also performed. A decubitus position, opposite to the side examined was another alternative position if the patient could not be in the prone position. The distal aspect of the leg to be examined was elevated with towels so that it was in the same level as the femoral vein. The interpretation of the ultrasonographic studies was based on the compressibility alone. A complete compressible vein was interpreted as normal. Partial or noncompressible vein was compatible with DVT.

The results of the compressive sonography was compared with those obtained from the contrast venography. The causes of the false positive and false negative ultrasonographic results was analyzed.

Results

Twenty-five contrast venographies were performed, 13 studies were interpreted positive for DVT and 12 studies negative for DVT. In the venographic positive DVT patients, the ultrasonography showed 11 DVT positive studies and 2 DVT negative studies. All of the venographic negative studies also showed to be negative ultrasonographic studies. So, the compressive ultrasonography has a sensitivity of 86% and a specificity of 100%.

In one of the two false negative ultrasonographic studies, the venogram showed only non-filling of the anterior tibial vein but the popliteal vein was normal. Another ultrasonographic false negative patient showed occlusion of the superficial femoral vein and a patent saphenous vein was misinterpreted as a patent superficial femoral vein.

Visualization of the vein below the popliteal vein was poor. Only few cases that the proximal tibial or peroneal veins were observed and it was difficult to assess the compressibility of the lumen.

The normal ultrasonographic study was shown in Figure 1, one of the ultrasonographic positive case was shown in Figure 2 and the one false negative case was illustrated in Figure 3.

Discussion

Venous thrombi will typically form within the muscular venous plexi of the calf and spread contiguously to the tibioperoneal veins. In 20% of cases they spread to the popliteal venous segment and the superficial femoral vein, and finally involve the common femoral vein. This pattern of involvement is thought to occur in the majority of lower extremity DVT cases. Occasionally, there is thrombus spreading to the iliac veins and into the inferior vena cave (6). Studies looking into the location of DVT after an episode of symptomatic pulmonary embolism have shown the involvement of femoral or popliteal veins in most instances (7). In 10 to 20% of cases, only calf vein thrombi have been observed. The presence of obstructive venous thrombosis helps to stimulate the development of collateral pathways for blood flow. The perforating veins that communicate between the superficial and deep veins help to shunt the blood flow into the

greater and lesser saphenous veins. A collateral pathway through the deep muscular branches of the thigh often forms a path between the popliteal vein and the profunda femoris vein.

Venous ultrasound uses three important diagnostic criteria to determine the presence of acute deep vein thrombosis (8). The first is the direct visualization of thrombus as an echogenic structure lying within the lumen of the vein. The second is the measurement of the changes caused by the presence of thrombosis within the vein lumen. These indirect signs are passive distention of the vein by the acute thrombus and loss of normal venous compressibility when slight pressure is exerted on the skin overlying the vein. The third relies on the detection of a change in the flow dynamics within the vein.

The single most important criterion for making the diagnosis of acute deep vein thrombosis remains to be the loss of compressibility of the vein. A normal response is complete collapse of the lumen of the vein before any distortion in the artery. Loss of venous compressibility or failure to appose the luminal surfaces of the walls of a vein is considered diagnostic of acute vein thrombosis. This simple observation remains the most sensitive and most specific criterion for diagnosing acute obstruction and nonobstructing deep venous thrombosis of the femoral and popliteal venous segments.

The sensitivity of 87% and specificity of 100% was quite similar to the reports from many authors (3, 9 ,10, 11, 12) One of the false negative ultrasonographic study was that the patient had thrombosis in anterior tibial vein only. Many investigators believed that clot limited to a calf location was ultimately of little clinical significance, but the possibility of extension to the popliteal system did exist. (13) The another false negative case of us could actually not have happened if we examined the misinterpreted veins more carefully.

The sources of error during venous compression ultrasound stated by Polak (8) were 1. below-knee (infrapopliteal) thrombus 2. segmental vein incompressibility (adductor canal) 3. possible chronic DVT 4. nonobstructing focal DVT 5. vein duplication 6. iliac vein thrombosis and 7. Profunda femoris DVT.

References

1. Hirsh J, Hill RD, Raskob GE. Clinical features and diagnosis of venous thrombosis. J Am Coll Cardiol 1986: 8: 114B-127B.
2. Bettmain MA, Robbins A, Braun SD, et al: Contrast venography of the let: Diagnostic efficacy, tolerance and complications ratio with ionic and non-ionic contrast media. Radiology 1987, 165: 113-116.
3. Cronan JJ, Dorfman GS, Scola FH, Scheppes B, Alexander J. Deep vein thrombosis: US assessment using vein compression. Radiology 1987; 162: 191-194.
4. Raghavendre BN, Horh SC, Hilton S, Subramanyam BR, Rosen RJ, et.al. Deep venous thrombosis: Detection by probe compression of vein. J Ultrasound med 1986; 5: 89-95.
5. Rabinov K, Paulin S. Roentgen diagnosis of venous thrombosis in the leg. Arch Surg 1972; 104: 134-144.
6. Browse N. Diagnosis of deep vein thrombosis. Br Med Bull 1978; 34: 163-167.
7. Browse NL, Thomas M. Source of non-lethal pulmonary emboli. Lancet 1974; 1: 258-259.
8. Polak JF. Peripheral vascular sonography. A practical guide. Baltimore: Williams & Wilkins, 1992.
9. Sullivan ED, Peter DJ, Cranley JJ. Real-time B mode venous ultrasound. J Vasc Surg 1984; 1: 465-471.
10. Ragjavendra BN, Rosen RJ, Lam S, Rile S, Horii SC. Deep venous thrombosis: Detection by high-resolution real-time ultrasonography. Radiology 1984, 152: 789-793.
11. Ojarasporn V, Ekmahachai M., Sivasomboon C, Prapakorn V. Ultrasound diagnosis of deep vein thrombosis. Thai J. of Radiology 1990, 27: 101-109.
12. Salzman EW. Venous thrombosis made easy. N Engl J Med 1986; 314: 847-848.
13. Moreno-Cabral R, Kistner RL, Nordyke RA. Importance of calf vein thrombophlebitis. Surgery 1976, 80: 735-742.

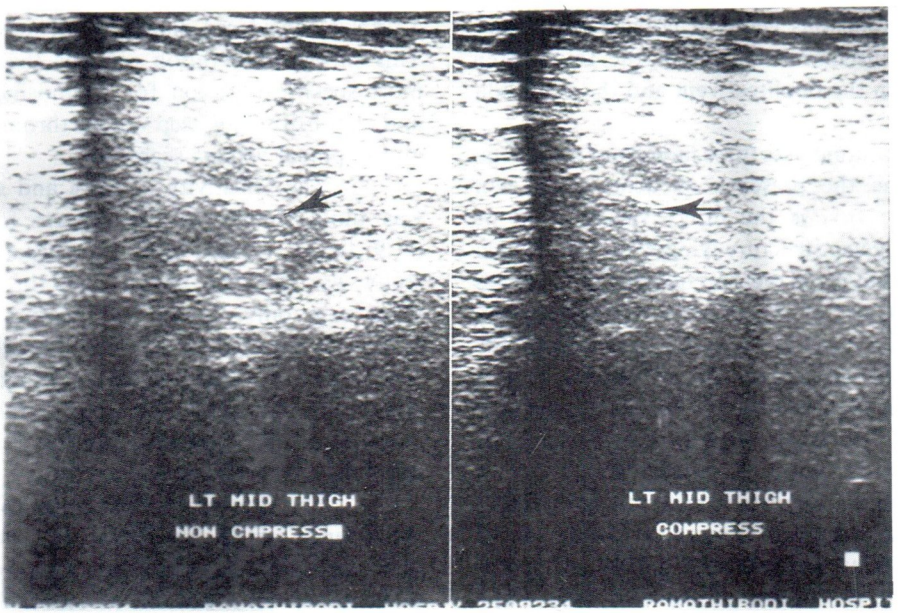

Fig. 1a left - non compressed ultrasonographic study of the femoral vein at mid thigh
right - compressed ultrasonographic study of the femoral vein at mid thigh showed completely collapsed venous lumen (arrow).

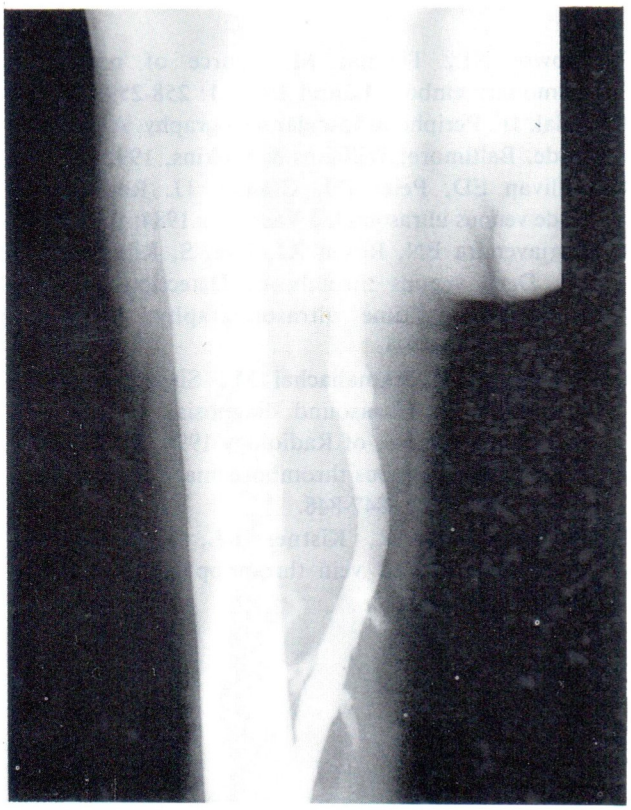

Fig. 1b normal venography at mid thigh, the level of the above ultrasonographic study.

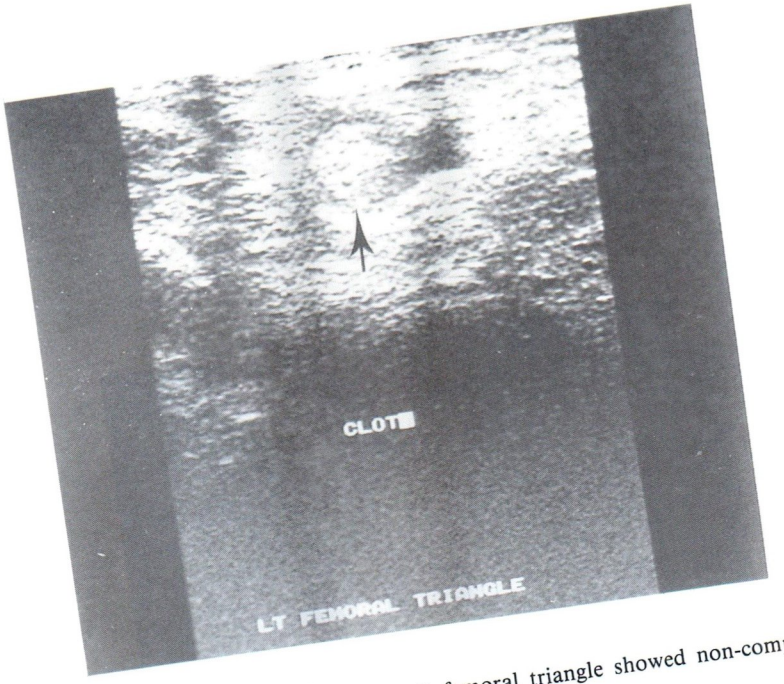

Fig. 2a Compressed ultrasonographic study of the lt femoral triangle showed non-compressible vein with clot inside, a true positive case.

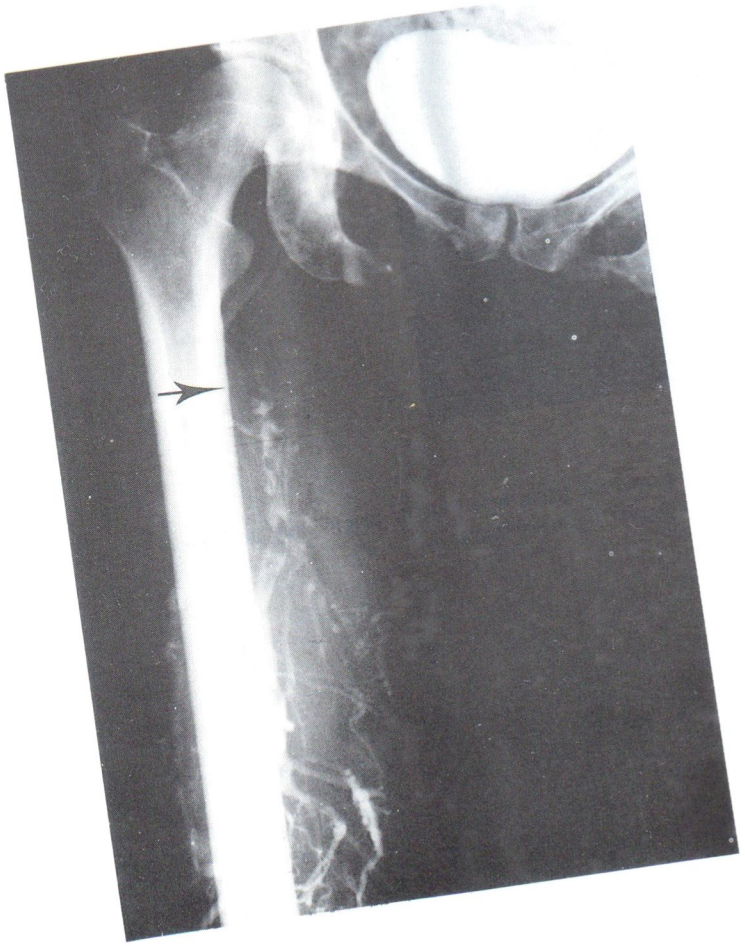

Fig. 2b Contrast venography, corresponding level of sonography was arrowed.

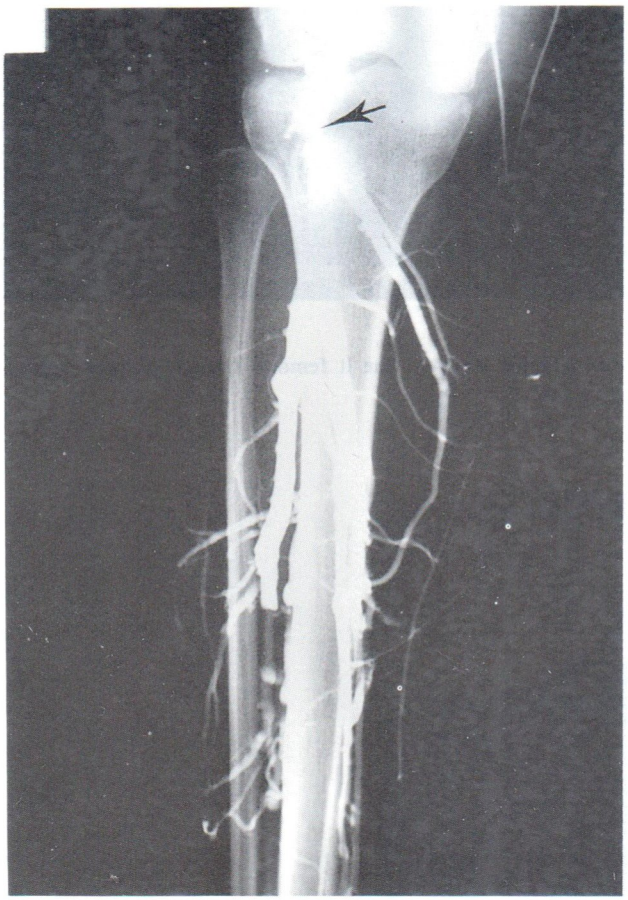

Fig. 3 contrast venography showed complete occlusion of the anterior tibial artery at its origin only and the rest of the deep vein appeared normal, producing false negative ultrasonography.

BENIGN VS MALIGNANT THYROID NODULES:SONOGRAPHIC EVALUATION

R. Supartmeta[1], P. Pekanan[1],
J. Chatchavala[1], S. Hiranpat[1]

Abstract.

Retrospective review of the ultrasonographic examination of the 119 thyroid nodules was performed. All cases had surgically and pathologically proved. The study included 64 benign and 53 malignant nodules. Definitive findings for benign nodules were purely cystic and predominantly cystic mixded nodules and for malignant nodules were extrathyroidal muscular invastion, vascular encasement and cervical lymphadenopathy. The suggestive findings for malignant nodules were hypoechoic solid pattern and rim calcification. The inconclusive findings were the features of the margin of the nodules, hetero or homogeneity of the tissue, iso and hyperechoic solid nodules.

Key words: Thyroid nodules, Ultrasonography

Introduction

Nodular thyroid disease is a relatively common disorder. In the patient with nodular thyroid disease the clinical challenge is to distinguish the malignant nodules from the benign ones and to identify those patients for whom surgical excision is indicated. The ability of high-resolution sonography to depict small, nonpalpable thyroid nodules is unsurpassed by any other imaging method. Solid nodules as small as 3 mm and cystic nodules as small as 2 mm can be visualized sonograhically. No single sonographic criterion can reliably differentiate all benign thyroid nodules from malignant nodules. We, therefore, reviewed the sonographic thyroid nodules examinations, to evaluate which sonographic characters could help to differentiate benign from malignant nodules.

Materials and Methods

A retrospective study of the thyroid nodules by ultrasonography was performed during the year 1986 to 1992 in Ramathibodi Hospital. Only the nodules that were surgically removed and pathologically examined were included. There were 64 benign nodules and 53 malignant nodules. The sonographic examination of the neck was performed with the patient in a supine position. The patient's neck was hyperextended. High frequency 7.5 MHz transducer was used. The sonographic features of the thyroid nodules, including margination, the presence of the hyperechoic foci or calcification, the echo pattern and extrathyroidal invasion or cervical lymphadenopathy were analyzed.

[1]Department of Radiology, Faculty of Medicine,
Ramathibodi Hospital, Rama 6 Street, Bangkok 10400, Thailand

Results

Table 1. Pathologic diagnosis of 117 thyroid nodules and number of the nodules for each pathology

Pathologic dx		No. (% of total benign or malignant nodules)
BENIGN:	Nodular goiters	43 (67)
	Adenoma	15 (24)
	Cystadenoma	6 (9)
	Total	64 (100)
MALIGNANT:	Papillary carcinoma	31 (58)
	Follicular carcinoma	13 (25)
	Mixed papillary&follicular CA	7 (13)
	Hüerthle cells tumor	1 (2)
	Medullary carcinoma	1 (2)
	Total	53 (100)

Note: Coexistent multinodularity included 4 cases of multinodular goiter, 1 case of triple nodules of cystadenoma, 2 cases of nodular goiter and papillary carcinoma, 2 cases of multicentric mixed papillary and follicular carcinoma, 5 cases of multicentric papillary carcinoma and one case of multicentric follicular carcinoma.

Table 2. Correlation of the margin of the nodules with the numbers of the benign and malignant nodules

Features of the margin	No. (%) of benign N.	No. (%) of malig. N.
Well defined (± Halo sign)	39 (53%)	34 (46%) Total 73
Ill defined	25 (57%)	19 (43%) Total 44
Note: No. of the benign nodules with halo sign was 19 (30%)		
No. of the malignant nodules with halo sign was 17 (32%)		

Table 3. Presence or absence of hyperechoic foci or calcification in the nodules, correlating with benign and malignancy

Calcification in the nodules	No. (%) of Benign N.	No. (%) of malign. N.
Presence	15 (23)	30 (57)
Absence	49 (77)	23 (43)
Note: Rim calcificatioin was found in 2 follicular carcinoma, 1 mixed papillary follicular carcinoma and 1 adenoma		

Table 4. Correlation of echo pattern with the numbers of benign and malignant nodules

Echo pattern	No.(%) of benign N.	No. (%) of malignant nodules	
Pure cystic nodules	3 (100)	0 (0)	T = 3
Mixed pattern cystic predominant	18 (100)	0 (0)	T = 18
	20 (59)	14 (41)	T = 34
Solid pattern solid predominant	23 (37)	39 (63)	T = 62

Table 5. Homogeneity and heterogeneity of the echo in solid pattern nodules with the number of the benign and malignant nodules

	No. (%) of benign N.	No. (%) of malignant N.	
Homogeneity	3 (43)	4 (57)	T=7
Heterogeneity	20 (36)	35 (64)	T=55

Table 6. Echogenicity of the solid pattern, correlating with the benign and malignancy

Echo pattern	No. (%) of benign N.	No. (%) of Malignant N.	
Hypoechoic	5 (23)	17 (77)	T=22
Iso or hyperechoic	18 (45)	22 (54)	T=40

Table 7. Correlation between the extrathyroid invasion and types of malignant nodules

Extension of lesion	Histology of malignant nodules
Cervical lymphadenopathy alone	Papillary Ca (2 cases)
Invasion of Strap muscles alone	Follicular Ca (2 cases)
	Papillary Ca (1 case)
Invasion of Strap muscles and longus colli muscle	Follicular Ca (1 case)
Invasion of Strap m., longus colli m. encasement of carotid a. and cervical lymphadenopathy	Medullary Ca (1 case)

Note: No benign nodules were associated with extrathyroidal involvement

Discussion

Most thyroid nodules are not true neoplasms of the thyroid gland but are due to cycles of hyperplasia and involution of thyroid lobules that result in fusion of localized colloid-filled follicles and are known as colloid or adenomatous nodules (1). The desscriptive terms adenomatous goiter, nontoxic nodular goiter, and colloid nodular goiter are used interchangeably when multiple nodules such as these are present in an otherwise normal patient (1). Epithelial-lined, simple thyroid cysts are rare pathologically (1). The benign follicular adenoma, unlike a colloid nodule, is a true thyroid neoplasm characterized by complete fibrous encapsulation of the nodule. Adenomas are not believed to have malignant potential (1). The overwhelming majority of thyroid nodules are benign (2,3,4). The relatively small benign nodules in our study was due to medical treatment in many benign nodules. Primary thyroid cancer can occur in several histologic forms. Papillary carcinoma (including the so-called mixed papillary and follicular carcinoma) is the most common form of thyroid cancer, accounting for 75-90% of all cases (5,6). Similar incidence was also shown in our series.

The appearance of the outer margin was not a reliable indicator to differentiate between benign and malignant nodules, agreeable by the opinion of Charboneau et al (1).

Calcification can be detected in 13% of all thyoid nodules, and the location and pattern of calcification has predictive value to distinguish benign from malignant lesions (7). Peripheral or egg-shell like calcification is a reliable feature of a benign nodule but occurs in only a small percentage of benign tumors (1). We had several cases of rim calcification in slightly more number in malignant nodules, probably due to the analysis in our series was done only in the operated nodules and had discarded many benign ones which has not been operated upon. When the internal calcifications are fine and punctate throughout the nodule, papillary cancer is a very likely diagnosis but if they are multiple, large and coarse, the benign noduldes are most likely (1). We have

found hyperechoic foci or calcification only twice in the malignant nodules, in comparison with those shown in benign nodules; however, the pattern of the calcification was not analyzed.

A nodule that has a significant cystic component is usually proved to be a benign colloid nodule or an adenomatous nodule that has undergone central degeneration or hemorrhage. Rarely, thyroid cancer, particulary the papillary variety, may exhibit varying amounts of cystic changes and can appear indentical to a benign degenerated adenoma (8,9). We did not found purely cystic nodules or cystic predominant mixed nodules to be malignant nodules, all were benign nodules. The solid nodules with or without homogeneity of the tissue occured in similar incidence in benign and malignant nodules. The hypoechoic solid nodules occured three times more in malignant nodules than the benign ones. If we considered that the benign nodules occured more than malignant nodules, then statistically, probably more benign nodules contains hypoechoic character (1). The iso or hyperechoic nodules were seen slightly more in malignant nodules, the opposite thing was reported by Solbiati et al (7).

The halo sign was seen equally in benign and malignant nodules in our series. It had been found in the other series in 70% of benign nodules (10) and in 15% of thyroid cancer (7,11). Histologically, it is not known whether this halo represents the capsule of the nodule or compressed adjacent thyroid parenchyma. In some cases, color Doppler flow imaging has shown that the halo is caused by vessels located around the periphery of the nodules. More recently, it has been proposed that a thin, complete peripheral halo is more likely to be seen with a benign nodule, whereas a thick, incomplete halo is more suggestive of malignancy (7). Color Doppler flow imaging has been reported to show increased vascularity with autonomously functioning thyroid adenomas as well as with thyroid carcinomas (12,13)

In conclusion; from our data, the only definitive findings of benign nodules is purely cystic and predominantly cystic mixed lesion and for malignant nodules is extrathyroidal invasion and cervical lymphadenopathy. Internal calcification occurred twice more in malignant nodules whereas hypoechoic solid pattern occurred three times more in malignant nodules. Other features were seen in similar incidence in both benign and malignant thyroid nodules.

Reference

1. Charboneau JW, Reading CC and James EM. Thyroid, Parathyroid and Cervical lymph Nodes. In : Wilson SR eds. American Roentgen Ray Society, Ultrasound; Categorical Course Syllabus. 1993: 217-225
2. James EM, Charboneau JW, Hay ID. Thyroid sonography. In: Rumack CM, Wilson SR, Charboneau JW, eds. Diagnostic Ultrasound. ST. Louis: Mosby Year Book, 1991
3. Rojecski MT, Gharib H. Nodular thyroid disease: evaluation and management. N Engl J Med 1985; 313: 428-436
4. Van Herie AJ, Rich P, Ljung B-ME, et al. The thyroid nodule. Ann Intern Med 1982:96: 221-232
5. Hay ID. Thyroid cancer. Curr Ther Hematol Oncol 1988: 3:339-342
6. Hay ID. Thyroid nodules and thyroid cancer. Med Interne 1989: 63: 2601-2604
7. Solbiati L, Vincenzo C, Ballarati E. Ultrasonography of the neck. RCNA Sept. 1992: 30(5): 941-954
8. de los Santos ET, Keyhani RS, Cunninghamm JJ; Mazzaterri EL. Cystic thyroid nodules: the dilemma of malignant lesions. Arch Intern Med 1990, 150: 1422-1427
9. Hammer M, Wortsman J, Folse R. Cancer in cystic lesions of thethyroid. Arch Surg 1982: 117: 1020-1023
10. Scheible W, Leopold GR, Woo VL, et al. High resolution real time ultrasonography of thyroid nodules. Radiology 1979; 133: 413-417
11. Propper RA, Skolnick ML, Weinstein BJ, et al. The nonspecificity of the thyroid halo sign. JCU 1980: 8:129-132
12. Fobbe F, Finke R,Reichenstein E, et al. Apprearance of thyroid diseases using color -coded duplex sonography. EUR J Radiol 1989: 9:29-31
13. Hodgson KJ, Lazarus JH, Wheeler MH, et al. Duplex scan derived thyroid blood flow in euthyroid and hyperthyroid patients. World J Surg 1988: 12: 470-475

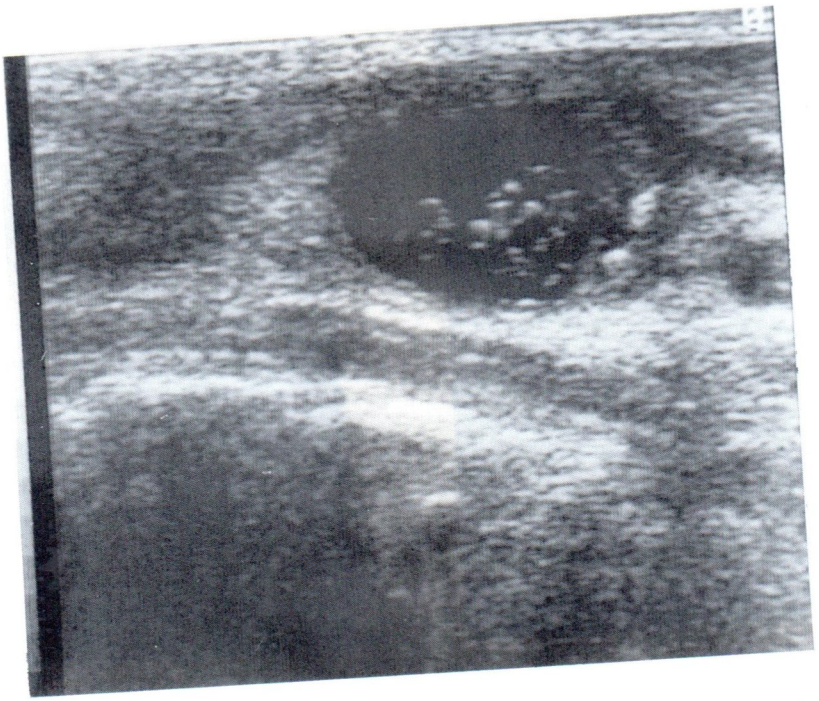

Fig.1 Nodular goiter. Two calcified foci at periphery of the mixed predominant cystic nodule.

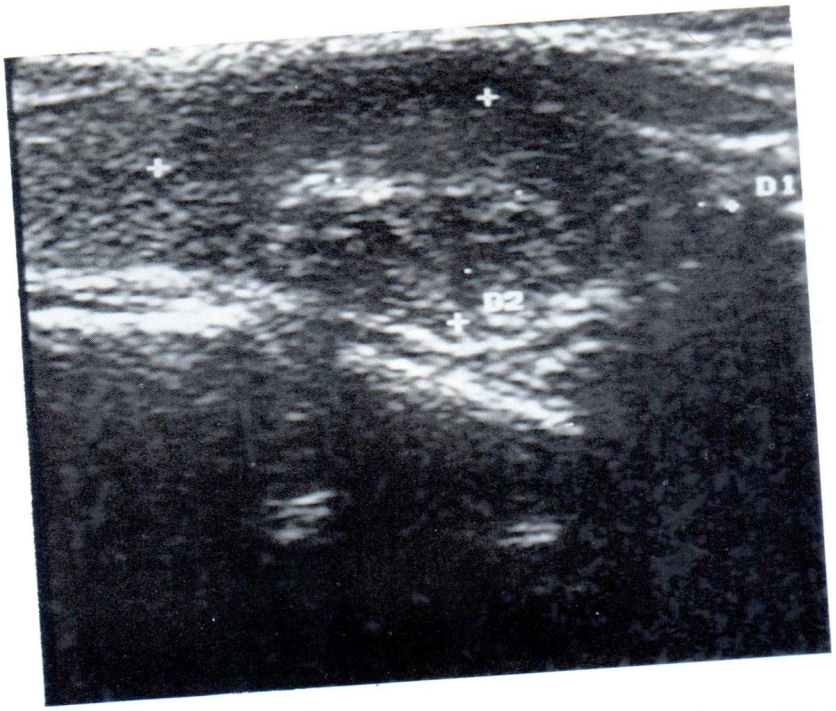

Fig.2 Papillary carcinoma. Calcified or hyperechoic foci in the solid (Hypo + Hyperechoic) nodule

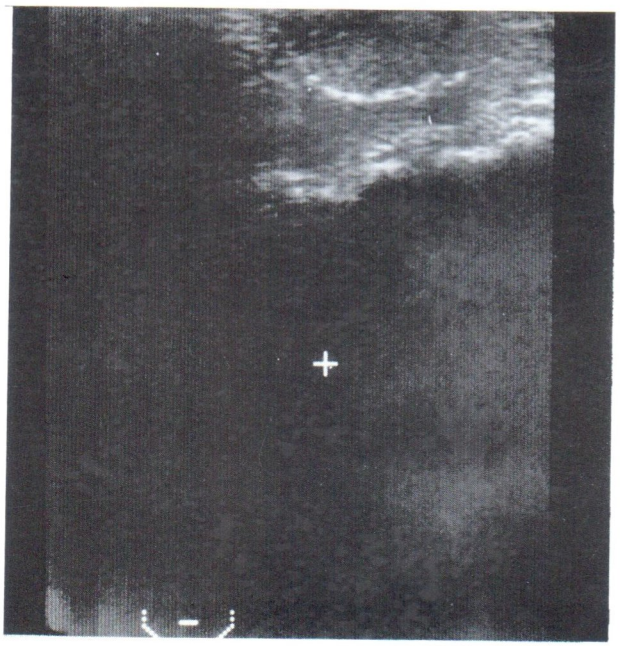

Fig.3 Papillary-folicular carcinoma.
Hypo + hyperechoic nodule with calcified rim.

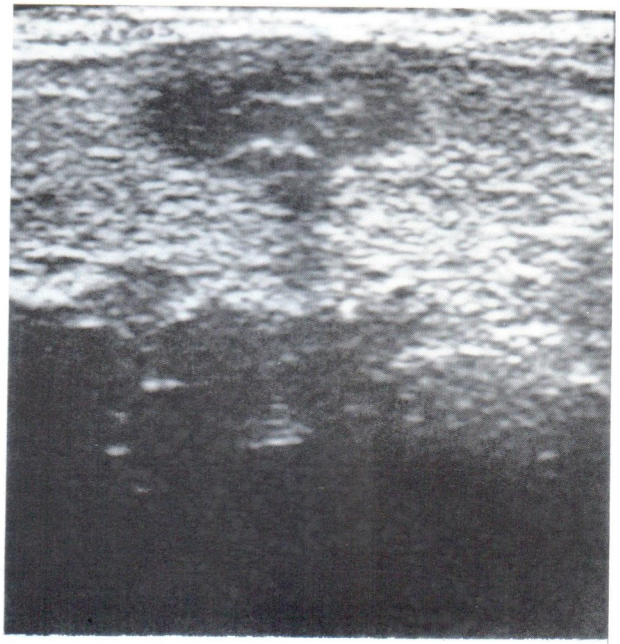

Follicular carcinoma.
Calcification in low echoic nodule.

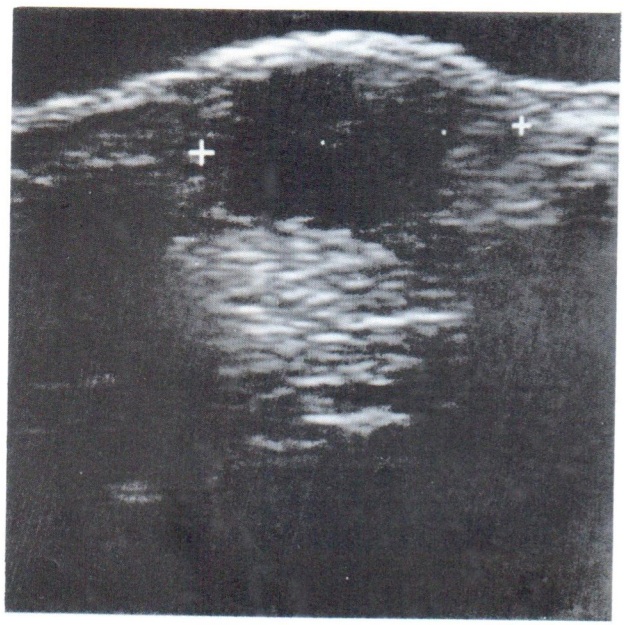

Fig.5 Nodular goiter. Mixed echoic pattern, with cystic predominant nodule.

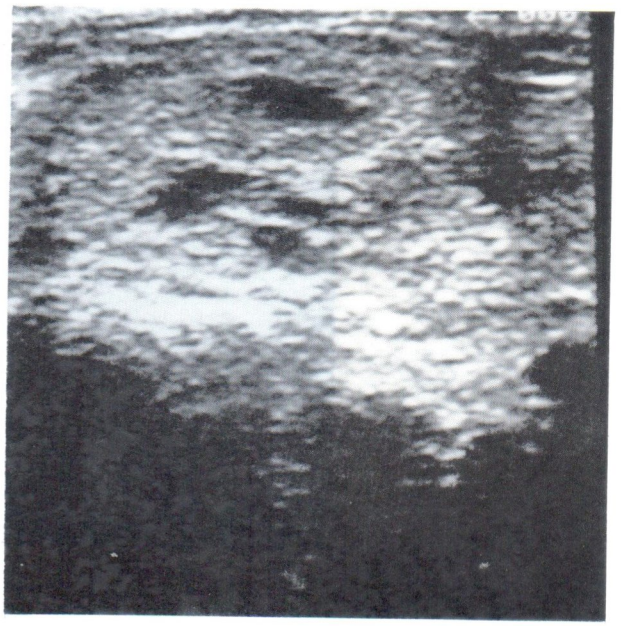

Fig.6 Nodular goiter. Mixed echoic pattern, with solid predominant nodule.

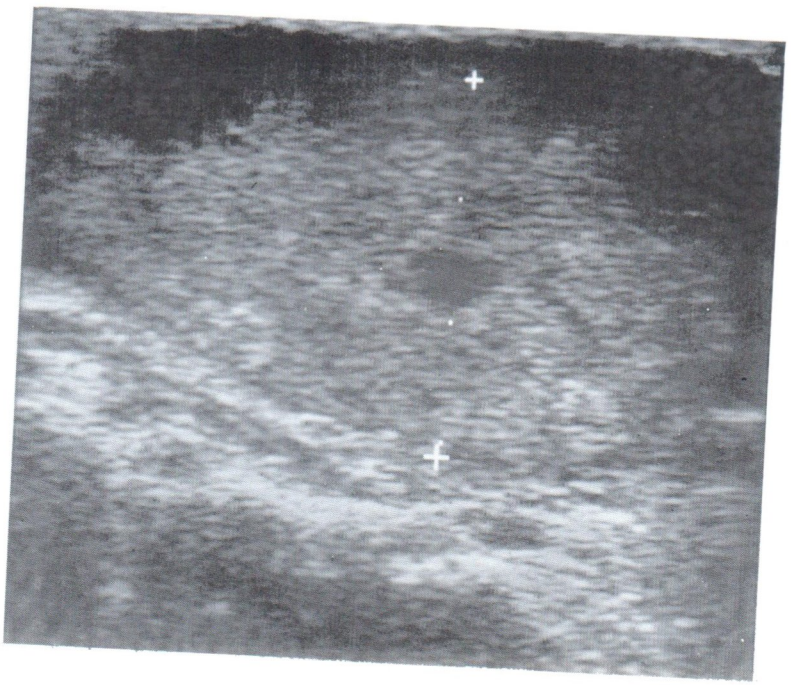

Fig.7 Follicular carcinoma. Mixed echoic pattern, predominantly solid pattern nodule.

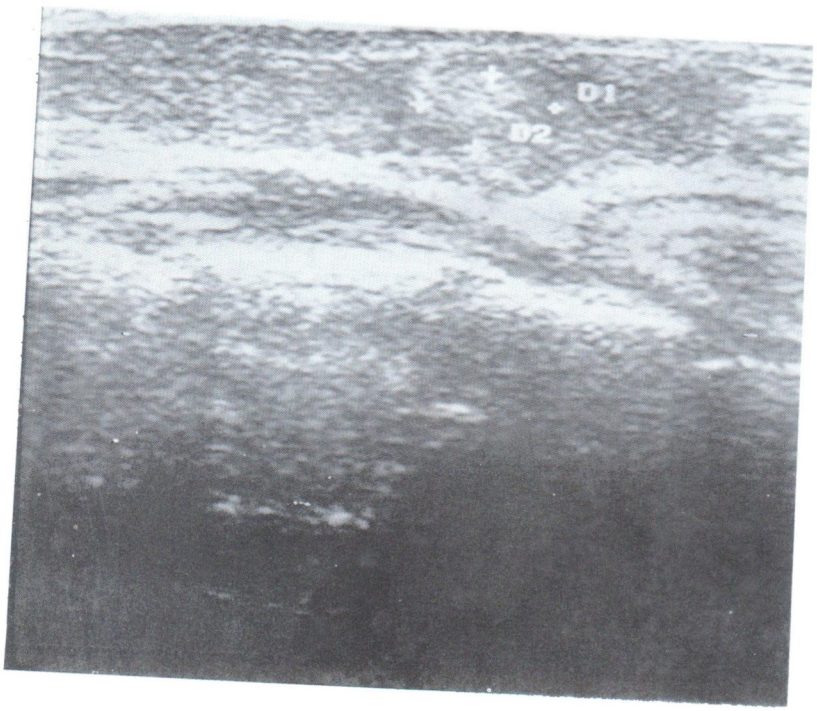

Fig.8 Papillary carcinoma. Hyperechoic solid nodule.

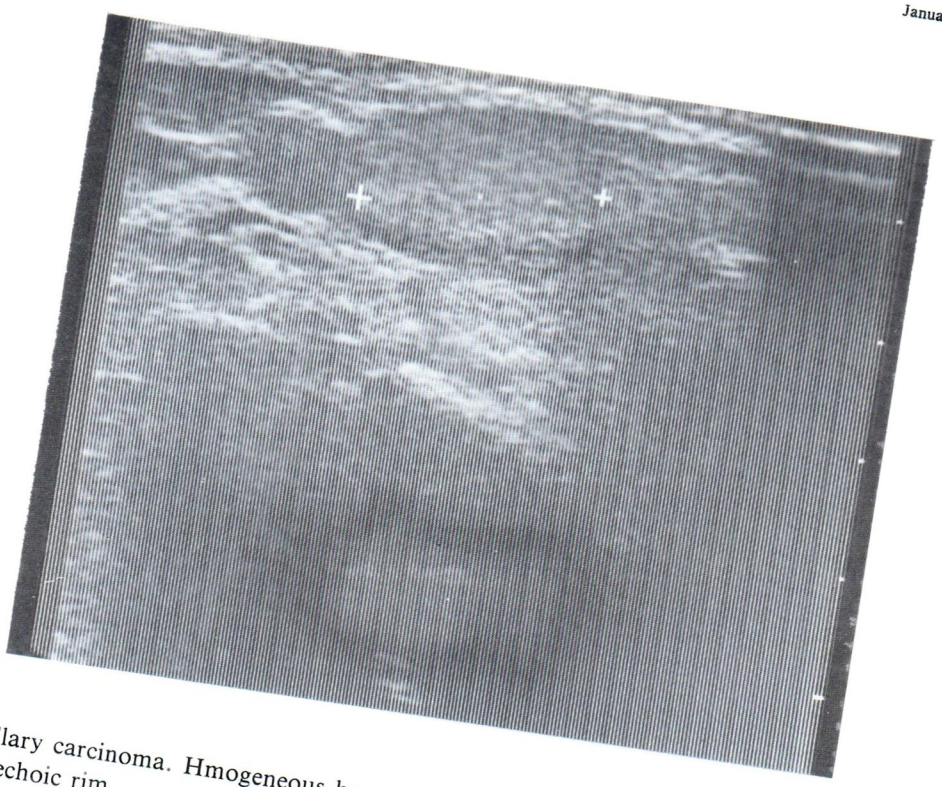

Fig.9 Papillary carcinoma. Hmogeneous hyperechoic nodule with well defined margin and partially hypoechoic rim.

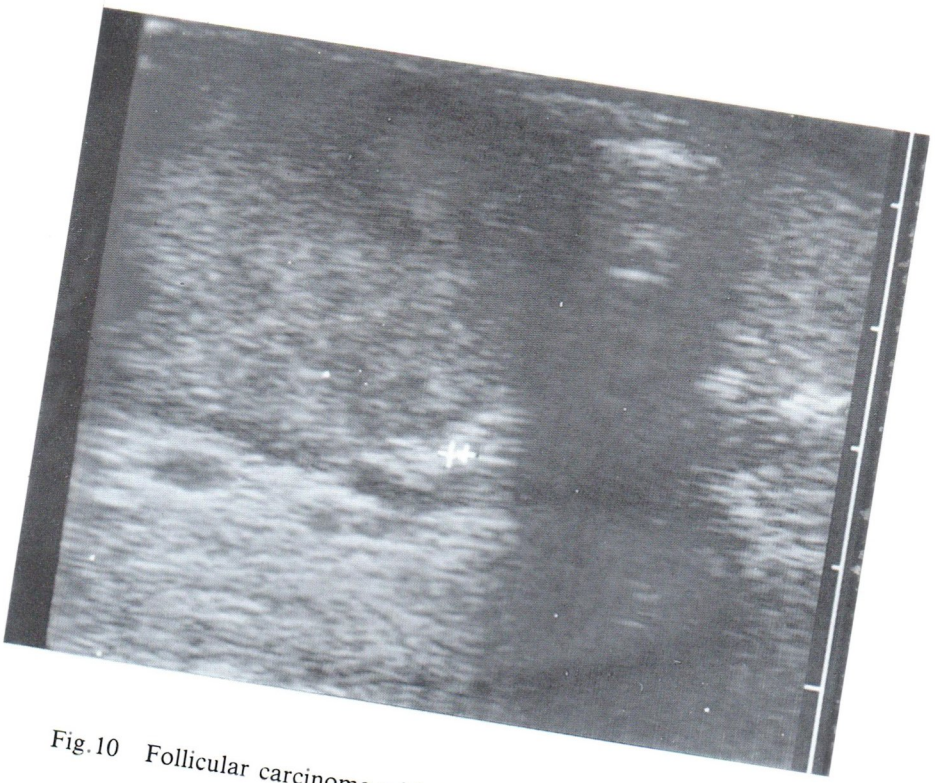

Fig.10 Follicular carcinoma with invasion of the strap muscle.

THE ASEAN JOURNAL OF RADIOLOGY

Excavated endoexoenteric form of lymphoma

P. Pekanan[1], S. Nirapathopongporn[1],
S. Chaovisit[1], P. Siriwongpairat[1]

Pictorial Essay

The principal radiologic features of lymphoma of the small bowel, as described by Marshak and colleagues (1) were multiple nodular defects, an infiltrating form, a polypoid form (intussuscepting), an endoexoenteric form with excavation and fistula formation, and a predominantly mesenteric invasive form with extraluminal masses. Aneurysmal dilatation has been considered the major radiologic finding in some reports (2). The infiltrating form was the most frequent radiologic finding, closely followed by the cavitary form (3).

Replacement of the muscularis and destruction of the autonomic nerve plexus by lymphoma may cause the bowel wall to give way and bulge focally. Aneurysmal dilatation tends to involve predominantly the unsupported, antimesenteric side of a small bowel segment. The contour may revert to normal after treatment; however, perforation is a life-threatening complication (4). For this reason, complete resection should be attempted whenever possible before chemotherapy (5).

Focal infiltration may lead to localized perforation into a sealed-off space, usually between the leaves of the mesentery. This cavitary form of non-Hodgkin's lymphoma usually denotes a primary small bowel origin. The irregular contour of the excavation, its relation to the mesenteric border of a small bowel loop, the fact that it contains air and debris and the generally thin soft tissue space separating it from adjacent bowel, distinguish cavitary lymphoma from a barium-containing cavity within an exoenteric leiomyosarcoma. An aneurysmal dilatation or sacculation may superficially resemble the lymphomatous cavity; it is, however, likely to involve the antimesenteric side of a bowel segment and to be in continuity with the bowel lumen proximally and distally. Cavitary lymphoma requires surgical excision, at times of a considerable extent of the involved bowel.

References

1. Marshak RH, Lindner AE, Maklansku D: Lymphoreticular disorders of the gastrointestinal tract: roentgenographic features. Gastrointest Radiol 4: 1030120, 1978.
2. Craig O, Gregson R: Primary lymphoma of the gastrointestinal tract. Clin Radiol 32: 63-71, 1981.
3. Gilchrist AM, Herlinger H, Carr RF, et al: Small bowel lymphoma, a radiologic pathologic correlation. In Herlinger H, Megibow A (eds): Gastrointestinal Radiology Review, Volume 1. New York: Marcel Dekker, 1990, pp 187-211.
4. Maglinte DDT: Malignant tumors. In Gore, Levine, Laufer (eds): Textbook of gastrointestinal radiology, Volume 1. Philadelphia: W.B. Saunders Company, 1994, pp. 916.
5. Baildam AD, Williams GT, Schofield PF: Abdominal lymphoma-the place for surgery. J R Soc Med 82: 657-660, 1989.

[1] Department of the Radiology, Ramathibodi Hospital, Rama 6 Street, Bangkok 10400, Thailand.

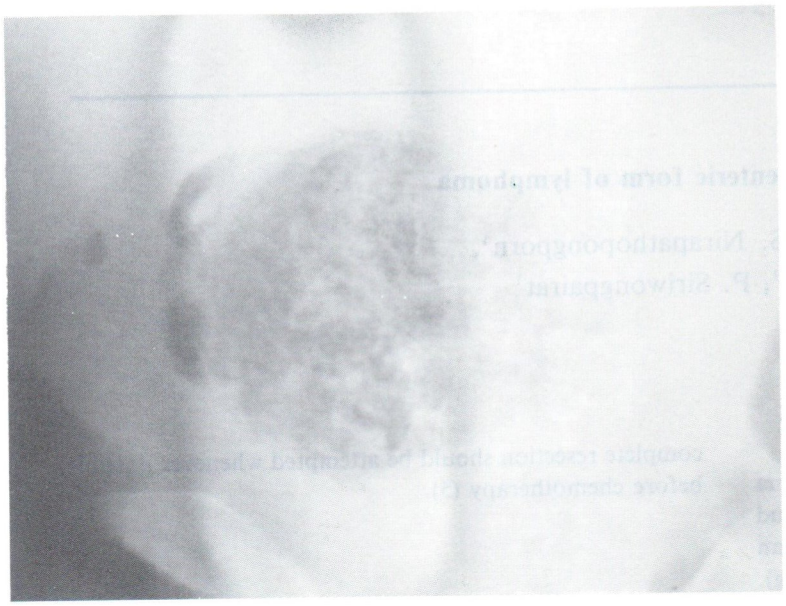

Fig. 1 Plain film of the abdomen showed gas containing mass at rt, paramedian upper part of the abdomen, simulating gauze abscess. The film was obtained when the patient had abdominal pain, post 600 rads radiotherapy for malignant lymphoma.

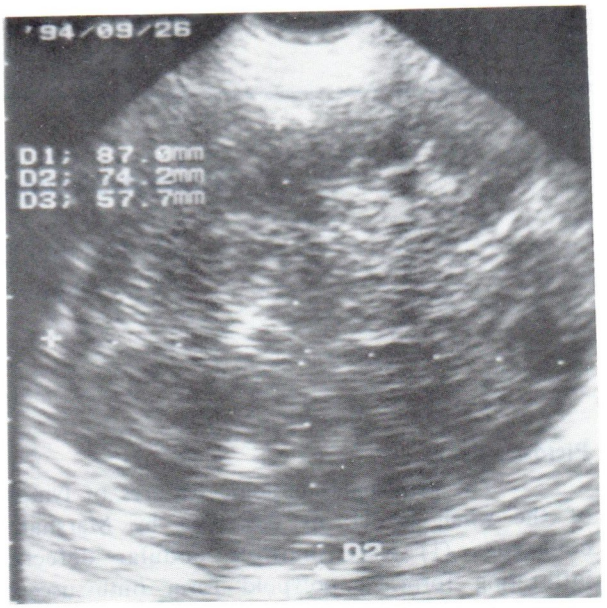

Fig. 2 Ultrasonography in the region of the mass showed round mixed hypo and hyper-echoic pattern.

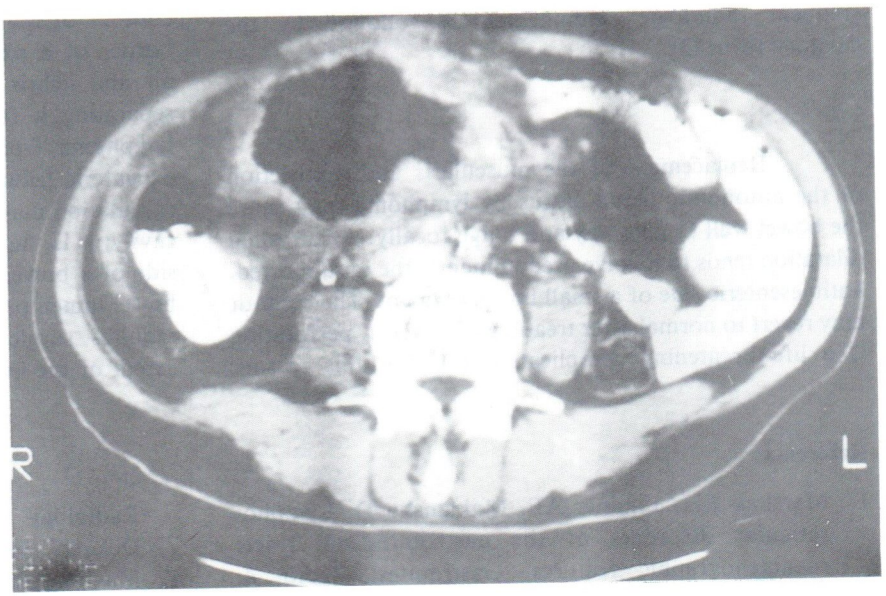

Fig. 3 Large mass in the abdominal cavity with large cavity and thickened irregular wall, oral contrast CT scan of the region of the mass.

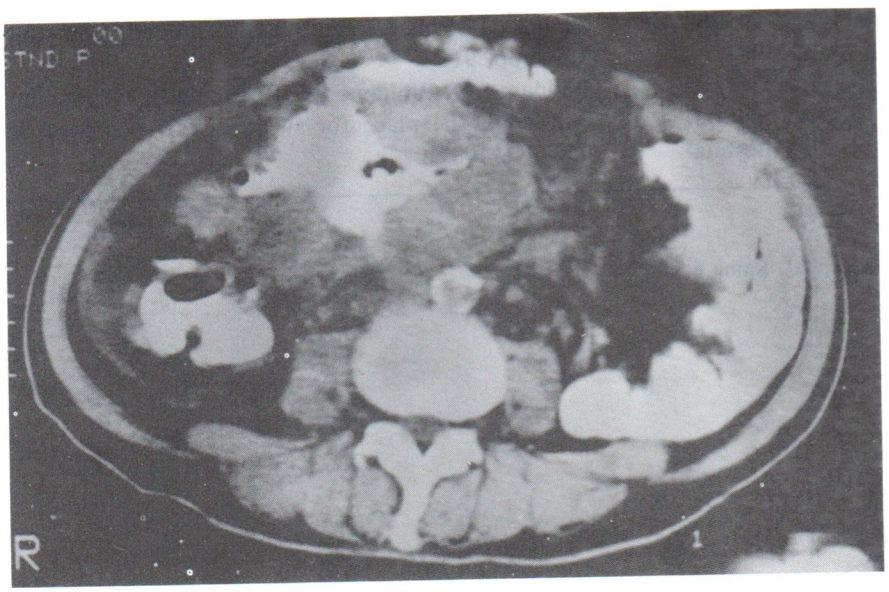

Fig. 4
The mass contains the ingested contrast medium in the previously mentioned cavity in Fig. 3, indicating continuation of the cavity with the bowel lumen.

Spiral CT Angiography in the Olfactory groove meningioma with 3-D Reconstruction.

K. Osathavanichvongs[1], P. Pekanan[2], A. Prapa sinsap[3], P. Jaroensuwan[4]

Pictorial Assay

Spiral CT angiography is a news, minimally invasive technique for vascular imaging,calcified and densely enhanced lesion imaging that made possible by combining two recently developed techniques: slip-ring CT scanning and computerized three-dimensional (3D) reconstruction (1). The purpose of this essay is to illustrate the appearance of the densely calcified olfactory groove meningioma relating to the surrounding vessels, the base of the skull and the adjacent brain, using this technique.

Technique

At Urupong Medical Center, a spiral CT scanner capable of performing 32 rotations in 32 sec at 120 kV and 300 mA has been used (Elscint CT twin, Elscint Ltd., Haifa, Israel). The raw data from the 32 rotations can be processed to yield multiple overlapping in 32 sec, a high level of intravascular contrast can be maintained throughout the acquisition by mechanical injection of 100 ml of 300 mgI/ml contrast material via an antecubital vein at a rate of 2 mm/sec with a scan delay of 60 sec. A table speed of 3.75 mm/sec is used, and images of 2.5 mm-thick sections are reconstructed every 1 mm, resulting in a maximum of 150 images of 2.5 mm-thick sections, each of which overlaps 1.5 mm with its adjacent section. In obtaining the CT scan, a field of view 250 mm, zoom 1.25, 512 × 512 matrix is used.

Non i.v. contrast scan of the brain is performed to locate the lesion, and to determine the cut levels. Then the spiral CT angiography was performed to cover the whole lesion.

The CT data currently can be used to produce vascular images in three different ways: shaded surface display, maximum intensity projection, and curved planar reformatting (2). The figures in this article are examples of the shaded surface display technique plus cut 3D images which requires more time and operator input than the other techniques but the advantage that it provides excellent anatomic detail without visualization of overlapping structures. The program used allows the operator to define lower and upper Hounsfield unit that encompass the actual density of the opacified lumen, the bony structures, the calcified and enhanced lesion (highlight threshold technique). The volume definition technique with manual subtraction of the irrelevant structures is combined using connecting algorithm. Later the 3D images (done by loading axial CT images and selecting multiple desired plane of CT images) is brought to superimpose the 3D surface images in the real-time mode. The processing time is 3 hrs.

The images obtained can help the neurosurgeons to plan for the operation better.

[1] Institute of scientific research, development and technology, Mahidol university, Pinklao-Nakornchaisri Street, Bangkok, Thailand.

[2] Department of Radiology, Ramathibodi Hospital, Rama 6 Street, Bangkok 10400, Thailand.

[3] Section of Neurosurgery, Prasat Hospital, Rajvithi Street, Bangkok, Thailand.

[4] Section of application specialists, Urupong medicall center, Theoddamri Street, Bangkok 10300, Thailand.

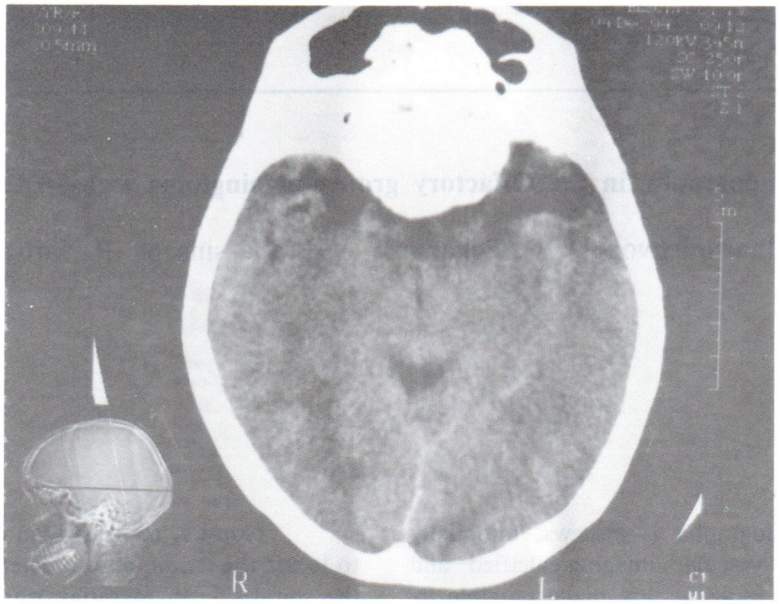

Fig. 1a Non i.v. enhanced CT scan of the brain at basal frontal region (third ventricular level). showed "bone density" round mass at midline basal frontal lobe, projecting into posterior frontal sinuses.

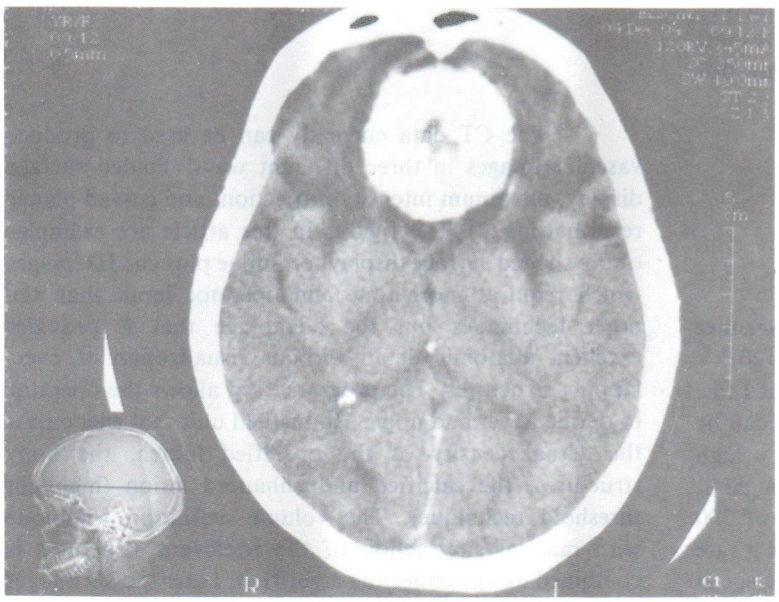

Fig. 1b Non i.v. enhanced CT scan of the brain at slightly higher level (inferior frontal horn level) showed this heavily calcified mass anterior to the frontal horns with surrounding brain edema.

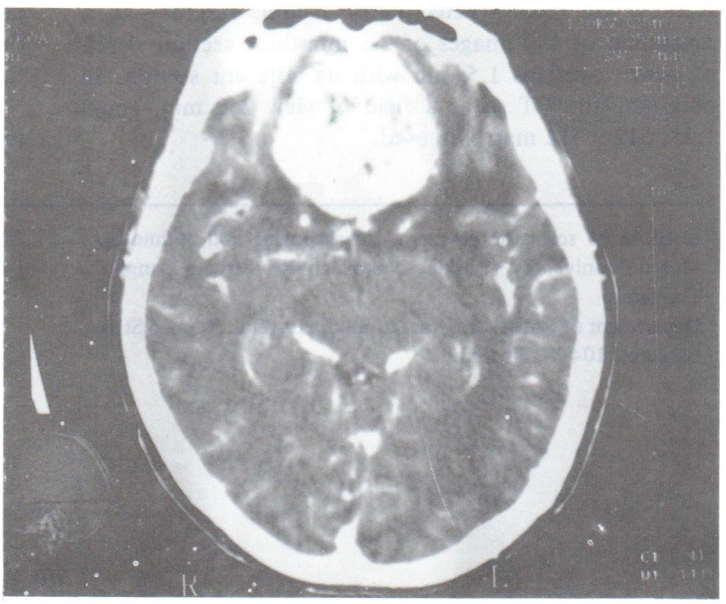

Fig. 2a I.V. enhanced CT scan of the brain at the mass region, showed no significant enhancement of the already dense mass.

January - April 1995 Volume I Number I

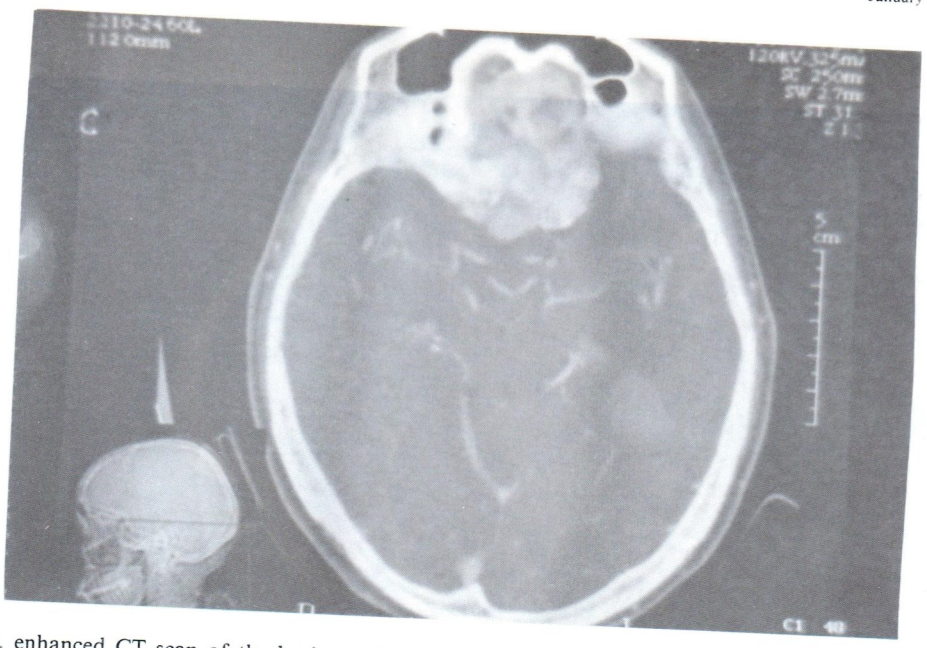

Fig. 2b I.V. enhanced CT scan of the brain at the mass region, adjusting window width and level showed soft part of the lesion.

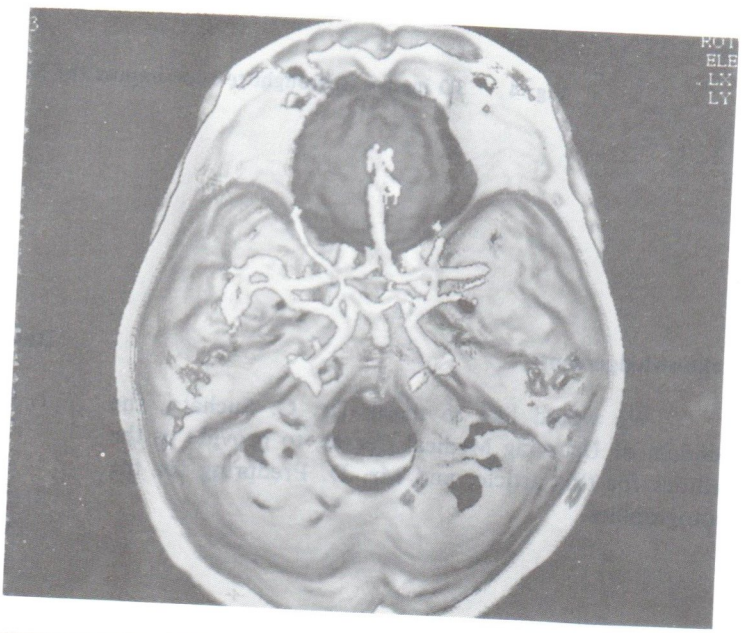

Fig. 3a 3D surface image of the mass, relating vessels and bony parts, view from above.

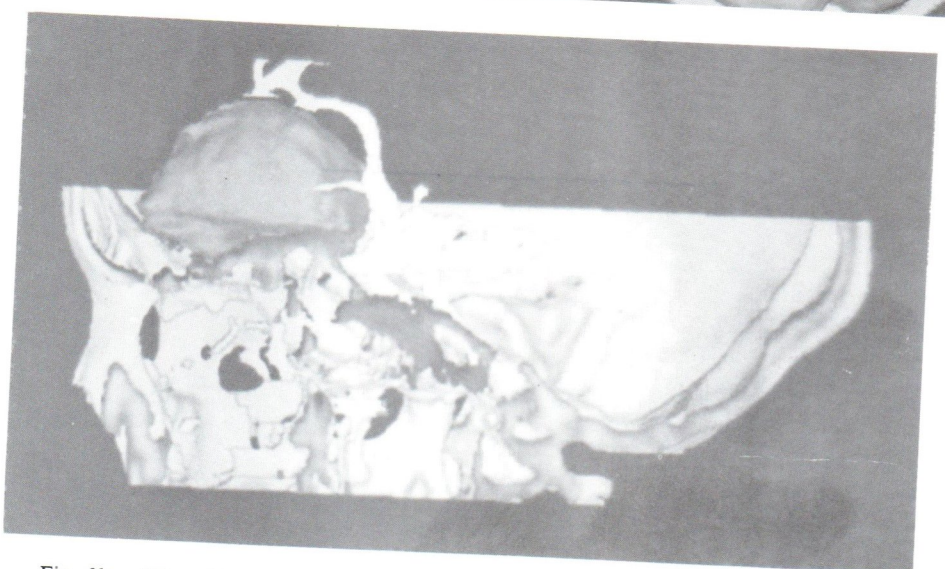

Fig. 3b 3D surface image of the mass, relating vessels and bony parts, side view.

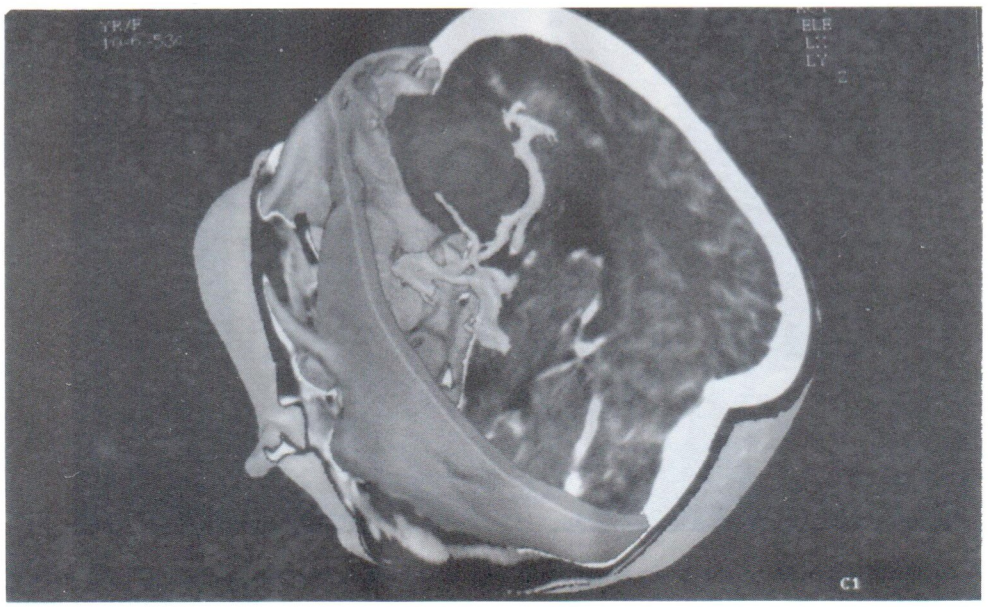

Fig. 4 3D images is brought to superimpose the 3D surface images in the real time mode.

Acknowledgement:

We would like to thank Dr. C. Suchato, the president of Urupong Medical Center, to provide us the facilities for this article, and Mr. D. Predpring for the photographies.

References:

1. Dillon EH, Leeuwen MSV, Fernandex MA, Mali WPTM. Spiral CT angiography. AJR 1993; 160: 1273-1278.
2. Vahlensieck M, Lang P. Chan WP, Grampp S, Genant HK. Three-dinensional reconstruction : parts I and II. Eur Radiol 1992; 2: 503-510.

Conventional Contrast Study in Demonstration of Branchial Cleft Fistula: A Report of Three Cases with Review of the Literatures.

Darunee Boonjunwetwat*
Varunee Stapatayawong**

Abstract:

Anomalies of the branchial apparatus are one of the common benign congenital neck mass. We have reported three cases of the branchial cleft fistula. One is the anomaly of the second branchial cleft and the other two cases are the anomaly of the third ones. Clinical presentations, rediographic contrast studies, revisions of the anatomy, embryology and differential diagnosis of the mass are included.

Key words: Branchial Cleft fistulae : radiograpic contrast studies. Revisions of Anatomy, Embryology and differential diagnosis. 3 cases report.

Abnormal remnants of the branchial cleft and pouch is one of the common benigh congenital neck mass. (2) Most branchial anomalies which present as fistulae, sinuses and cysts are considered to be derived from second branchial cleft remnants. Third and fourth branchial cleft sinuses are rare. (5)

METERIALS AND METHODS

Cases Report:

Case 1: A 34 years old man presented by a right neck mass with purulent discharge from a skin opening adjacent to the mass. The mass was noted since he was 4 years of age. He also had a feeling of discharges dripping in the right side of the pharynx corresponding to the neck mass. Physical examination revealed a cystic mass about 4×3 cm. in size with a small skin opening at the inferoposterior aspect of the mass situated at the lower part of the anterior border of sternocleidomastoid muscle. There was a purulent discharge coming out from the right tonsillar fossa when squeezing the cystic mass in the neck. The fistulogram was performed by injection of the contrast medium via the skin opening. The study showed the contrast medium filling the tract which is about 1 cm. in diameter and connected with the right tonsillar fossa of the oropharynx. (Fig. 1)

An operation was performed. The cystic mass was found beneath the sternocleidomastoid muscle with an external opening at the lower one third of the anterior border of this muscle. The fistulous tract was passing cephalad superficial to the common carotid artery and extending between the internal and external carotid artery with an internal opening into the right tonsillar fossa. Total excision was done and the final diagnosis was a second branchial cleft fistula.

* Chulalongkorn University Hospital.
** Bangkorlam Municipality Hospital.

Case 2: A 22 year old woman came with a complaint of sore throat and a left neck mass for 7 days. She has had the same symptoms repeatedly on and off for about 10 times since she was 10 years old. Recurrent suppurative thyroiditis was the provisional diagnosis. Her neck mass had disappeared after the inflammation subsided by medical treatment. She was treated with antituberculous drugs for two years without improvement. Incision and drainage of the neck mass was also performed three times in the past. Physical examination revealed a left neck mass, size about 4×4 cm. with signs of inflammation. The mass moved with swallowing. Surgical scars were also noted over the mass. After having been treated with antibiotics, the inflammation and the mass disappeared. Indirect laryngoscopy, later performed, was normal. Esophagogram revealed a tract originating from the apex of the left pyriform sinus and terminating in the area of the left lobe of thyroid gland, as shown in fig. 2.

Operation was performed with complete ligation of the tract.

Case 3: A 23 years old woman presented with a tender neck mass for 4 months. Previously, she had this same symptoms twice, three years and one year ago respectively. On each occasion, she was treated by antibiotics and drainage of pus with disappearance of mass and complete recovery of the inflammatory symptoms. Physical examination revealed left inflammatory thyroid nodule. The diagnosis of recurrent suppurative thyroiditis was given. The indirect laryngoscopy and fiberoptic laryngoscopy were performed but no abnormality were detected in the glottis or pyriform sinuses. No fistulous tract or opening can be demonstrated. Later, esophagogram was performed and a sinus tract was demonstrated at the left pyriform sinus terminating at the area of left lobe of thyroid gland as shown in fig. 3.

Operation was performed with complete ligation of the tract.

Discussion:

The branchial apparatus consists of a series of six mesodermal arches that are seperated from each other externally by ectodermally lined branchial clefts and internally by endodermally lined pharyngeal pouches. (Fig. 4) By the end of the fourth weeks of gestation, four well defined pairs of branchial arches are visible externally. Shortly there after, the second arch increases in thickness and proliferates caudally to meet the enlarging epicardial ridge of the fifth arch. The second, third and fourth branchial clefts becamed enclosed in an ectodermally lined cavity, the cervical sinus of His. Eventally, this sinus becomes obliterate by the apposition and fusion of its walls, yielding a smooth uniform contour to the external surface of the neck. The endodermal derivatives of the pharyngeal pouches then migrate to their final position. (5) Differentiation of the branchial apparatus to the structures of the neck are shown in table 1.

In each branchial arch, an aortic arch connecting the ventral and dorsal aortas developed. The first two pairs are involuted, by the time the sixth pairs is formed. The artery of the first persists forming the common and proximal part of the right subclavian artery. The fifth arch arteries involuted and the sixth pair forms the pulmonary arteries. (Fig. 6)

The anomalies are classified into sinus, fistula and cyst. Sinus is an incomplete tract that usually open externally and rerely internally. Fistula communicates to both internally and externally. Cysts have no communication neither internally nor externally. On the basis of the precise location of the anomalies, they can be classified according to their proposed pouch or cleft of origin.

1. First branchial anomalies.

It may originate anywhere along the nasopharynx, middle ear cavity or external auditory canal and external anteriorly or posteriorly to the pinna, or below the angle of mandible, involving the parotid gland or lying medial or superficial to it. (Fig. 7)

2. Second branchial anomalies.

The external opening is typically along the anterior border of the sternocleidomastoid muscle around the junction of the middle and lower thrid. Deep to platysma, along the carotid sheath, it then passes deep between the internal and external carotid arteries. After crossing over the hypoglossal and glossopharyngeal nerve, it then extends upward to end near the tonsillar fossa. (fig. 8)

3. Third branchial anomalies.

It passes from an external opening in the lower neck along the line of the anterior border of the sternocleidomastoid muscle, ascending in relation to the corotid sheath and passes deep posterior to the internal carotid artery between the glossopharyngeal nerve above and hypoglossal nerve below, piercing the thyrohyoid membrane to enter the pyriform sinus. (Fig. 9)

4. Fourth branchial anomalies.

It arises internally from the apex of pyriform sinus, penetrating the thyrohyoid membrane behind the fold of the internal laryngeal nerve. On the left, the fistula would loop around the aortic arch and on the right around the sublcavian artery. Thereafter, the tract ascends to the common carotid artery passing over the hypoglossal nerve and descends to an external opening in the lower neck along the anterior border of sternocleidomastoid muscle. (Fig. 10)

The clinical presentation of the patient with first branchial cleft anomalies is a recurrent periauricular swelling, a sinus in the periauricular region, a mass in the external auditory canal, a dimple or depression in the floor of the canal, granulations or polyps in the floor of the canal or a chronic discharge from the ear in a normal tympanic membrane. (7)

The second branchial cleft anomalies, patients came with a history of recurrent discharge or infection of a sinus in the lower part of the neck, or a neck mass.

The rare third and fourth branchial anomalies presented with recurrent neck abscess or recurrent acute suppurative thyroiditis (usually on the left side)

The patient may present with only a cystic neck mass without other symptoms. So we must differentiate them from other conditions. These included:

1. Thyroglossal duct cyst - usually midline.
2. Parathyroid cyst - rare, near inferior border of Thyroid.
3. Thyroid cyst - related to thyroid, anterior to carotid artery, and internal jugular vein.
4. Cervical thymic cyst - lower neck.
5. Cystic hygroma - usually posterior to carotid artery and internal jugular vein.
6. Cystic metastasis - usually in the posterior triangle, behind carotid artery and internal jugular vein.
7. Thyroid neoplasm - rare.
8. Dermoid cyst - usually upper neck.
9. Teratoma and cystic neuroma - symptoms related to nerve involvement.

Conclusion:

We presented three cases of branchial cleft fistula, with preoperative radiographic contrast studies showing the fistulous tract connecting the upper digestive tract and the skin opening. These studies had help the surgeon in identifying the fistulous tract and its course and planning of the operation can be done prior to surgery.

Esophagogram is useful for demonstrating the tract leading to proper diagnosis and thus proper management.

TABLE 1
Differentiation of the Branchial Apparatus

Location	Cleft(Ectoderm)	Arch(Mesoderm)	Pouch(Endoderm)
First	External ear canal	Mandible, muscles of mastication, fifth CN., malleus and incus	Eustachian tube, tympanic cavity, mastoid air cells
Second	Cervical sinus of His	Muscles of facial expression, body and lesser horns of hyoid, CN 7,8	Palatine tonsil
Third	Cervical sinus of His	Superior constrictor muscles, internal carotid artery, CN 9, greater horn and body of hyoid	Inferior parathyroid thymus, pyriform fossa
Fourth	Cervical sinus of His	Thyroid and cuneiform cartilage, CN 10, aortic arch, and right subclavian artery, part of laryngeal muscles.	Superior parathyroid, Apex of pyriform sinus
Fifth and sixth	None	Portions of the laryngeal muscles and skeleton, inferior pharyngeal constrictor muscle, CN 11	Parafollicular "C" cells of the thyroid gland.

CN = CRANIAL NERVE

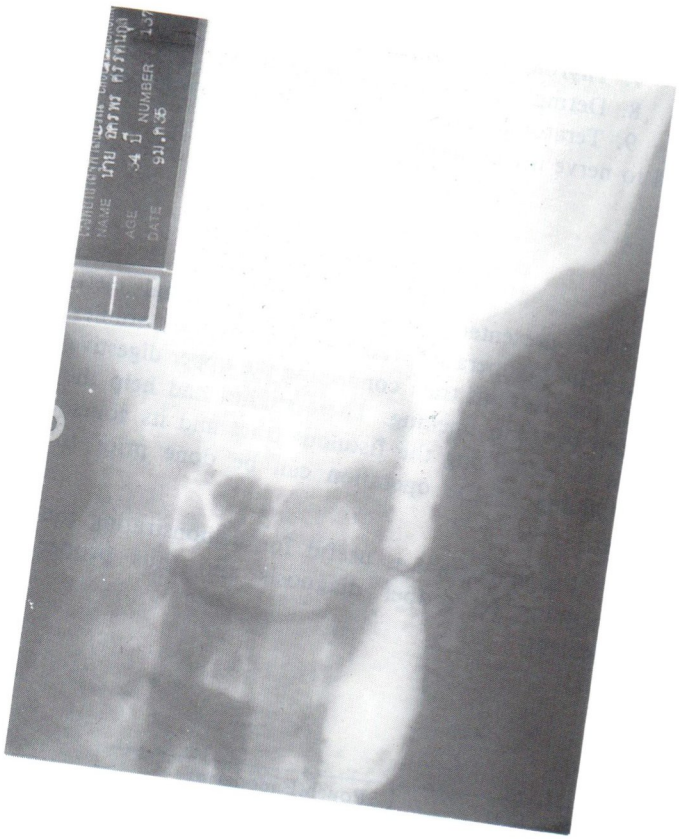

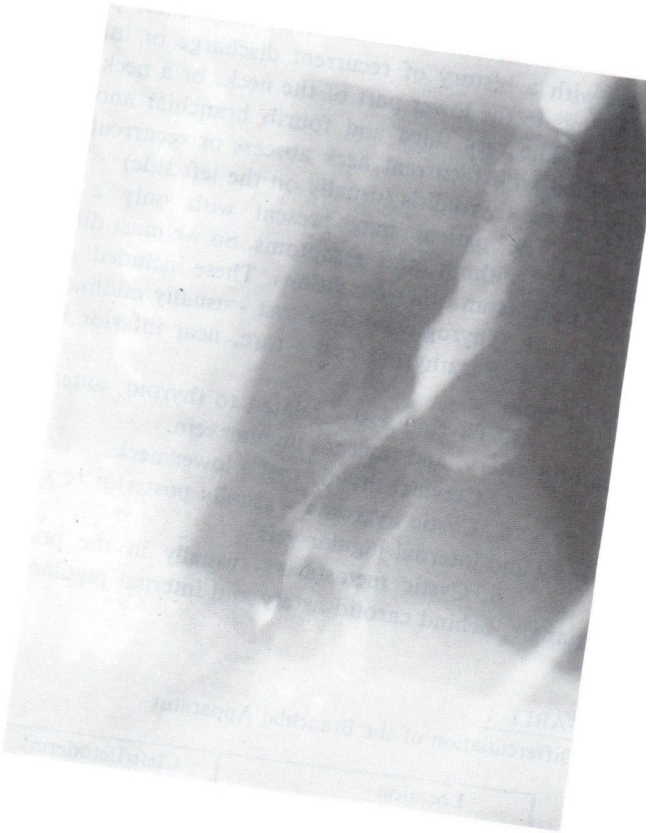

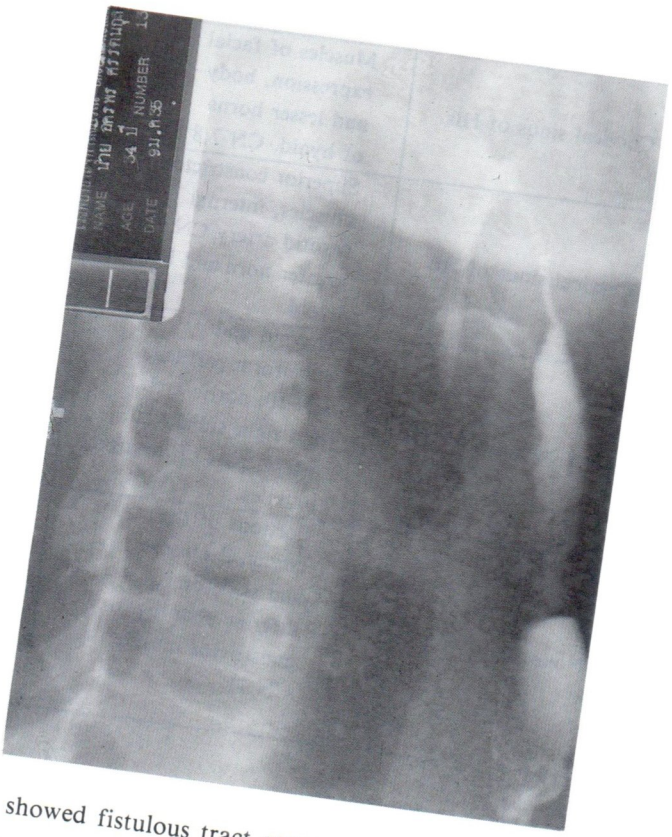

Fig.1 Case 1 Fistulogram showed fistulous tract connected with right tonsillar fossa (AP, lateral and left anterior oblique view).

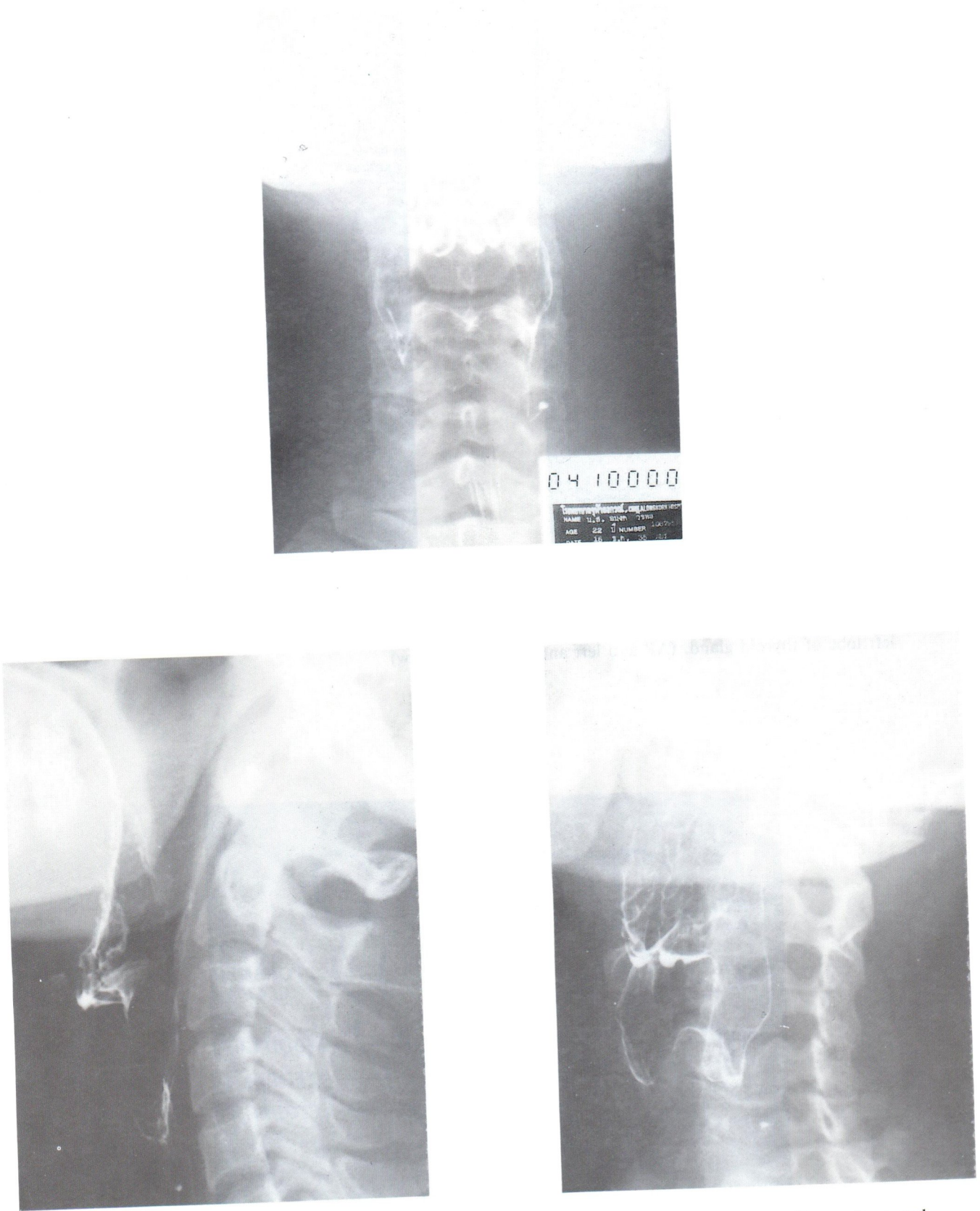

Fig.2 Case 2 Esophagogram showed sinus tract originating from the apex of left pyriform sinus and terminating in the area of left lobe of thyroid gland. (AP, lateral left anterior oblique view)

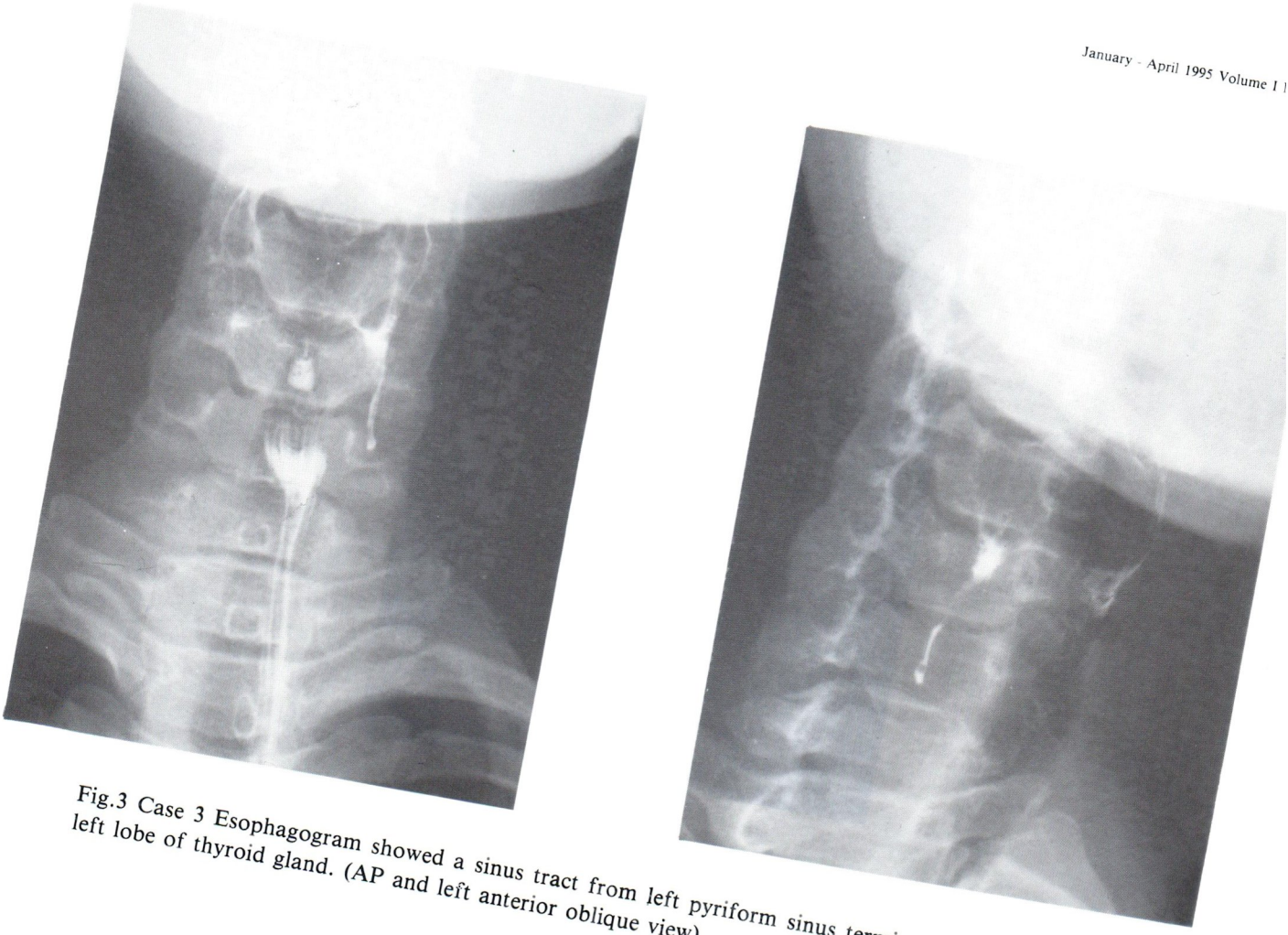

Fig.3 Case 3 Esophagogram showed a sinus tract from left pyriform sinus terminating at the area of left lobe of thyroid gland. (AP and left anterior oblique view)

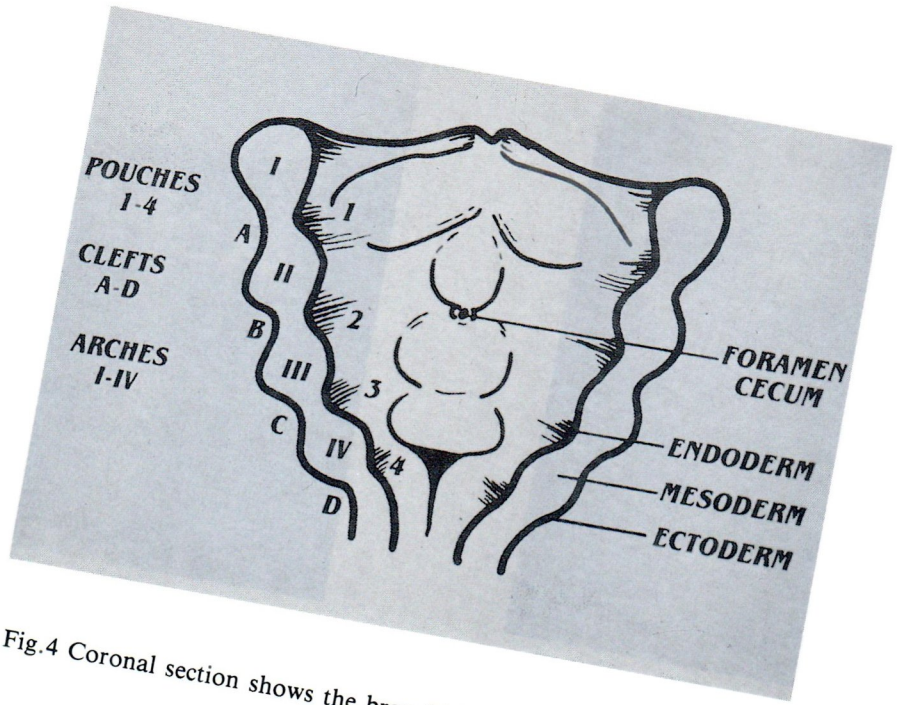

Fig.4 Coronal section shows the branchial pouches, clefts and arches.

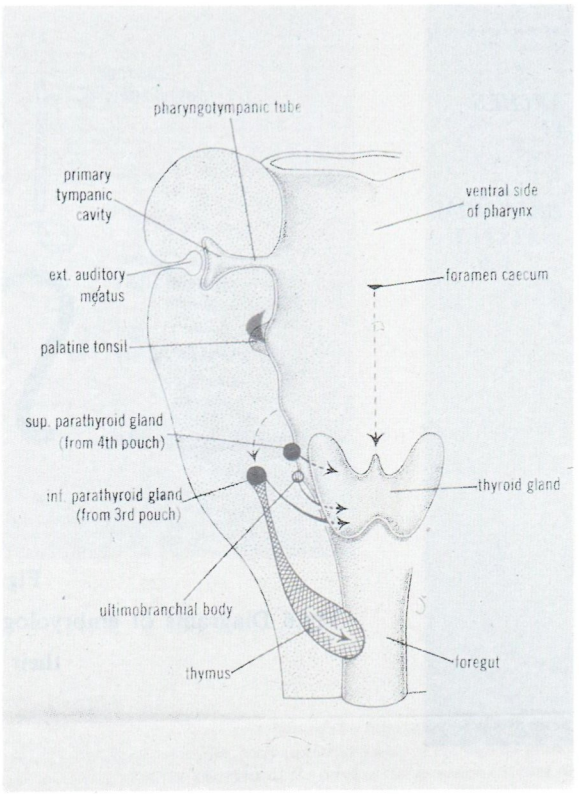

Fig.5 a

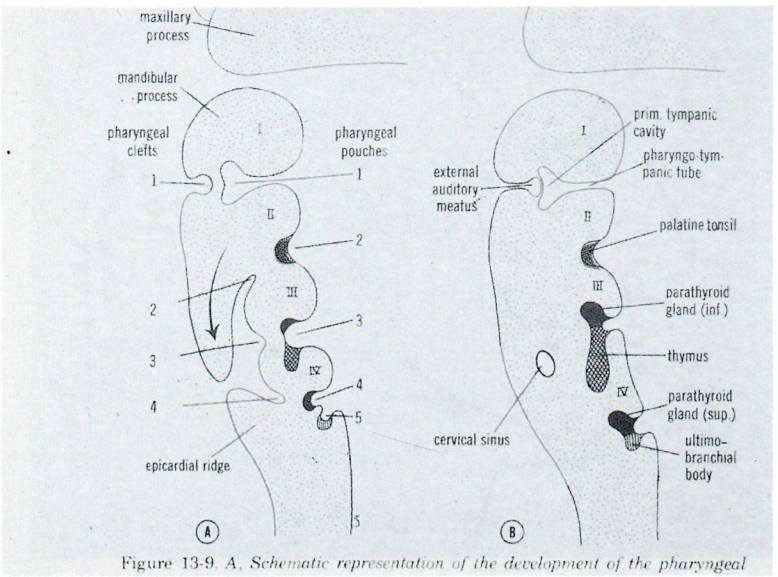

Figure 13-9. *A, Schematic representation of the development of the pharyngeal*

Fig.5 b

Fig.5 a and b Developement of the pharyngeal clefts and pouches.

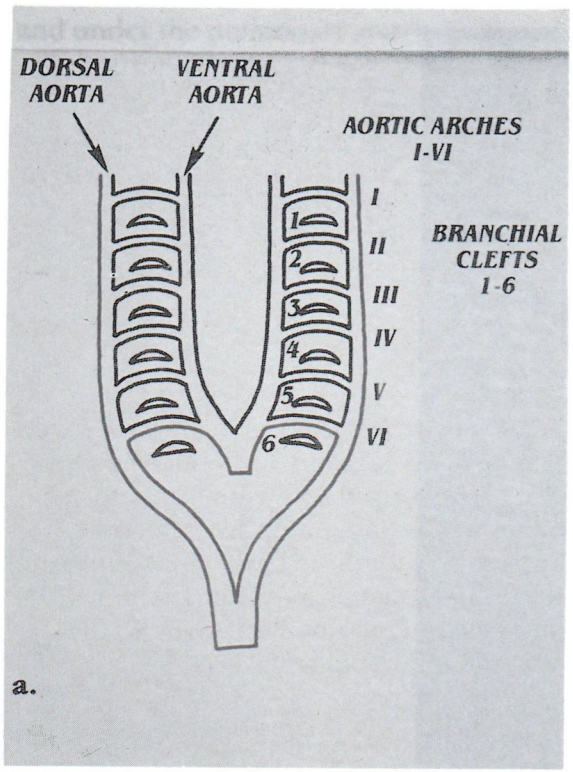

Fig.6 a

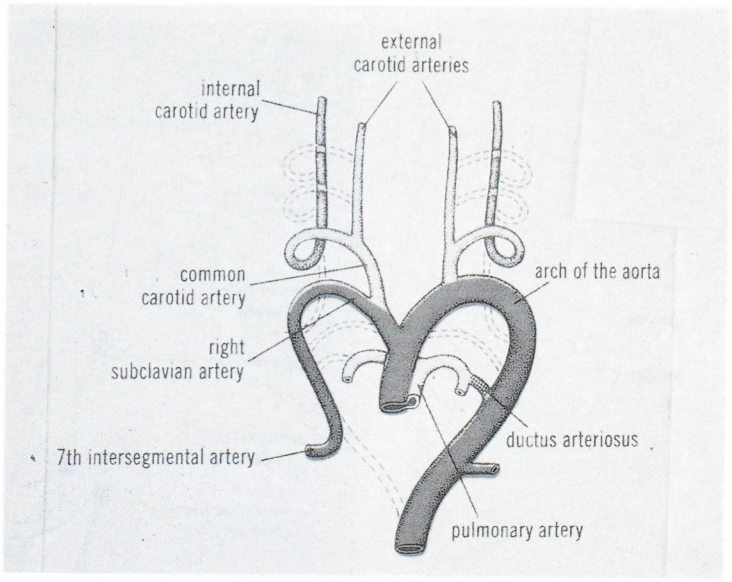

Fig.6 b

Fig.6 Diagrams of embryology of the aortic arch arteries and their relations to the branchial clefts.

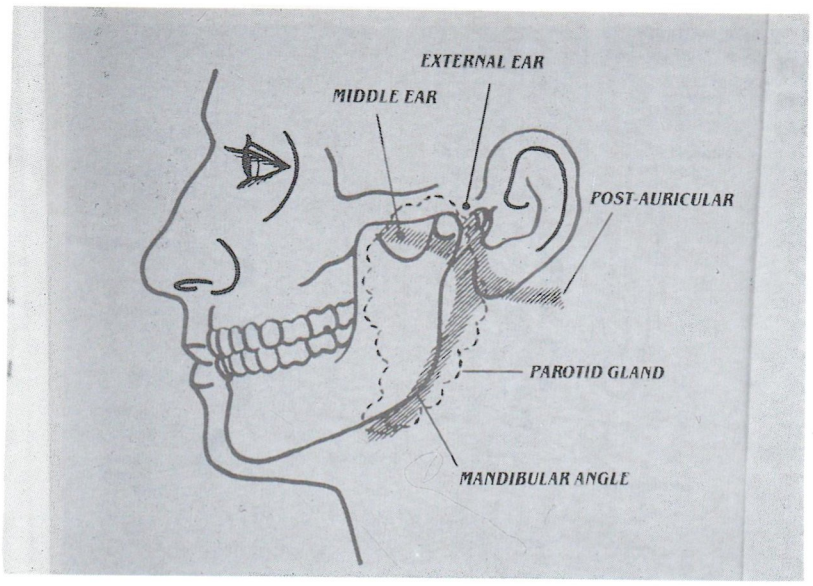

Fig.7 Diagram showed the course and relationships of 1st branchial anomalies.

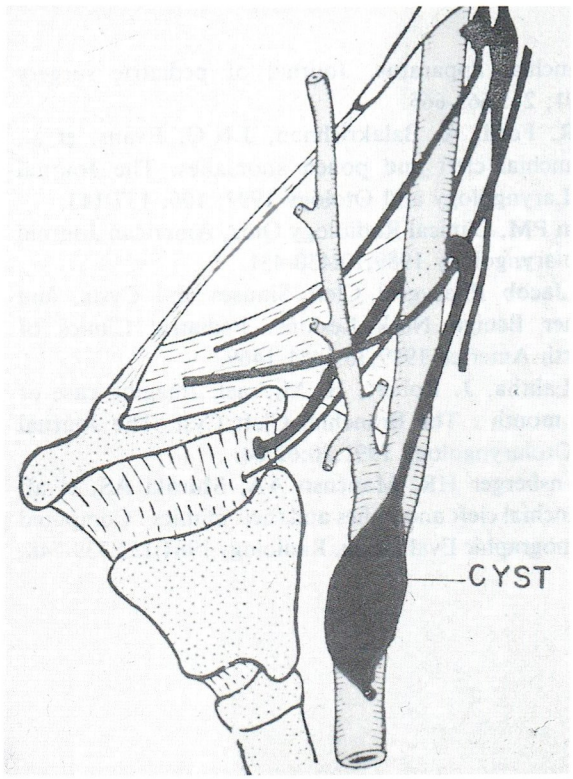

Fig.8 Diagram showed the course and relationship of 2nd branchial anomalies.

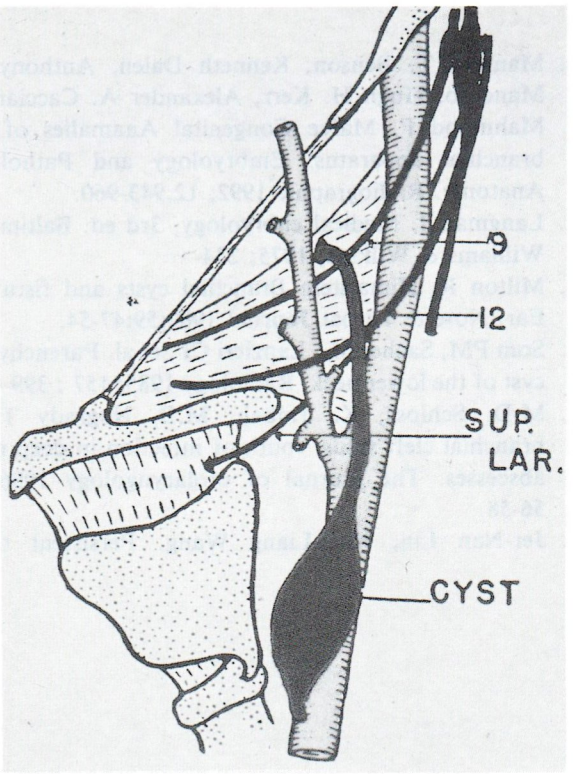

Fig.9 Diagram showed the course and relationship of 3rd branchial anomalies.

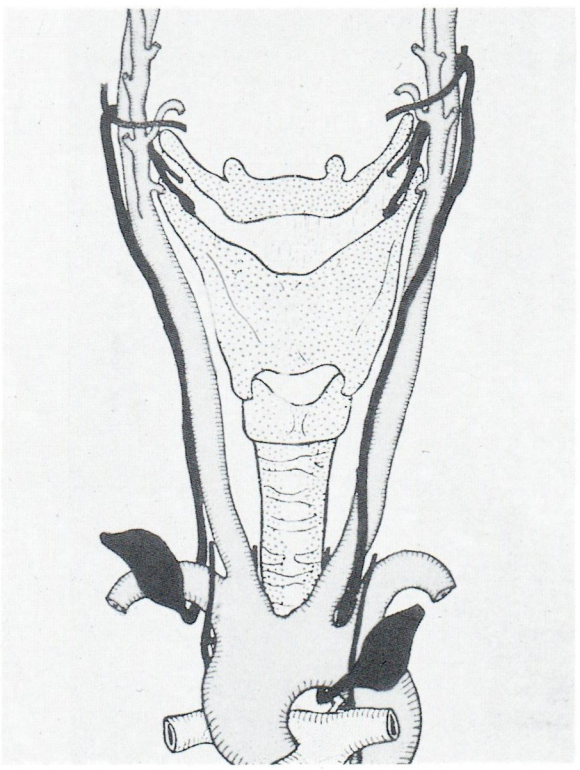

Fig.10 Diagram showed the course and relationship of 4th branchial anomalies.

REFERENCE:

1. Manferd T. Benson, Kenneth Dalen, Anthony A. Mancuso, Hugh H. Kerr, Alexander A. Cacciarelli, Mahmood F. Mafee Congenital Anamalies of the branchial apparatus: Embryology and Pathologic Anatomy. Radiographic 1992; 12:943-960.
2. Langman J. Medical enbryology, 3rd ed. Baltimore: Williams & Wilkins, 1975; 234-
3. Milton R. Himalstein Branchial cysts and fistulas : Ear, Nose & Throat Journal 1980;59:47-54.
4. Som PM, Sacher M., Lanzieri CF, et al. Parenchymal cyst of the lower neck. Radiology 1985; 157 : 399-406.
5. M.D. Schloss, K. Taibah, M.B. Nogrady Third branchial cleft sinus: routh of infection in deep neck abscesses. The journal of otolaryngology 1986:15; 56-58.
6. Jer-Nan Lin, Kuei-Liang Wang. Persistent third branchial apparatus. Journal of pediatric surgery 1991; 26: 663-665.
7. G.R. Ford, A. Balakrishnan, J.N.G. Evans, et al. Branchial cleft and pouch anomalies. The Journal of Laryngology and Otology 1992; 106: 137-143.
8. Som PM, Clinical Radiology Quiz, American Journal Otolaryngology 1989;10:430-431.
9. F. Jacob Pharygeal Cleft Sinuses and Cysts, and Other Benign Neck Lesions. Pediatric Clinics of North America 1989;36:1451-1469.
10. S. Lalitha, J. Robert, H. Michael. Imaging case of the month : The Branchial Cleft Cyst. The Journal of Otolaryngology 1991;20:62-64.
11. Harnsberger HR, Mancuso AA, Muraki AS, et al. Branchial cleft anomalies and their mimics : Computed Tomographic Evaluation. Radiology 1984;152:739-748.

The Role of Radiation Therapy in the treatment of Intracranial Tumours.

Prof. Kawee Tungsubutra, M.D., D.M.R.T. (England), D.Sc. (Hon.), F.C.R.T. (Thailand).

Abstract

The role of radiation therapy in the multimodalities treatment of intracranial tumours has been discussed. Surgery is used both for the diagnosis and the treatment of intracranial tumours. Radiation therapy has the role in both radical and palliative treatment. Local irradiation is used with the aim to reduce the size of the tumour, for alleviating pressure symptoms, to relieve obstruction of the flow of CSF to reduce hydrocephalus after the shunting operation, and to reduce the incidence or to prevent the recurrences after removal by surgery. Brain bath for palliative treatment of metastatic brain tumours and prophyllactic brain irradiation for the tumours which are notorious for brain metastases. Whole CNS irradiation is used to prevent the seedling of some tumours through the CSF. It may also be used in Leukaemias after the peripheral blood and the bone marrow pictures has been controlled by chemotherapy. The values of Radiation therapy in different kinds of intracranial tumours has been discussed.

Radiation therapy of Intracranial tumours, palliative and radical treatment, local and whole CNS irradiation, prophyllactic and supplementary irradiation to other modalities treatment.

Introduction:

Multimodalities treatment should be the treatment of choice for the management of intracranial tumours. Surgery is the first line of attack not only to have the correct diagnosis for further management but also, at the same time, will serve for the primary treatment by total, subtotal or partial removal of the mass or even only obtaining tissue for biopsy. Immediate decompression of the tumour mass which pressed on the surrounding structures or relieve the obstruction of the CSF. which has already affected the normal function of the nervous system. With the progress of the new technology, CT and MRI can help in the localization of the tumour not only the site of the lesion but also the size, extension, number of lesions, whether it be a solid, cystic or the mixture of the two components. The modern medical imaging will also tell the effects or damages of the brain that the tumour has caused such as hyrocephalus, atrophy etc. MRI with different relaxation techniques and different pulse sequence techniques can sometime tell a clue to the nature of the tumour such as a germ cell sensitive tumour or a malignant teratoma in the pineal region, the extent of edema versus the tumour mass,[11] etc. With modern equipments in radiotherapy post-operative radiation therapy can be given with more accuracy, with the help of a Simulator, delivering a high total tumour dose by a high dose-rate brachytherapy, or supervoltage teletherapy techniques. Chemotherapy as an adjuvant treatment to surgery and radiotherapy with a single or multiple drugs has ben explored by definite protocols, as well as chemical radioprotectors and radiosensitisers.[2, 5, 6, 7, 8] Some has organized a multi-institutional protocols to treat certain

Kaweevej Clinics, 318 Tarksin Road, Dhonburi, Bangkok 10600, Thailand.

tumours and to collect the results of the treatment which may be standardized and comparable so as to have a statistical significant results.[18]

Intracranial tumours were referred for radiotherapy after having elective surgery, palliative surgery by shunting for C.S.F. drainage, open biopsy or merely clinical and CT or MRI findings of cerebral metastasis from the known primary lesion treated previously from other hospitals.

The incidence of brain tumours or intracranial tumours population base data collected in 1988 was 31 per 100,000 population in Thailand.[21]

Methods and Materials

During 1987 to 1990, a four years period, 237 cases of intracranial tumours were referred for Radiotherapy at the National Cancer Institute. Bangkok, Thailand. Among these cases, there are 166 primary brain tumours and 71 metastatic brain tumours from known primary tumours of various sites.

Table I. Intracranial tumours referred for radiotherapy.

Type	Histological Diagnosis	Number	Totel
Primary	Gliomas	89	166
	Pineal tumours	17	
	Pituitary tumours	10	
	PNETS	10	
	Medulloblastoma	9	
	Ependymoma	3	
	Craniopharyngioma	3	
	Lymphomas	4	
	Leukaemia	1	
	Meningioma	8	
	No histological diagnosis	12	
Secondary	Metastatic tumours	71	71
	Total	237	237

Malignant Gliomas

Table II. Age distribution of Gliomas grade I-III and Glioblastoma Multiforme.

Age distribution	Gliomas grade I-III	Glioblastoma Multiforme
5 - 9	2	2
10 - 19	6	0
20 - 29	12	6
30 - 39	16 (35)	3
40 - 49	7	8
50 - 59	5	13 (26)
60 - 69	2	5
70 and over	1	1
Total	51	38

Fig. I Bar Chart shows the difference in peak incidence between gliomas and G.M.

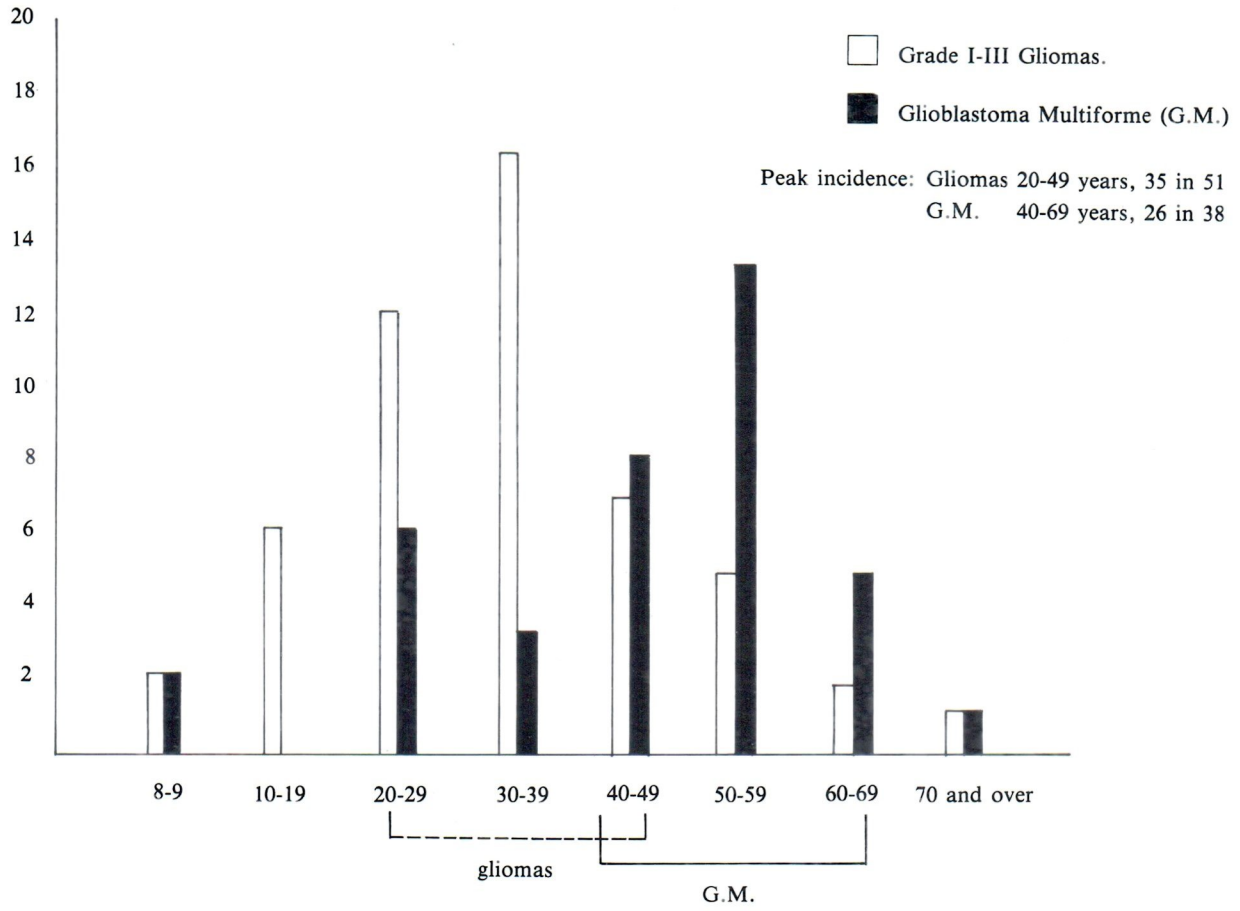

Table III. Lobes distribution among gliomas grade I-III and Glioblastoma Multiforme.

Lobe	Gliomas Grade I-III	Glioblastoma Multiforme
Frontal	25	5
Parietal	13	7
Temporal	1	5
Occipital	3	9
Cerebellum	5	—
Fronto-Temporal	—	2 ┐
Tempero-Parietal	—	3 ├ 11
Tempero-Occipital	—	6 ┘
Corpus Callosum	1	—
Medulla Oblongata	1	—
Parasella	2	1
Total	51	38

Note: Gliomas grade I-III are confined in one lobe and mostly in the operable sites. Glioblastoma Multiforme are spreading into the adjacent lobes or in the sites difficult to have total removal of the tumours.

Malignant Gliomas

The patients were referred for radiotherapy mostly after total removal of the tumours or subtotal removal of the visible tumours or partial removal of the part which may not be risky for operative death or neurological dificit after operation. In some cases, the tumour may have been removed piece meal or only some tissues may have been removed for biopsy. The 89 cases referred between 1987-1990 having the histological diagnosis as malignant glioma are reviewed and divided into two groups. The first group are those classified as Astrocytomas, Oligodendrogliomas or mixed Astrocytoma and Oligodendroglioma, Grade I-III which are altogether 51 cases. The second group are those classified as Glioblastoma Multiforme or the undifferentiated malignant gliomas. There is no significant difference in sex distribution in both group, male: female = 28:23 in the first group and 21:17 in the second group respectively. The youngest ages were about 7-8 years while the oldest ages were 71-72 years nearly the same in both groups. The peak incidence in the more differentiated form of malignant glioma are between 20-49, while in Glioblastoma Multiforme are between 40-69, about 2 decades older.

Pineal Tumours

17 cases are pineal and CNS germ cell tumours. These are the tumours which are found in the midline principally in the pineal area or anteriorly around the third venticle and suprasella region. In these 17 cases, there are 12 males and 5 females. The ratio between male: female = 2.4:1. The peak age incidence is between 12-24 years, i.e. 10 cases or 58.82% of the total cases. The youngest age was $13\frac{3}{12}$ years and the oldest was 59 years.

Table IV. Age distribution in Pineal tumours.

Age	Number
10 - 19	5] 10
20 - 29	5]
30 - 39	3
40 - 49	2
50 - 59	2
Total	17

Primitive Neuro-Ectodermal Tumours (PNETS) 10 cases

sex incidence; male : female about 2:1. There were 7 males and 3 females. The lowest age was $1\frac{5}{12}$ years and the oldest age was $10\frac{7}{12}$ years. The peak incidence was between 3-6 years. There were 6 cases or 60% of the total cases found between 3-6 years of age.

Medulloblastoma. 9 cases

sex incidence; males 5 : females 4. age incidence: lowest age found was 11 months and the oldest age 18 years.

Ependymoma 3 cases

Our three cases are adults, age 45, 49 and 64 years old. The first two cases were female and the oldest one was a male patient.

Craniopharyngioma 3 cases

All cases are female aged 12, 23 and 34 respectively.

Pituitary tumours 10 cases

All cases are chromophobe adenomas and came to see the doctor because of the reduction of the lateral field of visions with an evidence of enlargement of sella turcica seen in the lateral view of the skull. The lowest age found was 10 years old. 50% of the cases were more than 50 years old. In the 10 cases, there were 7 female and only 3 male patients. There were also symptoms of hormonal deficit in the patients found in active sexual life, between the age of 32 to 49. There were oligomenorrhea in the female patients and decrease libido in the male patients. In our male patients there were also decrease in the sex characteristics e.g. the growing of the beard and the sternal hair were diminished.

Meningioma 8 cases

The sex incidence is equal in male and female 4:4. The lowest age is 21 years old and the oldest is 76 years old. There are two in the frontal lobe, two in the mid temporal fossa, three in the occipital region and one is in the parasella region of the middle fossa. It has been observed that all of the cases, the tumours are in the Lt. side. Two patients who had the tumours in the frontal region, one was referred for post-operative radiotherapy after the 3rd recurrence post subtotal removal, another one was referred after the 1st recurrence post subtotal removal. These two cases have no recurrence after post-operative radiotherapy for 2½ years.

Lymphoma and Leukaemia.

4 cases were non-Hodgkin Lymphoma. In all cases, there are also lymph node involvement which proved to be lymphoma. The lesions in the brain are found by symptoms indicating lesions in the brain and confirmed by C.T.

1 case was leukaemia referring for radiotherapy after having chemotherapy.

Brain lesions with no histological report available

12 cases with evidence of lesion in the brain without histological confirmation were also referred for radiotherapy. The diagnosis in these cases were done by the C.T. or MRI, together with clinical symptoms. These tumours are in the brain stem, Thalamic, Pontine or Third ventricle regions where the surgeon considered too risky to obtain the tissue for histologic diagnosis. These patients had palliative surgery by doing V-V. shunt or V-A. shunt according to the perference of the surgeons. All of these patients had some degree of hydrocephalus prior to shunting operation.

Metastatic Carcinoma to the Brain 71 cases

sex incidence : male 54 cases versus female 18 cases. In 18 female cases, two cases had a primary lesion in the breast. One had a single lesion in the frontal lobe, age 52 who is a long term survivor, another one had multiple lesions in the brain who had brain bath for 40 Gy with a good palliative value or having a good quality of life. 4 cases had primary lesion from different sites, one had a primary in the scalp, one had a primary from melanoma of the face, one had a primary from Ca. Cervix and another one from a choriocarcinoma. All these 4 cases are short term survivors between 3-8 months.

The rest 12 cases had metastazised from bronchogenic Ca., 4 were squamous cell type but 8 were adenocarcinoma. The 4 squamous cell type cases had multiple lesions while 6 adenocarcinoma cases also had multiple lesions and 2 cases had single lesion, one in the frontal lobe, another one at the parieto-temporal lobe. Both solitary lesions in the brain had total removal with local irradiation at the tumour beds by 3 fields technique or two wedges fields technique.

In 53 male patients, the youngest age 40, the oldest age 78, there were only two cases who had a primary lesion in other sites apart from bronchogenic Ca. These two cases, one had a primary lesion from Ca. Thyroid papillary type, another one from the renal cell Ca. Both of these cases had a single metastasis in the frontal lobe and had frontal lobectomy and post-operative local radiotherapy. Both are long term survivors with good quality of life.

51 cases had a primary lesion in the bronchus, the detail of which can be seen in table V.

Table V. Detail of 51 brain metastasis cases from bronchogenic Ca.

Cell type	Cases	Multiple	Single	Lobe	No	Rt.	Lt.
Squamous cell	6	5	1	frontal	1	1	—
Large cell-undiff.	2	2	—	—	—	—	—
Adenocarcinoma	43	25	18	frontal	12	7	5
				parietal	2	2	—
				temporal	2	2	—
				Fronto temporal	2	1	1

Results and Discussion.

Over the past 25 years there has been progressive improvement in the results of treating intracranial tumours either a primary or a metastatic ones. There are several reasons for this which include advances in neurological imaging leading to more accurate localization, improvements in neurosurgical techniques, better peri-operative care, wider use of megavoltage equipments and techniques including greater and more precise dosage delivered to the tumour and the introduction of chemotherapy.[2, 3, 4,5,6, 7]

Since the introduction of CT Scanning, it is clear that in patients with inoperable tumours situated deeply within the cerebral hemispheres, radiotherapy alone often decrease tumour bulk, reduce neurological disability and prolongs active life sometimes for many years. The treatment of the entire cerebro-spinal axis by irradiation has become mandatory for the control of medulloblastoma, germinomas and high grade ependymomas especially when occuring in the posterior fossa. In a substantial number of patients with intracranial tumours, tissue will not be available for histological diagnosis at the time of referal for radiotherapy either because of frank inoperability or because the hazards associated even with biopsy were considered to be unduly great.[2, 6]

Malignant Gliomas.

There is good evidence that survival of children and adults with intracranial gliomas in increase by routine post-operative radiotherapy compared with surgery alone.[2, 6] Reviews of the literatures show the value of conventional radiotherapy for high grade gliomas in the adult but fails to show a clear advantage for radiosensitizers, hyperfractionation, acceleration or particle radiotherapy, which have been studied to date. For low grade gliomas, the survival of oligodendroglioma patients was greater than those with astrocytoma but the difference was less marked in the long term.[4] No difference in survival was found between grade I and grade II astrocytoma. Low grade astrocytoma, may progress to greater malignancy. This process is related to the natural biology of the tumour and not to previous radiotherapy since progression to greater malignancy may appear spontaneously or after surgery alone. A number of retrospective studies have suggested a beneficial role for radiotherapy in low grade astrocytomas incompletely resected at surgery. In low grade oligodendroglioma the role of radiotherapy is less clear. Although a survival advantage could not be demonstrated, there was a trend toward a lowering of the recurrence rates in patients with subtotally excised solid tumours who received radiation therapy.[4, 5, 8, 19, 20] Since this is our primary report, therefore our follow up period is still so short. In term of survival we have observed the survival in two categories, the short term and the long term. The short term survirors are those who survive only 6-8 months after radiotherapy, complete or incomplete course. The long term survivor are those who survive longer than 8 months after the completion of the radiotherapy course. Those who hae no complete course of radiation by any reason, never have long term survivor. In the patients with glioma grade I-III: there are 74.50% long term survivors while in the patients with Glioblastoma Multiforme only 18.42% are long term survivors. One important factor which may have the impact on survival is the extent of surgery prior to radiation. The majority of the patients in the low grade glioma group had the tumour in the frontal lobes which are amendable for total removal while those in the high grade glioma or Glioblastoma Multiforme group had the tumour already spread into 2 lobes and difficult to have total removal. (table III)

In both groups, the important prognostic factors are : the extent of surgery whether it was a total removal or a subtotal or partial removal of the mass, the general condition of the patients and the dose of the radiation received. In both groups, the technique of radiation are those for a local irradiation of the tumour bed or the residual tumour by 3 fields technique or a wedge pair technique giving a daily dose of 180 cGy/day, five times per week with a wider margin for the Glioblastoma Multiforme. The total tumour does was 5500-6500 cGy in $6\frac{1}{2}$-7 weeks

Pineal Tumours.

In the past, attempts to obtain tissue from pineal tumours were associated with a very high morbidity. Torkildsen proposed that these tumours should be treated by shunting procedure and irradiation.[11] Irradiation may be used as a therapeutic "diagnostic" test in cases which tissue can not be taken for biopsy. Tumours in these areas may be classified into two groups, the radiosensitive and the radioresistant tumours. The radiosensitive group consisted of the germ cell tumours and the pineoblastoma. The radioresistant group consisted of the malignant teratomas and the non-germ cell tumour (pineocytoma and gliomas).

The tumours in these groups we have given a limited volume irradiation to a dose of 20 Gy as localized by the C.T. and the simulator. If the tumours respond well as evaluated by C.T. after a "Diagnostic" therapeutic approach, we shall regard that it is a sensitive tumour which may have a high incidence of cerebro-spinal fluid seeding.[11] These patients are subsequently treated by whole craniospinal axis radiotherapy whereas resistant tumours are continued to have the treatment to local field alone. In our series, there are 9 short term survivors (die within 6-8 months) and 8 long term survivors who are follow up from 1 to 3 years. The long term survivors are those having the sensitive tumours and 7 in the 8 long term survivors having the age below 24, only 1 case having the age above 24. The 9 short term survivors are those

having the resistant tumours, not responding after the dose of 2000 cGy and 5 of the 9 patients have the age above 24 with poor general condition. Interestingly the other 4 short term survivors are under 12 years old and received incomplete radiotherapy course. For the sensitive tumours, we deliver 50 Gy to the local tumour and 30 Gy to the remaining brain and spinal cord. We start with a local irradiation with a limited field to the tumour, a dialy dose of 180 cGy/day performing the "diagnostic" therapy to a dose of 20 Gy then evaluation was made by a CT. If it proved to be a senstive tumour then cerebro-spinal axis irradiation will be made giving a daily dose of about 150-160 cGy/day. If the tumour proved to be a resistant one, then a further local irradiation will be given to a tumour dose of 50 Gy - 55 Gy.

Factors affecting the prognsis:

1. General conditions of the patient prior to radiotherapy is given.
2. Neurological symptoms or deficits prior to surgical treatment is given which depend on the duration of symptoms before seeking medical treatment.
3. The surgical intervention whether it was only V-P or V-A shunting, with or without partial removal or biopsy.
4. The Radiotherapy received is completed or not.

Anyhow, the tumour types and neurological performance status are the most important factors predicting the probability of survival.

The factors which may affect the patients to have complete radiotherapy course or not are:

1. Poor general condition before treatment.
2. Parents are uneducated and stop bringing their children to have a long course of radiotherapy.
3. Parents stop rdiation therapy and seek the old Thai traditional medicine

We concluded that shunting and radiosensitivity testing remains the treatment of choice for tumours in the pineal region.

Primitive Neuro-Ectodernal Tumours (PNETS).

Highly malignant anaplastic tumours similar in histological appearance to medulloblastoma are called Primitive Neuro-Ectodernal Tumours (PNETS) They may occur in the cerebral hemispheres of children and young adults. These tumours are highly malignant and generally run a rapidly fatal course. The biological behaviour, therapeutic response and prognosis of patients with medulloblastoma are different from the PNET group which confined to certain cerebral hemisphere tumours. The survival was influenced by the proportion of the tumour that was undifferentiated. All patients with more than 90% of the tumour undifferentiated died by 30 months, compared with those when tumours were less than 90% undifferentiated are long term survivors.[6] In our 10 cases, 6 cases died rapidly within 6-8 months, only 4 cases are long term survivors who are still alive and are followed up 1-3 years. These 4 cases are $3\frac{9}{12}$, 4, 4 and 7 years old and had good general condition and telerated the radiotherapy until having completed the course. We have irradiated the whole cerebro-spinal axis to a dose of 3000 cGy in 6-$7\frac{1}{2}$ weeks with a daily dose of 150-180 cGy.

Medulloblastoma.

Medulloblastoma is the frequent type of posterior fossa tumours found in children and also is the most malignant. Surgery is the most important initial measure against this disease.

The aims of surgery are to relieve C.S.F. hypertension and relieve local pressure effects, safe the failing vision, obtain tissue for biopsy, stage the tumour and reduce the tumour mass as much as possible prior to radiotherapy. Most failures in the treatment for medulloblastoma have been due to local recurrence in the posterior fossa. CT and MRI scanning will reveal the size and extent of any residual tumour in the posterior fossa after surgery and/or radiotherapy. Myelography and CSF cytology after craniotomy may reveal sub-clinical spinal deposits.[6] In our 9 cases, 4 were dead within 6-8 months after treatment, all of which are below 3 years of age. Among the 5 long term survivors, all were children older than 3 years except 1 patient age $1\frac{6}{12}$ years whose general and neurological performance status was good after subtotal removal of the mass.

Treatment factors associated with a long term survival, was complete or subtotal resection of the primary tumour, as opposed to partial removal. A radiation dose to the posterior fossa of 55 Gy or more and the cerebro-spinal axis radiation of 3000 cGy were given in a period of 7-8½ weeks according to the tolerance of the patients.

Ependymoma. 3 cases.

All of our case are found in adults age 45, 49 and 64 respectively. They presented with the symptom of headache and increased intracranial pressure. C.T. revealed a mass in the lateral, 3rd and 4th ventricle respectively. Operation was done in the first case for biopsy only, but in the second and third cases, shunt and biopsy was done. Histological reports were low grade ependymoma in all cases. Brain bath was given in all cases to a dose of 3000 cGy in 4-4½ weeks and a booster dose of 2000 cGy were given by reduced field to posterior fossa only. After that, irradiation of the spinal axis were also

done to a total dose of 3000 cGy in 4-4½ weeks. For all patients with high grade tumours and for all those with tumours of any grade situated in the posterior fossa, we recommend irradiation to the whole cerebro-spinal axis. The potential value of prophylactic cerebro-spinal irradiation compared with local cerebral irradiation was supported by the reduced risk of tumour seeding associated with neurospinal axis irradiation. Two of our cases who had complete course of radiation are long term survivors while another one died in 8 months and we have to stop the radiation before she received the full course.

Craniopharyngioma. 3 cases

The ages of these 3 cases were 12, 23 and 34 years old respectively. All had the chief complaint of lossing lateral field of vision due to optic chiasma compression. The operation was done for decompression and also for partial removal of the tumours. In all cases the lateral view of the skull showed no enlargement of the sella turcica. C.T. of the skull showed suprasellar tumours at the parasellar region and having the cystic part extending anteriorly.

After partial removal of the tumour, local irradiation was given to a total tumour dose of 5500-6000 cGy in 6-6½ weeks with a daily dose of 180 cGy day, 5 sessions a week.

All of them are long term survivor with recovery of the field of vision.

In the largest series of the world's literature, Bloom presented the results of 122 patients managed by conservative surgery and post-operative irradiation of high dose level (50-60 Gy) yielding 5-10 year survivals of 85-74% respectively. The results of treatment are improved using Megavoltage therapy and the results in children are better than in adults.[6,18]

Even when the surgeon believes that total tumour removal has been accomplished and the patient makes a good post-operative recovery, many such cases still die of tumour recurrence.

In more recent reports where comparison has been possible between surgery alone and surgery with post-operative radiotherapy, distinctly superior results has been obtained for the combined treatment.[14,17]

Partial removal or even simple cyst aspiration combined with radical radiotherapy appear to give the best results. Children with recurrence after surgery alone can be salvaged by a conservative operation with radical radiotherapy.

Lymphoma 4 cases, Leukaemia 1 case.

All the 4 cases are systemic non-Hodgkin's Lymphoma with cerebral symptoms. C.T. reveal lesions in the brain. Brain bath has been given to a dose of 30-40 Gy with improvement of the cerebral symptoms. Chemotherapy has also been given for the systemic diseases. The result of treatment was unsatisfactory. There is only one case that survived over 1 year.

In the Leukaemia case, neuro-spinal axis irradiation was given after the blood picture has been recovered by chemotherapy. Neuro spinal axis irradiation was given to kill the leukaemic cells that has survived in the cerebro-spinal system because of the "blood-brain barrier".

Meningiomas. 8 cases

Histologically, meningiomas have been considered to be radioresistant and therefore the role of radiotherapy has been disputed.[13]

Radiotherapy prolongs survival in patients with incomplete resected or inoperable meningioma. Following radiotherapy alone, neurological improvement will occur in a significant proportion of patients with inoperable disease. Radiation with a tumour dose of not more than 1.8 Gy per fraction with treatment on a daily basis to a total tumour dose of 6500-7000 cGy result in minimal late morbidity.[6,13,15,16,18]

The result of treatment in our cases are satisfactory. 7 in 8 cases are long term survivors with reasonably good quality of life. One case having repeated recurrences for 3 times in a duration of 2 years, 1½ years and 1 year respectively, after surgery alone in the past, was referred for post-operative radiation therapy, and this time without recurrence for 4 years at present. Another one having recurrence 3 years after the fist operation without post-operative radiation therapy, also was referred for post-operative radiation therapy. These two cases the tumours were in the frontal area which is feasible for repeated surgery. The case who died after 8 months was the one who had the tumour at the middle fossa, parasellar region in which subtotal removal was not feasible because of the risk to morbidity and mortality. This case had only partial removal, the majority of the tumour remained intact. The observed transformation of these tumours to higher histological grade probably represent a natural progression of neoplastic tissue to frank malignancy.[13]

Table VI. 12 cases with no histological report, diagnosis were made by CT or MRI.

12.	Age	Sex	Site of the tumour	Survival after Brain Bath	
1.	4	m.	Brain Stem	died	2 months
2.	5 5/12	f.	Pontine tumour	died	2 months
3.	9 8/12	f.	Pontine tumour	died, abandon treatment	
4.	20	m.	3rd ventricle	died	3 months
5.	21	m.	Ventricular hydrocephalus	died	8 months
6.	26	m.	Ventricular hydrocephalus	died, abandon treatment	
7.	18	m.	Basal ganglion lesion	survive	1 year
8.	34	m.	Thalamic tumour Rt.	died, abandon treatment	
9.	38	f.	Brain stem tumour	died	3 months
10.	35	f.	Thalamic tumour Rt.	died, abandon treatment	
11.	58	m.	Brain stem tumour	died, abandon treatment	
12.	65	m.	Thalamic tumour	died, abandon treatment	

m. = male, f. = female

These are the cases which the tumours had block the path way of the C.S.F. and marked degree of hydrocephalus had occured. The patients mostly had poor general conditions and marked degree of neurological deficit had already established. Surgical intervention were feasible only doing V-P. or V-A shunt according to the preferential of the surgeon. The parents or the relative of the patients mostly discourage to have further radiation treatment and taking the patients back home after few radiation doses. Only one patient who had completed the radiation course survive for one year.

Pituitary Tumours.

The treatment of pituitary adenomas which have optic chiasma compression with unilateral or bitemporal heminopsia by surgical decompression and post-operative rediotherapy is well accepted. Total or partial removal of the tumours as much as feasible and post-operative radiotherapy with a limited fields always followed by recovery of the visual fields and long term survivors. Replacement therapy with hormones that are deficient, will make a good quality of life for the survivors.[1,6,18] In the 10 cases treated in our Institute, 9 cases did well. Only one case who died because of the operative complication. The patient was 66 years old, diabetic and weak. She died a few days after operation because of septicemia.

Metastatic Carcinoma to the Brain 71 cases.

It is our policy for matastatic brain lesions, if the primary has been controlled and had a solitary lesion in the brain, resection of the tumour and post-operative local irradiation is the treatment of choice. By this policy we have many long term survivors. If there are multiple lesions, whether the primary, lesion has been controlled or not, palliative radiation by brain bath will be given. Eventhough these cases with multiple lesions in the brain may be short term survivors, radiation therapy with brain bath will improve the neurological performance of the patients and thus improve the quality of the rest of their lives.

Conclusion:

We have treated 237 cases of intracranial tumours referred for radiotherapy post-operatively during 1987-1990, a 4 years period of which 225 cases having definite histological diagnosis and 12 cases having no histological diagnosis eventhough operation had been done but the tissue was not obtainable due to one or another reasons. There are 166 cases of primary lesions but another 71 cases are metastatic ones. All the metastatic cases had a history of a known primary tumour that had been treated by multimodalities therapy and having a proven histological diagnosis. The patients were following up for a varying period of 1-3 years. The results of treatment in each specific group of the tumours were analysed and prove to be satisfactory in comparison with the report elsewhere. The 5 years survival rate and long term results will be followed up and analysed in future.

From this study we have observed that adenocarcinoma of the lungs is the most frequent cell type which produce brain metastasis either being the multiple or a solitary ones. So it may be advisable to do a prophylactic brain bath in the patient with adenocarcinoma of the lung after the primary lesion has been controlled.

References:

1. Bloom H.J.G. Radiotherapy of pituitary tumours. In: Jenkins J.S., ed. Pituitary tumours, London: Butterworths; 1973:165-197.
2. Bloom H.J.G. Combined modality therapy for intracranial tumours. Cancer; 1975:35:111-120.
3. Bloom H.J.G. Recent results and research concerning the treatment of intracranial tumours. In: Chang C.H., Housepian, E.M., eds. Tumours of the Central Nervous system: modern radiotherapy in multidisciplinary management, New York: Masson Publishing; 1981:225-248.
4. Bloom H.J.G. Treatment of brain glioma in children. In: Bleehen, N., ed. Tumours of the brain, Berlin Spinger-Verlag; 1986:121-140.
5. Bloom H.J.G.; Glees, J.P. Chemotherapy of gliomas in adults and of medulloblastoma in children. In: Voth. D., Krauseneck, P., eds. Chemotherapy of gliomas. Berlin: Walter de Gruyter and Co., 1984:331-339.
6. Bloom H.J.G.; Glees J. and Bell J. The treatment and long-term prognosis of children with intracranial tumours. Int. J. Radiation Oncology Biol. Phys. 1990:18:723-745.
7. Bloom H.J.G. and Bessel, E.M., Medulloblastoma in adults: A review of 47 patients treated between 1952 and 1981. Int. J. Radiation Oncology Biol. Phys. 1990:18:763-772.
8. Bleehen N.M., Studies on High Grade Cerebral Gliomas. Int. J. Radiation Oncology. Biol. Phys., 1990:18:811-813.
9. Brada M.; Dearnaley D.; Horwich A; and Bloom H.J.G. Management of Primary Cerebral Lymphoma with Initial Chemotherapy. Int. J. Radiation Oncology Biol. Phys. 1990:18:787-792.
10. D' Angio G.J.; Rorke L.B.; Packer R.; Sutton L.; Zimmerman R.; Key Problems in the Management of Children with Brain Tumours. Int. J. Radiat. Oncol. Biol. Phys. 1990:18:805-810.
11. Dearnaley D.P.; A' Hern R.P.; Whittaker S. and Bloom H.J.G. Pineal and CNS Germ Cell Tumours; Int. J. Radiation Oncology Biol. Phys. 1990:18: 773-781.
12. Garcia, D.M.; Marks J.E.; Latifi H.R. and Kliefoth, A.B. Childhood Cerebellar Astrocytomas. Is there a role for postoperative Irradiation? Int. J. Radiation Oncology Biol. Phys. 1990: 18:815-818.
13. Glaholm J.; Bloom H.J.G.; and Crow J.H.; The Role of Radiotherapy in the management of Intracranial Meningiomas. Int. J. Radiation Oncology Biol. Phys. 1990:18:755-761.
14. Hoogenhout J.; Otten B.J.; Kasem I.; Stocling G.B.A.; Walder H.D. Surgery and Radiation therapy in the management of craniopharyngiomas. Int. J. Radiat. Oncol. Biol. Phys. 1984:10:2293-2297.
15. Jannoun L.; Bloom H.J.G. Long-Term Psychological Effects in Children Treated for Intracranial Tumours. Int. J. Radiat. Oncol. Biol. Phys. 1990:18:747-753.
16. King D.L.; Chang C.H.; Pool. J.L. Radiotherapy in the management of meningiomas. Acta Radiol. Ther. Phys. Biol. 1966:5:26-33.
17. Manaka S.; Teramoto A.; Takakura K. The efficacy of radiotherapy for craniopharyngioma. J. Neurosurg. 1985:62:648-656.
18. Rubin P., Inaugural Address: The past is the prologue for the future. Int. J. Radiat. Oncol. Biol. Phys. 1990:18:715-721.
19. Sheline, G.E. Radiotherapy for High Grade Glimas Int. J. Radiat. Oncol. Biol. Phys. 1990:18:793-803.
20. Whitton A.C.; Bloom H.J.G., Low Grade Glioma of the Cerebral Hemispheres in Adults. Int. J. Radiat. Oncol. Biol. Phys. 1990:18:783-786.
21. Vatanasapt V.; Titapant V.; Tangvoraponkchai V.; Pengsaa P. Cancer Incidence in Khon Kaen, Thailand, 1985-1988:46

Prediction of the site of the aneurysms in the region of the circle of Willis and the vicinity by CT scan

S. Hirunpat[1], P. Pekanan[1], P. Uttamakul[1], N. Ruxayos[1]

Abstract:

Retrospective study of the proved aneurysms, detected by i.v. contrast CT study in 21 cases, relating with the angiographic and surgical results. The aneurysms were mapped on the "pentagon" which was assumed to represent the circle of Willis. Paramedian anterior pentagon represented the site of anterior communicating artery aneurysm and the opposite posterior paramedian or median area was the site of basilar tip aneurysm. The lateral anterior corner was for the aneurysm of the horizontal portion (rare) of the middle cerebral a. or supraclinoid internal carotid a. The lateral posterior corner would be for aneurysm of the posterior communicating a, or distal internal carotid artery. Most of the aneurysms at the genu of the middle cerebral a. (more common than at the horizontal portion) were outside the petagon and were at the region posterior to the anterior middle cranial fossa. Rarer case of the anterior communicating a. was above the pentagon, seen between the floor of both frontal horns.

Key words: Aneurysms, circle of Willis, CT scan

Intracranial aneurysms represent the most common atraumatic cause of subarachnoid hemorrhage (7). The vast majority of saccular aneurysms are isolated lesions without any underlying predisposing factor. In less than 5 percent of cases, aneurysms are associated with septic emboli, head trauma, or neoplasia. Approximately 90 percent of saccular aneurysms occur in the anterior circulation in the region of the circle of Willis. Most commonly, specific sites of occurrence are the anterior communicating artery, posterior communicating origin, and middle cerebral artery bifurcation/trifurcation. Traditional methods of identifying the origin of aneurysms have rested upon either CT correlation of the site of the hemorrhage (8, 9) or angiographic morphologic changes in ruptured aneurysms. For instance, anterior interhemispheric blood correlated to ruptured anterior communicating aneurysms, whereas Sylvian fissure hemorrhage often indicates middle cerebral artery bifurcation aneurysm rupture.

Direct detection of the aneurysm by i.v. contrast CT scan is possible in the absent or faint subarachnoid blood. We study the possibility of accurate localization of the origin of these CT detected aneurysms.

[1] Department of Radiology, Ramathibodi Hospital, Rama 6 Street, Bangkok 10400, Thailand.

Materials and methods:

Retrospective study of the aneurysms in the region of the circle of Willis detected by enhanced axial CT scan of the brains was performed in 21 patients. Correlation of the sites of the aneurysms detected by CT scans with the angiographic and operative findings was done. The suprasellar cistern where the circle of Willis located was viewed as the "Pentagon". The enhanced aneurysms seen were mapped on this pentagon. The levels of the CT cuts where the enhanced aneurysms were visualized, were labelled as levels 1, 2, or 3.

The axial cuts at the posterior fossa were 4 mm in some cases and 10 mm in another cases. The level 1 was the cut that the sellar turcica, dorsum sella or the posterior clinoid process was visualized. The level 2 was the level that the suprasellar cistern was seen. The level 3 was the level that the 3rd ventricle was shown.

Results

Twenty-one patients studied were 11 males and 10 females. The age ranged from 29 to 71 yrs old. Subarachnoid hemorrhage was present in 18 cases and the focal neurological sign without subarachnoid hemorrhage in 3 cases. The size of the aneurysms were 4-14 mm, according to the CT findings and all were saccular type.

The detailed findings in the cases of the anterior communicating artery, basilar tips, internal carotid artery, posterior communicating artery and the middle cerebral artery were shown in Table 1, 2, 3, 4 and 5 respectively. The illustrated cases of the anterior communicating artery were shown in Fig. 1, of the basilar tip in Fig 2, of the internal carotid artery in Fig 3 and 4, of the posterior communicating artery in the Fig. 5 and of the middle cerebral artery in the Fig. 6 and 7.

The anatomic diagram of the circle of Willis is shown in Fig. 8. The summarized diagram of the aneurysms on the Pentagon and the labeled site of the aneurysm was seen in Fig. 9. The aneurysms outside the pentagon was illustrated in the diagrams of Fig. 10 and Fig. 11.

Table 1. Detailed analysis of the 9 aneurysms at the anterior communicating artery by CT scan

No.	Age	Sex	Aneurysm's size (mm)	Level	DMM(mm)	Side	Location on the pentagon
1.	55	M	10	2	5	Lt	
2.	55	M	6	2	2	Lt	
3.	71	M	10	1	5	Rt	
4.	52	M	8	1	4	Rt	
5.	49	F	8	2	0	Midline	
6.	45	M	4	2	2	Lt	
7.	58	M	14	2	0	Midline	
8.	53	F	8	2	4	Lt	
9.	62	M	5	3	2	Rt	

Note; DDM = distance from midline to the middle part of the aneurysm
* the aneurysm was at between floor of both frontal horns, cut level 3

Table 2. Detailed analysis of the 2 aneurysms at the basilar tip by CT scan

No.	Age	Sex	Aneurysm's size (mm)	Level	DDM(mm)	Side	Location on the pentagon
1.	67	F	12	1,2,3	0	midline	
2.	55	F	17	2	0	midline	

Table 3. Detailed analysis of the 2 aneurysms at the internal carotid artery by CT scan

No.	Age	Sex	Aneurysm's size (mm)	Level	DDM,DPC (mm)	Side	Location on the pentagon
1.	40	M	7	2	12, 9	Rt	
	the aneurysm was at the distal ICA bifurcation						
2.	60	F	6	2	10, 18	Lt	
	the aneurysm is at the supraclinoid portion						

Note; DPC = distance from prepontine cistern to mid part of the aneurysm

Table 4. Detailed analysis of the 3 aneurysms at the posterior communicating artery by CT scan

No.	Age.	Sex	Aneurysm's size (mm)	Level	DDM,DPC (mm)	Side	Location on the pentagon
1.	55	F	5	1	11, 8		
2.	68	F	11	2	10, 5		
3.	67	M	6	2	8, 7		

Table 5. Detailed analysis of the 5 aneurysms at the middle cerebral artery by CT scan

No.	Age	Sex	Aneurysm's size (mm)	Level	DDM (mm)	Side	Location on the pentagon
1.	29	M	10	2	36	Lt	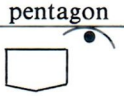
2. *	53	F	6	1	10	Rt	
3.	50	F	5	2	28	Rt	
4.	59	F	8	1	28	Lt	
5.	55	M	2	2	30	Rt	

* the aneurysm arose from the mid horizontal portion of rt MCA
Other aneurysms were from the region of the trifurcation/bifurcation of the MCA

Discussion

The circle of Willis is an interconnecting arterial polygon that surrounds the ventral surface of the diencephalon adjacent to the optic nerves and tracts (1). The normal circle of Willis is shown diagramatically in Figure 8. The following vessels comprise the circle of Willis: 1. the two ICAs 2. the horizontal (A l) segments of both anterior cerebral arteries 3. the anterior communicating artery 4. the two posterior communicating arteries 5. the horizontal (P1) segments of both posterior cerebral arteries 6. the basilary artery. (2). The ICAs, ACAs, ACoA, and their branches are sometimes termed the anterior circulation; the basilar bifurcation, PCAs, and PCoAs are collectively termed the posterior circulation (3). In normal patients the entire circle of Willis is only occasionally visualized on a single injection during cerebral angiography. Contrast enhanced spiral CT with maximum intensity projection can be used to obtain angiographic images of the circle and its major branches (4, 5, 6). Other noninvasive techniques for visualizing these vessels include magnetic resonance angiography (MRA) and transcranial doppler ultrasound.

The circle of Willis is actually "the Septagon", however, for simplicity, we drew "the Pentagon" to represent it. From this study, we could see from Fig. 9, that there were 5 locations where aneurysms sit on the Pentagon. The anterior communicating a. aneurysm would be at midline or paramedian part of the anterior Pentagon. The opposite midline posterior pentagon was the site of basilar tip aneurysm. The posterior right or left corner would be for aneurysm of the posterior communicating a. or distal ICA. The anterior corner of both sides would be for aneurysm of the horizontal portion of the middle cerebral a. or supraclinoid internal carotid a. The regions on the lateral wall of the pentagon anywhere between the anterior and posterior corners would be for aneurysm of the posterior communicating a. or distal internal carotid artery. These aneurysms which could be related to the circle of Willis (or the pentagon) must be seen at the cut levels 1 or 2.

There were aneurysms seen outside the pentagon. One case of the anterior communicating a. aneurysm that was located high (seen at cut level 3) between the floor of the frontal horns. The aneurysms of the genu of the middle cerebral a. would be posterior to the anterior wall of the middle cranial fossa.

By mapping the visualized enhanced aneurysm by CT scan on the pentagon, it help to locate the origin of the aneurysm.

Acknowledgment: We would like to thank Mrs. O.Jermjitpong and Mr.D.Predpring in helping us preparing the Manuscript.

References

1. Osborn AG: Introduction to Cerebral Aniograph, pp 33-48. Harper and Row, Hagerstown, 1980
2. Osborn AG: Diagnostic neuroradiology, pp 126. Mosby, St.Luis, 1994
3. Saeki N, Rhoton AL Jr: Microsurgical anatomy of the upper basilar artery and the posterior circle of Willis, J Neurosurg 46: 563-578, 1977
4 Napels, Marks MP, Rubin GD et al: CT angiography with spiral CT abd maximum intensity proection. Radiol 185: 607-610, 1992
5. Marks MP, Napel S, Jordan JE, Enzmann DR: Diagnosis of carotid artery disease: preliminary experience with maximum intensity-projection spiral CT, AJR 160: 1267-1271, 1993
6. Dillon EH, van Leeuwen MS, Fernandex MA, Mali WPTM: spiral CT angiography, AJR 160:1273-1278, 1993
7. Sahs AL, Perret GE, Locksley HB, et al (eds): Intracranial aneurysms and subarachnoid hemorrhage: A cooperative study. Philadelphia, JB Lippincott, 1969
8. Aaknaabu WS, Richardson AE: Multiple intracranial aneurysms: Identifying the ruptured lesion. Surg Neurol 9: 303-305, 1978
9. Scotti G, Ethier R. Melancon D, et al: Computed tomography in the evaluation of intracranial aneurysms and subarachnoid hemorrhage. Radiology 123:85-90, 1977

January - April 1995 Volume 1 Number 1

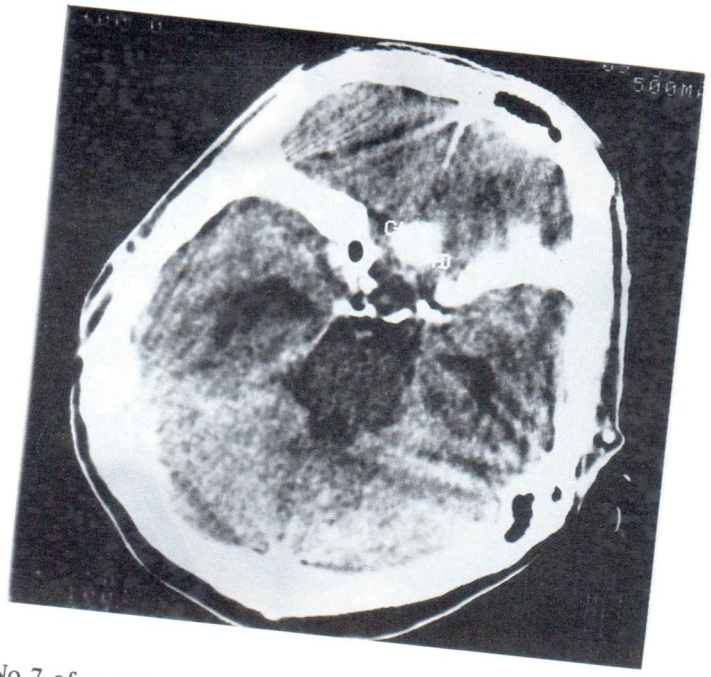

Fig.1a Case No.7 of anterior communicating a. aneurysm by i.v. enhanced CT scan

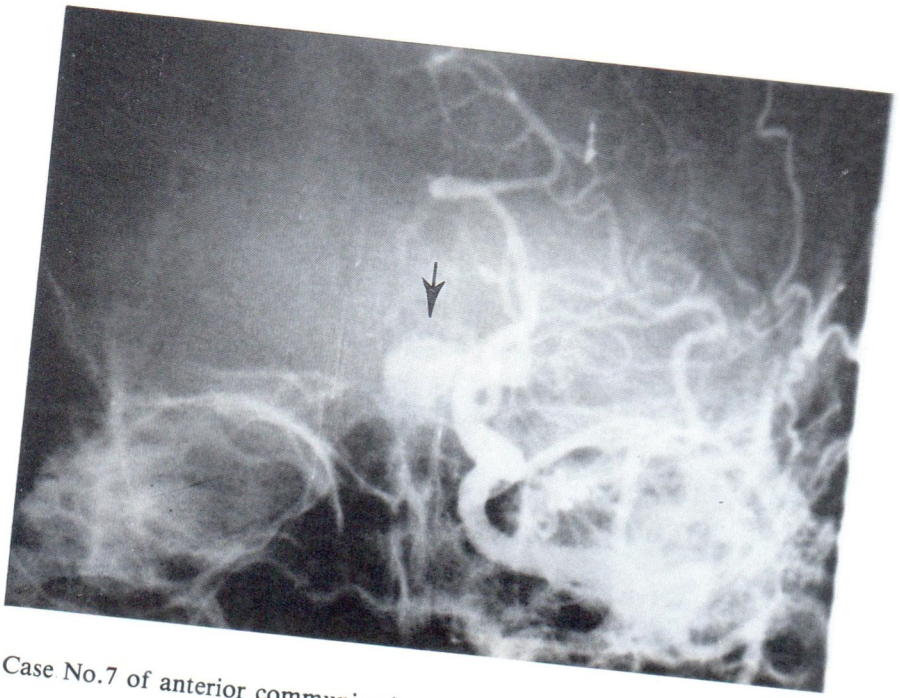

Fig.1b Case No.7 of anterior communicating a.aneurysm by conventional angiography

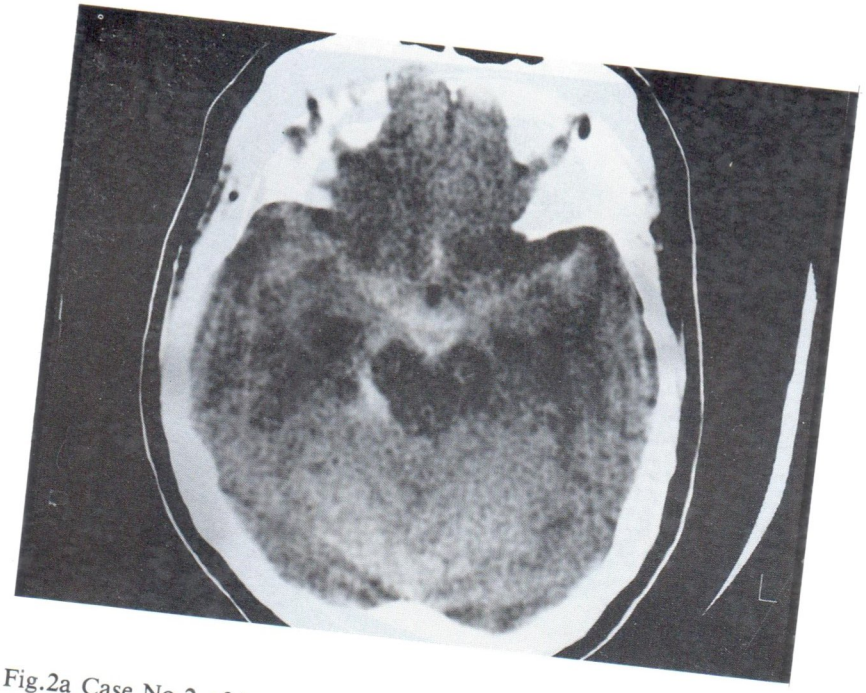

Fig.2a Case No.2 of basilar tip aneurysm by i.v. contrast study

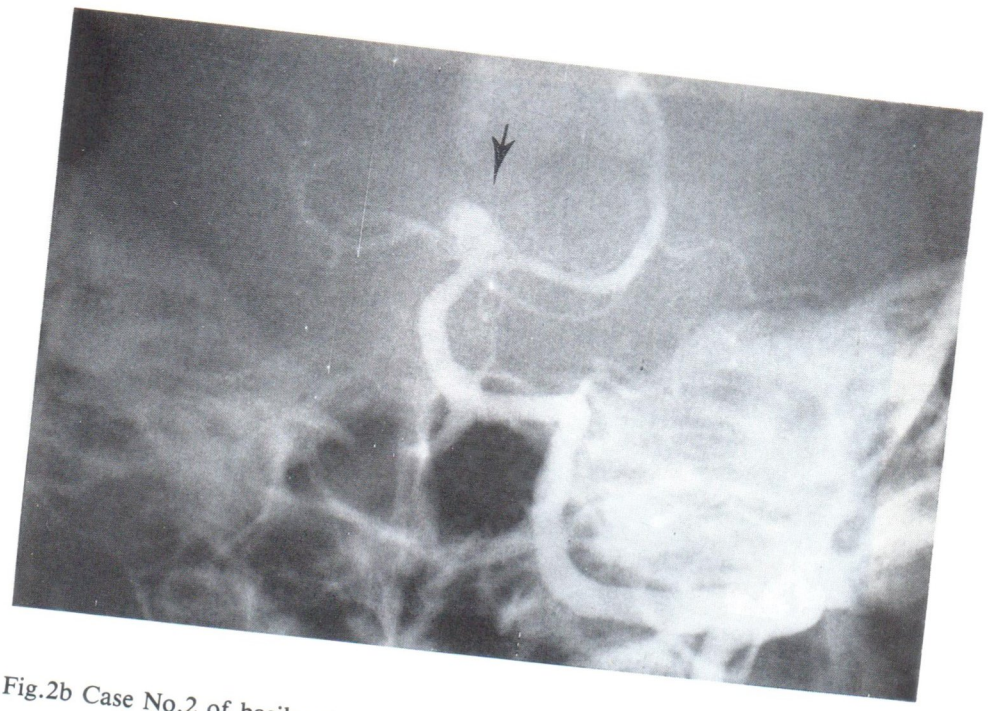

Fig.2b Case No.2 of basilar tip aneurysm by conventional angiography

January - April 1995 Volume 1 Number 1

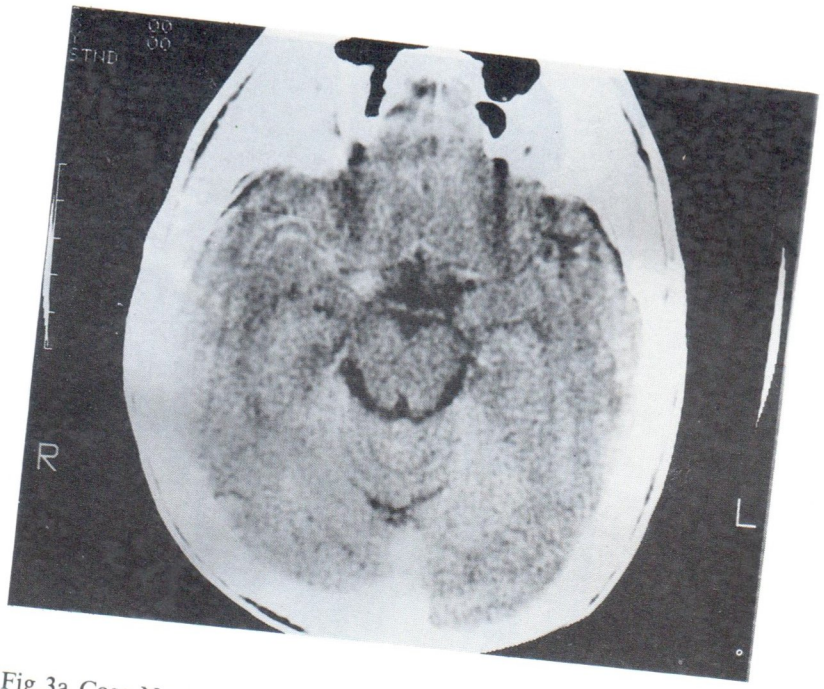

Fig.3a Case No.1of aneurysm at distal ICA by i.v. enhanced study

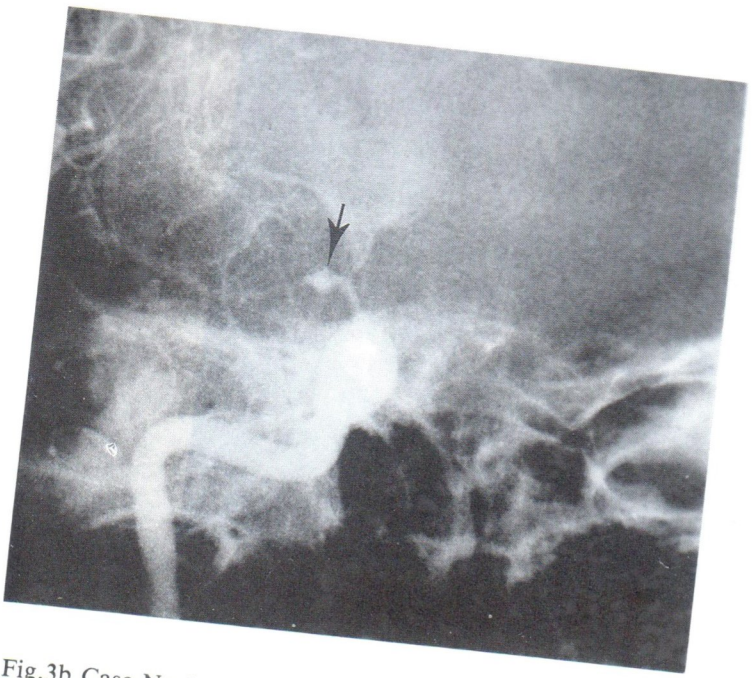

Fig.3b Case No.1 of aneurysm at distal ICA by conventional angiography

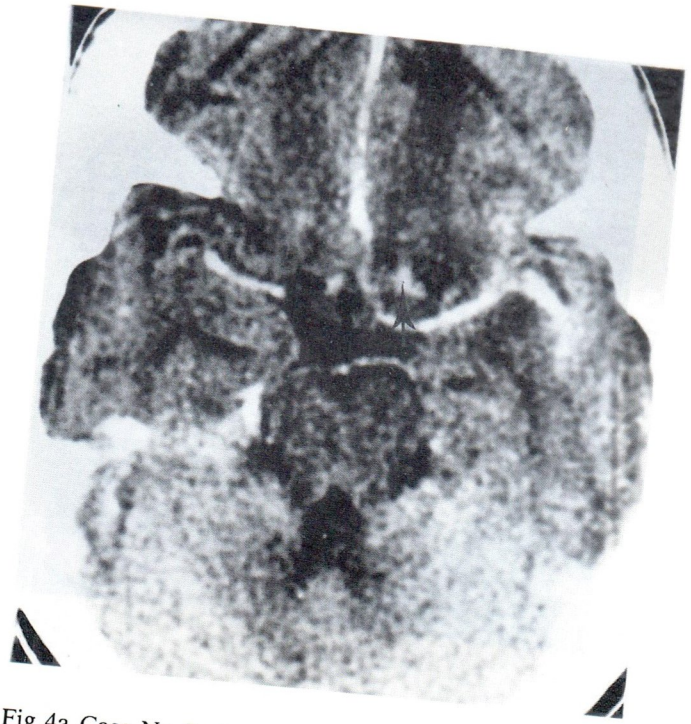

Fig.4a Case No.2 of aneurysm at supraclinoid internal carotid a. by i.v. enhanced CT scan

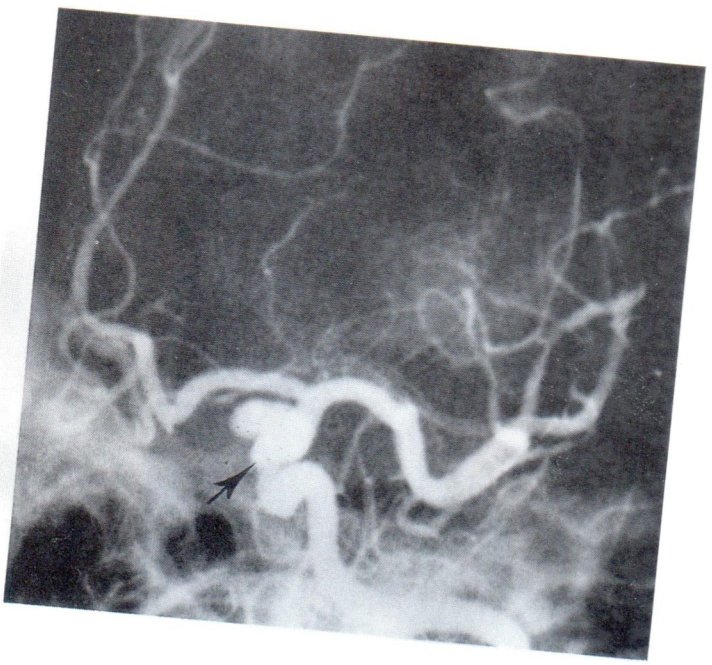

Fig.4b Case No.2 of aneurysm at supraclinoid internal carotid a. by conventional angiography

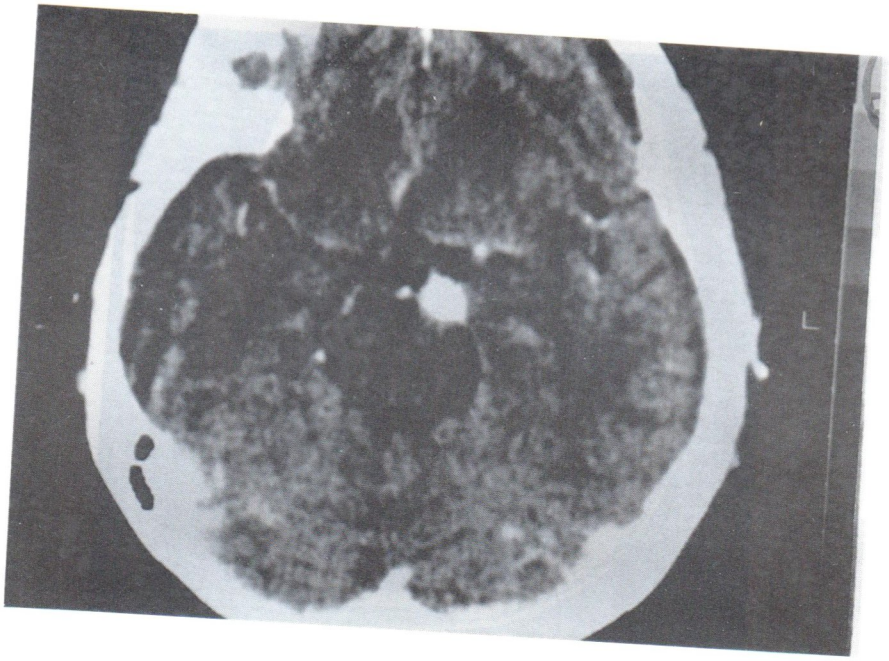

Fig.5a Case No.2 of posterior communicating a. aneurysm by i.v. enhanced CT scan

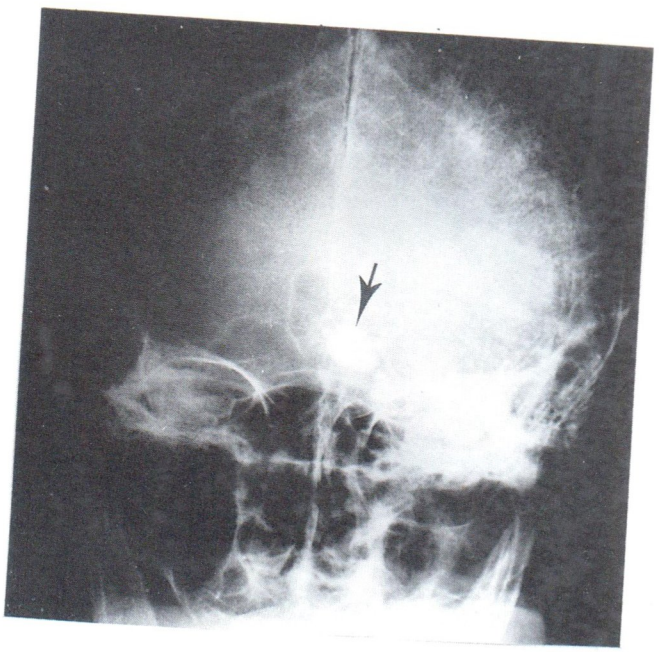

Fig.5b Case No.2 of posterior communicating a. aneurysm by conventional angiography

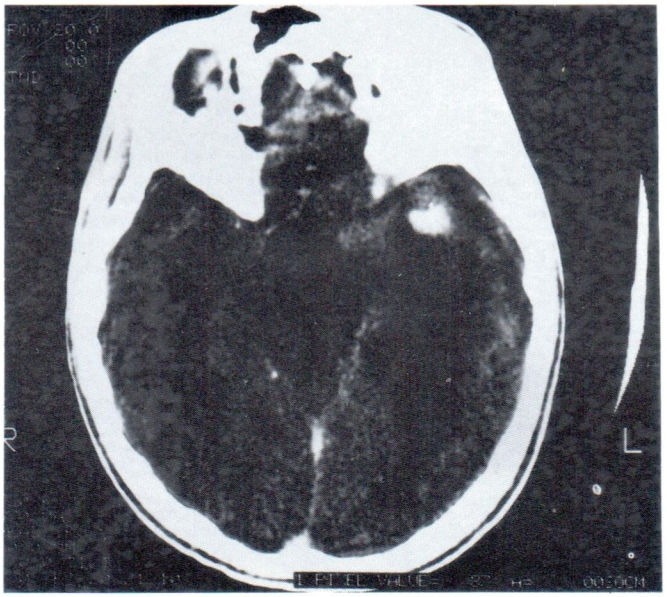

Fig.6a Case No.1 of middle cerebral a.aneurysm by i.v. enhanced CT scan

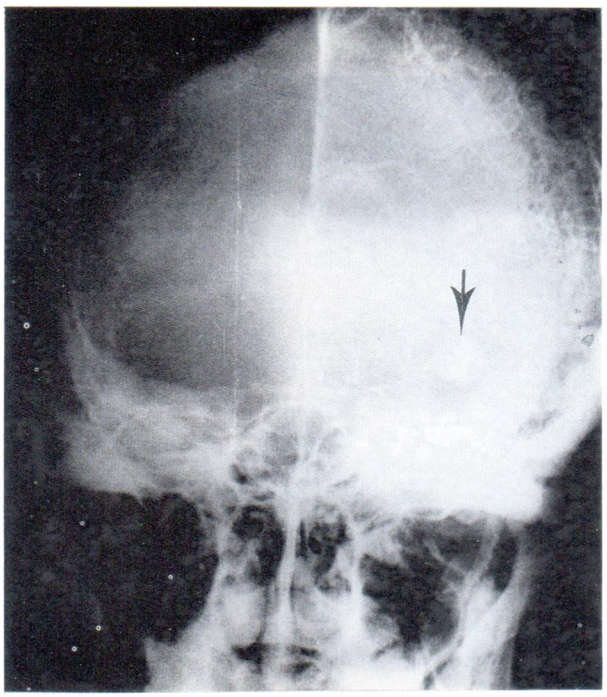

Fig.6b Case No.1of middle cerebral a. aneurysm by conventional angiography

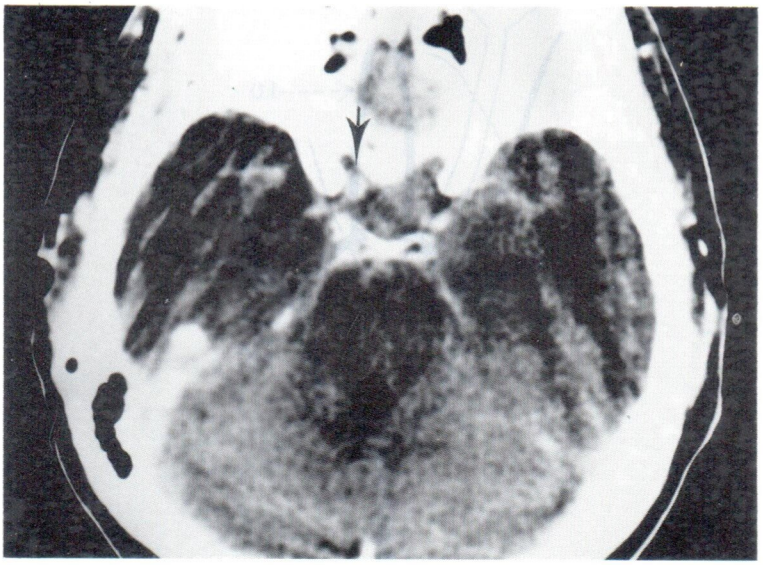

Fig.7a Case No.2 of middle cerebral a. by i.v. enhanced CT scan

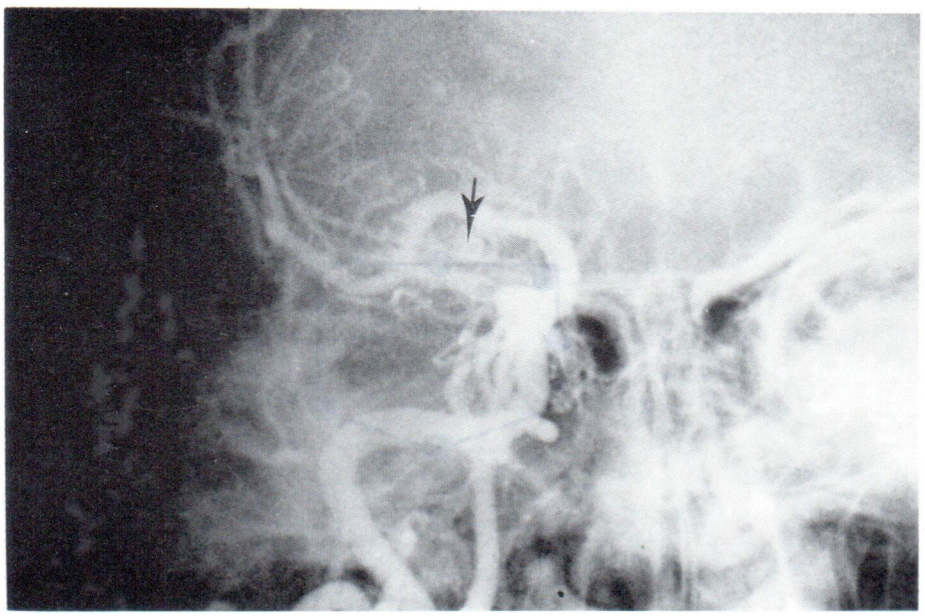

Fig.7b Case No.2 ofmiddle cerebral a. by conventional angiography

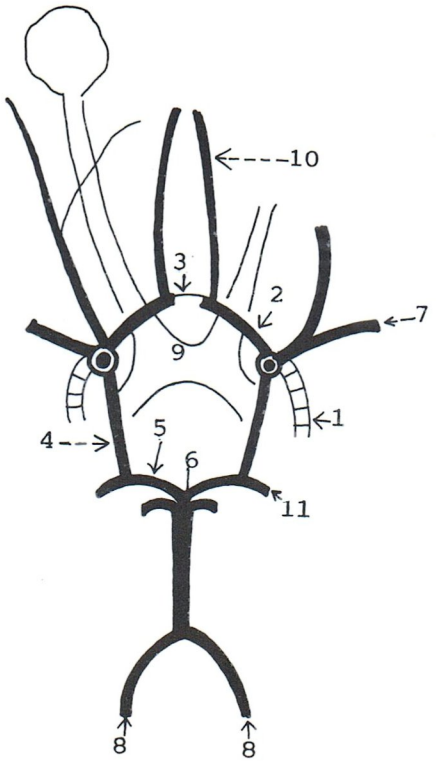

Fig.8 Anatomic diagram depict the circle of Willis. 1, Internal carotid artery (ICA). 2, Horizontal (A1) anterior cerebral artery segment. 3, Anterior communicating artery (ACoA). 4, Posterior communicating artery (PCoA). 5, P1 segment of posterior cerebral artery (PCA). 6, Basilar artery (BA) bifurcation. 7, Middle cerebral artery (MCA; not part of the circle of Willis). 8, Vertebral arteries (VAs; also not part of the circle of Willis). 9. Optic chiasm. 10, A2 (post communicating) ACA segment. 11, P2 (post communicating) PCA segment. (Modified from Osborn AG: Handbook of Neuroradiology, Mosby-Year Book 1991)

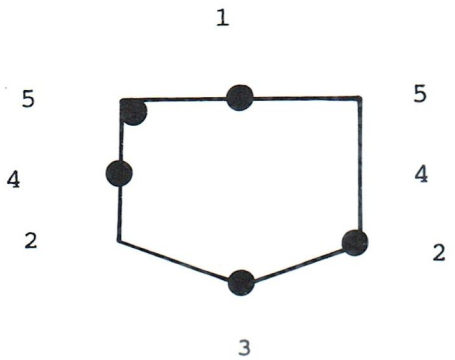

Fig.9 Summarized diagram of the aneurysms of thecircle of Willis, according to the locations on the "pentagon"
1 = aneurysm of anterior communicating artery
2 = aneurysm of posterior communicating artery vs distal ICA
3 = aneurysm of the tip of the basilar artery
4 = aneurysm of posterior communicating artery vs distal ICA
5 = aneurysm of horizontal portion of middle cerebral a. vs of supraclinoid ICA.

Fig.10 Aneurysm outside the circle of willis, at the genu of middle cerebral artery, approximately at the region posterior to mid curve of the anterior middle cranial fossa wall

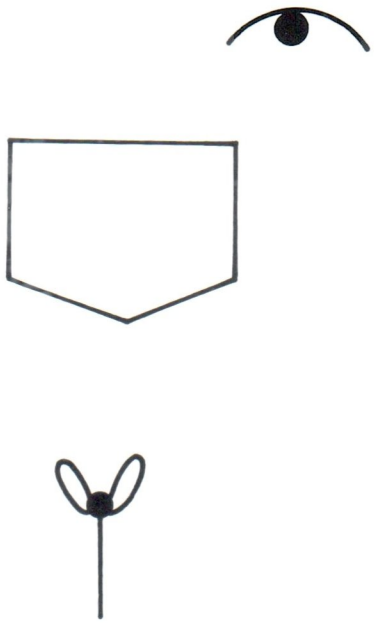

Fig.11 Aneurysm was shown at area 3, of anterior communicating a. between the floor of the frontal horns

Songsittivan Company Limited.

1017 Prachachuen Road, Bangsue,
Bangkok, Thailand. 10800